THE EPHRIN-A1/EPHA2 SIGNALING AXIS REGULATES GLUTAMINOLYSIS IN HER2-POSITIVE BREAST CANCER

By

Victoria Marie Youngblood

Dissertation

Submitted to the Faculty of the

Graduate School of Vanderbilt University

in partial fulfillment of the requirements

for the degree of

DOCTOR OF PHILOSOPHY

in

Cancer Biology

May, 2016

Nashville, Tennessee

Approved:

Jin Chen, M.D., Ph.D.; Advisor
Barbara Fingleton, Ph.D.; Chair
Rebecca Cook, Ph.D.
Melissa Skala, Ph.D.

ORIGINAL PUBLICATIONS

1. Youngblood VM, Kim LC, Edwards DN, Hwang Y, Santapuram PR, Lu P, Ye F Stirdivant SM, Brantley-Sieders DM, Chen J. *The Ephrin-A1/EPHA2 signaling axis regulates glutamine metabolism in HER2-breast cancer.* Cancer Res. 2016 (In Press).

2. Wang S, Amato KR, Song W, Youngblood V, Lee K, Boothby M, Brantley-Sieders DM, Chen J. *Regulation of Endothelial Cell Proliferation and Vascular Assembly through Distinct mTORC2 Signaling Pathways.* Mol Cell Biol. 2015 Apr;35(7):1299-313. doi: 10.1128/MCB.00306-14.

3. Youngblood V, Song W, Walter D, Hwang Y, Chen J, Brantley-Sieders D. *Elevated Slit2activity impairs VEGF-induced angiogenesis and tumor neovascularization in EphA2-deficient endothelium*. Mol Cancer Res. 2015 Mar;13(3):524-37. doi: 10.1158/1541-7786.MCR-14-0142.

3. Amato KR, Wang S, Hastings AK, Youngblood VM, Santapuram PR, Chen H, Cates JM, Colvin DC, Ye F, Brantley-Sieders DM, Cook RS, Tan L, Gray NS, Chen J *Genetic and pharmacologic inhibition of EPHA2 promotes apoptosis in NSCLC.* J Clin Invest. 2014 May 1;124(5):2037-49. doi: 10.1172/JCI72522.

This dissertation is dedicated to all breast cancer patients
for all their bravery and courage.

In Memoriam:
To my stepmother, Dolly Gallegos Youngblood

ACKNOWLEDGEMENTS

I am extremely gracious and appreciative of all those that have supported and encouraged me during my graduate training here at Vanderbilt. I would first like to thank my outstanding mentor, Dr. Jin Chen. This work would not at all been possible without her support and guidance. She constantly encouraged me to push beyond my scientific comfort zone, nurtured my scientific creativity, and she ultimately helped me become a better scientist. When first faced with the option of investigating tumor metabolism, it was Dr. Chen that provided me with the confidence and encouragement to take on such a task, for which I am eternally grateful. I would also like to express tremendous appreciation to my thesis committee: Drs. Barbara Fingleton (Chair), Rebecca Cook, and Melissa Skala. This group of talented scientists provided me with scientific guidance, helpful critiques, and invaluable insight in terms of forming hypotheses, data analysis, and presentation skills. Not only did they shape me into a better scientist, but they also served (and continue to serve) as strong role models.

I would also like to thank those who supported me financially during my graduate training, specifically to Dr. Paul Bock for the Mechanisms in Vascular Disease Training Grant (T-32 NIH/NHLBI 5T32HL007751-17) and the National Cancer Institute for the Pre-doctoral Ruth L. Kirschstein National Research Service Award (NRSA) (F31 FCA180407A). I would also like to acknowledge all the members of the Cancer Biology department for all of their daily help.

I want to thank the present and past members of the Chen lab: Dana Brantley-Sieders, Yoonha Hwang, Wenqiang Song, Shan Wang, Deanna Edwards, Laura Kim, Eileen Shiuan, Meghana Rao, Katherine Amato, Pranav Santapuram, David Vaught, Debbie Dorkoski, and Tammy Sobolik, as they have proved instrumental in my thesis

work. Each member played an integral role in my PhD training whether as a collaborator on a project, assisting with animal work, proof reading, or overall everyday encouragement. I would like to also highlight one member of the Chen lab, Dana Brantley-Sieders, for her scientific talents, support and friendship. She has been a fundamental part of my scientific training. She trained me in all of my angiogenesis techniques, helped me think out of the box and encouraged me day in and day out. For all this and more, I am tremendously grateful.

I must also acknowledge my past research mentors, Nancy Kanagy, Ph.D. from the University of New Mexico, and James Taylor, M.D. from the National Heart Lung and Blood Institute. Their introductions to biomedical and translational research were monumental to my successes and I am truly appreciative of their mentorship.

Lastly, I would like to acknowledge my friends and family. Their constant love and support without a doubt continued to propel me throughout my graduate training. My first year of graduate training was excessively difficult due to the passing of my stepmother, my uncle and my grandmother, and the hospitalization of my father. Despite these hardships my husband, my family and in-laws provided the utmost support. Thank you, mom and dad, Dolly, Dave, Daniel, Amorette, DJ, Michael, Nancy, Matt, Brenda, Justin, Katie, Emily, Zach, Mason, Della, Addie, and Lydia for everything. In addition, I would like to acknowledge my amazing roommate and friend, Brad, another Vanderbilt graduate student, that provided an incredible amount of support and friendship. I must also thank my dear friends that I met in graduate school, Liz, Kate, Hannah and Zoi. Thank you for your enduring friendship and fun times. Finally I must thank my husband, Zack. He stood by my side through every tragedy and triumph. His love and support go beyond what I knew possible and no words could possibly describe my gratitude. Thank you, Zack, and I love you.

TABLE OF CONTENTS

LIST OF TABLES

Table Page

LIST OF FIGURES

LIST OF ABBREVIATIONS

ABL—Abelson Murine Leukemia Viral Oncogene Homolog 1

ACC—Acetyl-CoA Carboxylase

ACLY—ATP Citrate Lyase

ADAM—A Disintegrin And Metalloproteases

ADP—Adenosine Diphosphate

ANOVA—Analysis of Variance

ATP—Adenosine Triphosphate

BrdU—Bromodeoxyuridine

CXCR4—C-X-C Chemokine Receptor Type 4

DAB—Diaminobenzidine Tetrahydrochloride

DAPI—4',6-Diamidino-2-Phenylindole

DCIS—Ductal Carcinoma *In Situ*

DMEM—Dulbecco's Modified Eagle's Media

DMSO—Dimethyl Sulfoxide

DOX—Doxycycline

EGF—Epidermal Growth Factor

EGFR—Epidermal Growth Factor Receptor

ELISA—Enzyme Linked Immunosorbent Assay

EPH—Erythropoietin Producing Hepatoma

Ephrin—EPH Family Interacting Proteins

ER—Estrogen Receptor

F-2,6-BP—Fructose 2,6-bisphosphate

FAK—Focal Adhesion Kinase

FASN—Fatty Acid Synthase

FBS—Fetal Bovine Serum

GCL—Glutamate cysteine ligase

GDH—Glutamate Dehydrogenase

GEF—Guanosine Nucleotide Exchange Factor

GFP—Green Fluorescent Protein

GLS—Glutaminase

GOT—Glutamate Oxaloacetate Transaminase

GPI—Glycosylphosphatidlinositol

GPT—Pyruvate Transaminase

GRB2—Growth Factor Receptor-Bound Protein 2

GS—GSH synthase

GSH—Glutathione Reduced

GST—Glutathione-*S*-transferase

GTP—Guanosine Triphosphate

HER2—Human Epidermal Growth Factor Receptor 2

HIF—Hypoxia Inducible factor

HK—Hexokinase

HRMEC—Human Retinal Microvascular Endothelial Cells

HUVEC—Human Umbilical Vein Endothelial Cells

IDC—Invasive Ductal Carcinoma

IF—Immunofluorescence

IFNγ—Interferon Gamma

IHC—Immunohistochemistry

KRAS—Kirsten Rat Sarcoma Viral Oncogene Homolog

LDH—Lactate Dehydrogenase

mAb—Monoclonal Antibody

MAPK—Mitogen Activated Protein Kinase

MMTV—Mouse Mammary Tumor Virus

MMP—Matrix Metalloproteases

MPMEC—Murine Pulmonary Microvascular Endothelial Cells

mTOR—Mammalian Target of Rapamycin

mTORC—Mammalian Target of Rapamycin Comlex

MYC—Avian Myelocytomatosis Viral Oncogene Homolog

OXPHOS—Oxidative Phosphorylation

PBS—Phosphate Buffered Saline

PCNA—Proliferating Cell Nuclear Antigen

PCR—Polymerase Chain Reaction

PDAC—Pancreatic Ductal Adenocarcinoma

PDZ—PSD95/Dig/ZO1

PET—Positron Emission Tomography

PFK—Phosphofructokinase

PI3K—Phosphatidylinositol 3 Kinase

PK—Pyruvate Kinase

PKM2—Pyruvate Kinase M2 Isoform

PPP—Pentose Phosphate Pathway

PR—Progesterone Receptor

Rac1—RAS Related C3 Botulinum Toxin Substrate 1

RHO-A—RAS Homology Gene Family, Member A

RIPA—Radioimmunoprecipitation Assay

RNAi—RNA Interference

ROS—Reactive Oxygen Species

RPMI—Roswell Park Memorial Institute Media

RTK—Receptor Tyrosine Kinase

SAM—Sterile-alpha-motif

SD—Standard Deviation

SEM—Standard Error of the Mean

SH2—SRC homology 2

shRNA—Small Hairpin RNA

siRNA—Small Interfering RNA

SREBP1—Sterol Regulatory Element Binding Protein 1

TCA—Tricarboxylic Acid

TNBC—Triple Negative Breast Cancer

TUNEL—Terminal Deoxynucleotidyl Transferase dUTP Nick-End Labeling

VEGF—Vascular Endothelial Growth Factor

VEGFR2—Vascular Endothelial Growth Factor Rector 2

vWF—von Willebrand Factor

α-KG—alpha-ketoglutarate

CHAPTER 1

INTRODUCTION

Overview

Breast cancer persists as the second leading cause of cancer related deaths of women in the United States despite advancements in early diagnosis and therapeutic treatments. Metabolic reprogramming is a hallmark of cancer and contributes to the initiation and progression of breast carcinomas by providing the molecular 'building blocks' that sustain viability and rapid proliferation. Enhanced glycolysis coupled with an increase in glucose consumption was originally believed to be the primary mechanism of aberrant metabolism. However, as the field of tumor metabolism has expanded, we now know glutamine also serves as a major nutrient source for tumor cells and that oncogenes can directly regulate the many branches of cell metabolism. EPHA2 receptor tyrosine kinase has recently been recognized as a major contributor to the initiation and metastatic spread of several cancers, including breast. Overexpression of EPHA2 is observed in breast cancer patient samples and correlates with poor prognosis and decreased survival. A unique characteristic of EPHA2 is its ability to function as either a tumor promoter or tumor suppressor depending on whether it is bound to its preferential ligand, ephrin-A1. In the absence of ephrin-A1, EPHA2 becomes overexpressed and signals in a ligand-independent manner that confers growth and motility. Although EPHA2 has oncogenic potential and signals through several oncotargets, the role of EPHA2/ ephrin-A1 in tumor metabolism, specifically in breast cancer, has yet to be elucidated. Herein, we describe the first functional evidence that links EPH/ephrin signaling to tumor cell metabolism. We used genetic, molecular and pharmacologic approaches to interrogate the mechanisms by which EPHA2 ligand-independent

signaling promotes tumorigenesis in the absence of its prototypic ligand, ephrin-A1. We discovered that the loss of ephrin-A1 leads to enhanced EPHA2 activity that augments glutamine metabolism and lipid accumulation to promote tumor growth in a HER2-positive model of breast cancer. Our data suggests that this upregulation of glutaminolysis is attributed to increased RhoA-dependent glutaminase activity. Furthermore, the work herein, also highlights ephrin-A1 as a diagnostic marker in some subtypes of breast cancer and presents EPHA2 as a potential therapeutic target in carcinomas that are dependent on glutaminolysis.

BREAST CANCER

Breast cancer remains the second leading cause of cancer-related deaths in women in the United States with an estimated 40,000+ death per year [1]. Though breast cancer can also arise in men, it occurs about once in every 100 cases of reported diagnoses [1]. Environmental factors such as body mass index, hormone replacement therapy and age are all linked to elevated risk, however much of the data that link environmental risk and breast cancer remain largely correlative [2]. The identification of germline mutations in the breast cancer susceptibility genes, *BRCA1* and *BRCA2*, introduced that some women have an inherited predisposition to breast cancer [3], yet approximately 85% of women diagnosed with malignancies of the breast have no first degree familial history of the disease [4, 5]. Thus the overexpression, deletion, or somatic mutations of critical growth regulating proteins can also significantly attribute to the transformation of mammary cells, tumor maintenance and metastatic spread.

Though the term 'breast cancer' describes all neoplastic formations of the breast, breast cancer is comprised of a variety of subtypes that are classified by their tissue of origin, histological appearance and molecular characteristics. Approximately 95% of breast cancers are carcinomas and arise from the epithelial cells within the

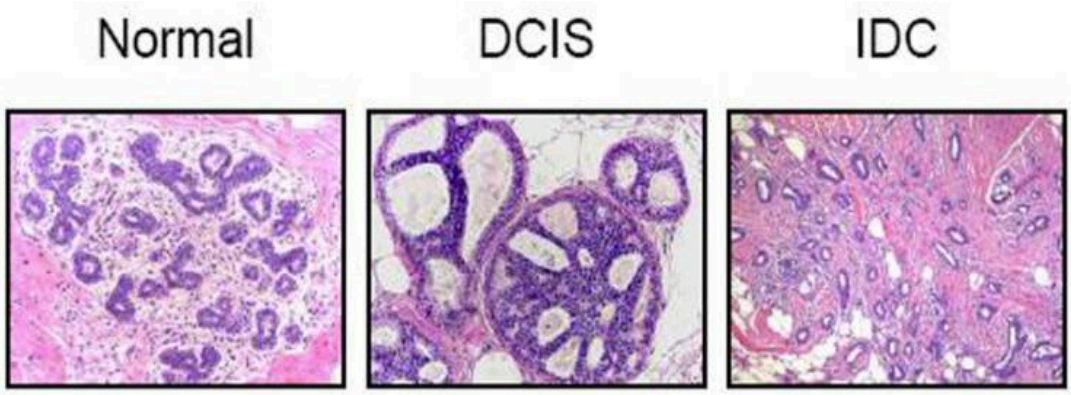

Figure 1.1 Histomorphological changes in mammary ductal tissue. Normal ductal tissue (left); ductal carcinoma *in situ* (DCIS) displays neoplastic growth confined to the ductal region (middle); invasive ductal carcinoma (IDC) displays neoplastic growth that has invaded the surrounding tissue (right) (Adapted from [6].

glandular tissue of the breast. Because the carcinoma arises from the glandular tissues, it can also be referred to as adenocarcinoma. A small percentage of breast cancers are sarcomas and these arise from the surrounding muscular or connective tissues.

Mammary carcinomas are primarily classified by their histological appearance and by their molecular characteristics. In histological classification, the carcinoma is classified by its tissue or cellular origin, such that ductal carcinoma originates from the inner lining epithelium of the ducts, and lobular carcinoma originates from lobules that supply the ducts with milk. They are further categorized by whether the carcinoma is limited to the epithelial region (*in situ*) or whether is has invaded into the surrounding stromal tissue (invasive) (Figure 1.1). Ductal carcinomas remain the most diagnosed subtype of breast cancer and invasive ductal carcinoma (IDC) accounts for approximately 55-80% of all breast cancers at the time of diagnosis. Due to the heterogeneity of all cancers, including breast, these carcinomas are further categorized based on molecular subtype. Currently, there are four major molecular subtypes of breast cancer: i) Luminal A, ii) Luminal B, iii) Triple

Negative/Basal-like, and iv) HER2 type. These subtypes, as highlighted in TABLE 1, are categorized by their protein expression patterns of progesterone receptor (PR), estrogen receptor (ER), HER2 receptor, and whether they exhibit a high degree of positive Ki67 staining. There are several smaller subtypes reported and with increased research it can be expected that additional molecular subtypes will emerge.

Molecular Subtype	Receptor Status	Prevalence	Reference
Luminal A	-ER+ and/or PR+ -HER2 negative -Low Ki67	40-70%	[7, 8]
Luminal B	-ER+ and/or PR+ -HER2+ or High Ki67	10-20%	[7, 8]
Triple Negative/Basel-like	-ER negative -PR negative -HER2 negative	15-20%	[7, 9-11]
HER2 type	-ER negative -PR negative -HER2+	10-20%	[7, 10, 12]

TABLE 1.1 Breast cancer molecular subtypes

Metabolic Reprogramming of Tumor Cells

In the early 1900's Otto Warburg described the phenomenon in which tumor cells utilize glucose in a manner different from non-cancerous cells. Non-cancerous cells convert glucose to lactate primarily under hypoxic conditions; yet, cancer cells perform this conversion despite adequate oxygen [13, 14]. This body of work launched decades of investigation into the mechanisms of how tumor cells are able

to utilize major nutrients to generate energy and 'building blocks' to support tumor cell viability and proliferation. We now know that glucose is not the only nutrient that tumor cells use for energy. Studies have revealed glutamine and lipids also serve as critical nutrient sources for tumor cells [15-17]. Because of their molecular structure, these molecules can serve as a rich nitrogen source for purine and pyrimidine synthesis and can also provide critical intermediates for ATP generation [16]. As the field of tumor metabolism has continued to broaden, researchers have also discovered that several oncogenes are at the epicenter of metabolic reprogramming [18-20]. For example, the PI3K/AKT/mTOR and RAS/MAPK pathways have both been implicated in metabolism reprogramming [19, 21, 22]. This discovery has, indeed, enhanced our understanding of tumor metabolism and has provided additional insight into the mechanism in which oncogenes regulate cell growth.

Glycolysis

In healthy and non-proliferating cells, ATP generation primarily relies on the highly efficient mitochondrial process of substrate oxidation in the TCA cycle and electron transport-coupled oxidative phosphorylation (OXPHOS). In this process, glucose is catabolized to pyruvate, which then enters the mitochondria. Pyruvate is then oxidized to acetyl-CoA and is combined with oxaloacetate to enter the TCA cycle and undergo OXPHOS.

Oxidative phosphorylation:

Glucose → Pyruvate → Acetyl-CoA → TCA cycle/OXPHOS → 36 ATP

In the event of hypoxia, rather than entering the mitochondria, pyruvate is instead reduced to lactate by the enzyme lactate dehydrogenase (LDH). Proliferating tumor cells, however, shift their bioenergetics to glycolysis as means to support macromolecule duplication even under aerobic conditions, a process also referred to as the "Warburg effect" [23, 24].

Glycolysis:

Glucose → Pyruvate → Lactate → 2 ATP

Warburg originally hypothesized that aerobic glycolysis became a dominant pathway in tumor cells because of dysfunctional mitochondrial OXPHOS [13]. However, later studies revealed that mitochondrial activity was intact in some tumors cells and that these cells can still utilize glucose for OXPHOS but instead preferentially use glycolysis [25]. The reasons for cancer cells to preferentially use glycolysis rather than OXPHOS are multifold. First, though glycolysis only produces 2 ATP molecules compared to 36 in OXPHOS per glucose molecule, glycolysis occurs at a greater rate thus producing a constant supply of ATP. Therefore, rapidly dividing tumor cells have an abundant amount of ATP to use readily without ever obtaining a high concentration of ATP [26]. This is beneficial for a rapidly dividing cell because elevated ATP concentrations can attenuate glycolysis by negative regulatory mechanisms, in which the rate-limiting enzymes, phosphofructokinase 1 (PFK1) and pyruvate kinase 1 (PK1) can be inhibited [27]. Second, glycolysis generates lactate as a final product that is subsequently transported to the extracellular space, thus generating a lactic acidotic environment that can contribute to tumor growth. For instance, inhibition of the lactate transporter, MCT1, inhibits lactate flux and impairs tumor cell growth and tumor angiogenesis [28]. Additional studies have further demonstrated that this acidotic environment confers cell viability in events of glucose deprivation and can promote cancer progression [29, 30]. Third, aside from generating ATP, glycolysis intermediates serve as critical precursors for the macromolecules necessary for the rapid proliferation of tumor cells [31]. Additionally, glutamine, another critical nutrient that can drive aberrant metabolism, can also serve as a precursor for fatty acid, purine and pyrimidine synthesis, and these pathways are augmented upon increased rates of glycolysis or hypoxia [16, 32]. Fourth, an accumulation of data also suggests that enhanced levels of reactive oxygen species (ROS) generated from OXPHOS can be cytotoxic [33, 34]. Thus reducing the activity of OXPHOS may aid in tumor cell viability. Incidentally, as

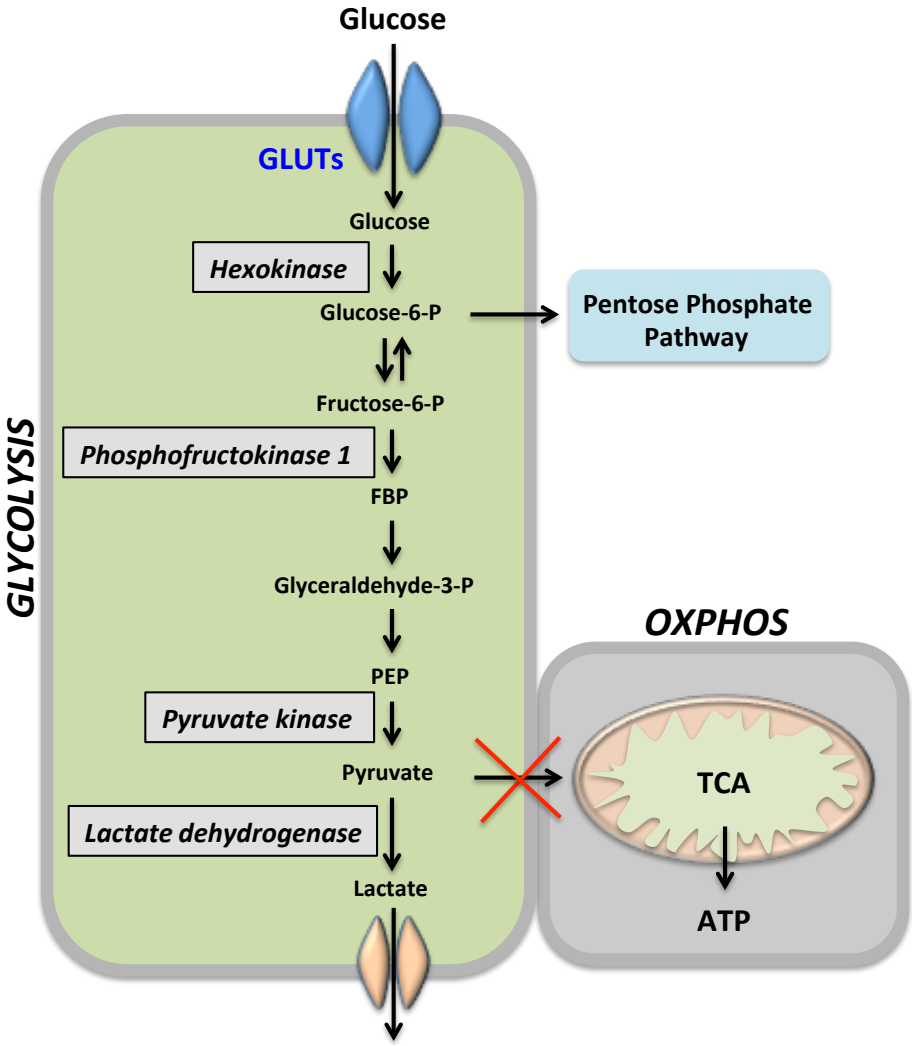

Figure 1.2 Glycolytic pathway. Schematic diagram of glucose being metabolized through the glycolytic pathway to generate lactate. Pyruvate is converted to lactate rather than undergoing mitochondrial oxidative phosphorylation (OXPHOS). Glycolysis intermediate, glucose-6-phosphate (glucose-6-P) can also be shunted to the pentose phosphate pathway. Major regulatory enzymes of glycolysis are listed.

tumor cells are reprogrammed for enhanced glycolysis, we subsequently see an enhancement of the regulatory proteins that facilitate this pathway (FIGURE 1.2).

GLUT transporters

Glucose first enters the cells by the GLUT family of glucose transporters, also referred by the gene name *SLC2A*. The GLUT family, which is comprised of 14

isoforms, is divided into 3 classes. Class I, also referred to as classical glucose transporters, is comprised of GLUT1-4 and GLUT14, and remains the most characterized class of GLUT transporters. Class II is comprised of GLUT5, 7, 9,and 11; and Class III incudes GLUT6, 8, 10, 12, and 13 [35]. GLUTs can have varying affinities for glucose, as well as for fructose and galactose. GLUT1, reported to have a high affinity for glucose, compared to the other isoforms, remains one of the most studied GLUT proteins [36, 37]. GLUT1 overexpression has been linked to most human cancers including pancreatic, breast, head and neck, renal, colorectal, lung and prostate [38-42]. Studies have also suggested that GLUT1 expression may also have prognostic value in that GLUT1 expression correlates with invasiveness and poor prognosis in patients with prostate and colorectal cancers [41, 42]. The transcription factor, hypoxia inducible factor 1 alpha, (HIF-1α), has been implicated as a key regulator of tumor metabolism and appears to be a critical regulator of GLUT1. Aberrant expression of the remaining Class I GLUT transporters has also been linked to several cancers. GLUT4, another highly studied GLUT facilitator, is regulated by p53 [43], and had been reported as a major regulator of glucose transport in several cancers, including breast [37, 44]. Its unlikely that the Class I GLUT transporters are solely responsible for glucose mobility in cancer cells, and additional investigations are further elucidating the roles of the remaining GLUT transporters in tumor metabolism.

Hexokinase

Once in the intracellular environment, glucose undergoes the first committed step of glycolysis by being enzymatically converted to glucose-6-phosphate (G6P) by the enzyme hexokinase (HK). There are four major mammalian isoforms of hexokinase, denoted as HK1, HK2, HK3, and HK4 [45]. However, hexokinase 2 (HK2) appears to be the critical HK isoform responsible for metabolizing glucose in glycolytic tumor cells, as evidenced by its overexpression in cancerous cells compared to normal cells [46]. Additionally, Patra *et al.* demonstrated that loss of HK2 inhibited tumor

initiation and growth in a *Neu*-driven mammary tumor mouse model, suggesting that HK2 may potentially serve as a therapeutic target in glycolysis-driven cancers [47].

Phosphofructokinase 1

The conversion of fructose-6-phosphate (F6P) to fructose-1,6-bisphosphate (FBP) by the enzyme phosphofructokinase 1 (PFK1) is considered the second committing step of glycolysis. The regulation of PFK1 plays a critical role in the continuation of glycolysis or whether metabolites are redirected to the pentose phosphate pathway (PPP)—a metabolic pathway that branches off of glycolysis that can also confer growth by enhancing NADPH and nucleotide generation. One mechanism in the regulation of PFK1 is by *O*-linked β-*N*-acetylglucosamine (*O*-GlcNAc) glycosylation at Ser529. This glycosylation can inhibit PFK1 activity [48] thus redirecting upstream metabolites to enter the PPP. Additionally, an abundant amount of ATP can also negatively regulate PFK1. Yet AMP and fructose 2,6-bisphosphate (F-2,6-BP) can activate PFK1 activity and F-2,6-BP can even override the inhibitory effect of ATP to further perpetuate glycolysis [49].

Pyruvate kinase

Pyruvate kinase (PK) converts phosphoenolpyruvate (PEP) to pyruvate, and generates ATP in the process. Similar to PFK, PK is also subjected to allosteric regulation by ATP and is specifically activated by fructose-1, 6-bisphosphate [27]. As a major regulator of glycolysis, it is no surprise that PK appears to be highly relevant in controlling tumorigenesis. The M2 isoform (PKM2), in particular, appears to be most relevant in human malignancies and is overexpressed in tumor cells [50]. Additionally, inhibition of PKM2 by siRNAs or pharmacologic approaches appears to decrease glycolytic flux and viability in tumor cells [51, 52], thus demonstrating its potential as a therapeutic target.

Lactate dehydrogenase

Lactate dehydrogenase (LDH) reduces pyruvate to lactate in the final step of glycolysis, and has been reported as overexpressed in a variety of breast cancer cell lines and tissues [53, 54]. Similar to many other regulatory proteins of glycolysis, its expression can be induced by both HIF-1α and MYC [20, 55]. LDH may also play a critical role in the maintenance of tumor glycolysis by preventing pyruvate from being converted to the OXPHOS precursor, acetyl-CoA. Fantin *et al*. used *in vitro* and *in vivo* models of breast cancer to demonstrate that knockdown of LDH not only reduced tumor cell growth, but was also able to significantly enhance mitochondrial OXPHOS [25].

PET imaging

The dependence of cancer cells on increased glucose uptake has been exploited for use in clinical oncology. [^{18}F]fluorodeoxyglucose positron emission.tomography (FDG–PET) imaging, also know as PET scan, relies on a radioactive glucose analogue, in which the oxygen atom is replace with fluorine-18, to be consumed in a similar manner as glucose [56]. The analogue is transported into the cell by GLUT transporters and undergoes phosphorylation by HK. Because this analogue is lacking its oxygen atom, it cannot undergo the following reaction and is thus trapped in the cell until it undergoes natural decay. The analogue remains trapped for a period of time that allows it to be visualized. In this capacity, PET scans remain a relevant tool in the diagnosis and monitoring of cancers after treatment [56]. Figure 1.3 demonstrates the use of PET scans to monitor the efficacy of chemotherapy treatments in cancer patients. The PET scan images are from a patient before and after chemotherapy treatment.

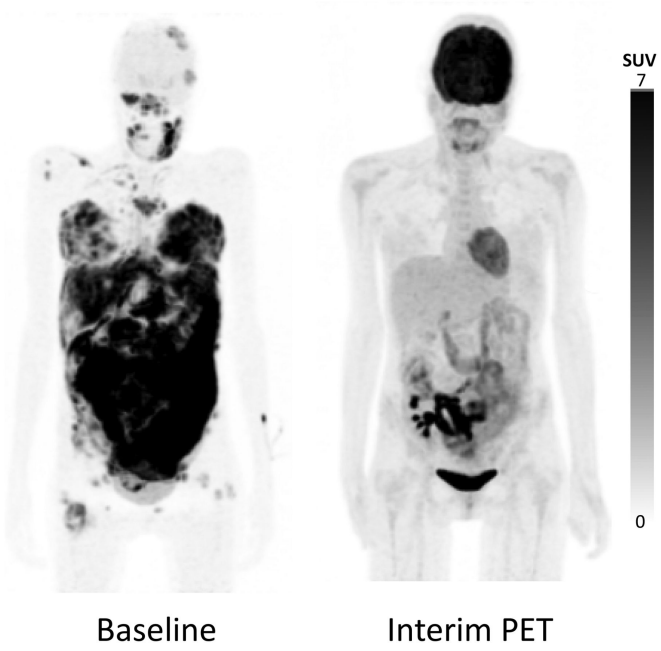

Figure 1.3 ^{18}F-FDG–PET images pre- and post- therapy. Baseline image showed multiple nodal lesions in the diaphragm and extranodal lesions in breast, intestines, and bone marrow (left); ^{18}F-FDG–PET image after 4 cycles of therapy showed a dramatic metabolic response in all nodal and extranodal lesions (right). ^{18}F, radionuclide fluorine 18; FDG, fluorodeoxyglucose; PET, positron emission tomography (Adapted from [57])

Glutamine metabolism in cancer

Glutamine is an abundant amino acid that plays a central role in healthy cell and tumor cell metabolism by serving as a critical precursor for nucleic acids, fatty acid synthesis and cellular energetics [15, 16]. Though mammalian organisms can readily absorb glutamine from exogenous sources, they also have the capability for synthesizing glutamine, thus making it a non-essential amino acid.

Glutamine metabolism greatly contributes to malignant growth by means of glutaminolysis [16, 58], and by regulating redox homeostasis through the generation of glutathione [59] (Fiugre 1.4). The process of glutaminolysis (also referred to as anaplerosis) describes the events of glutamine metabolism in which glutamine is

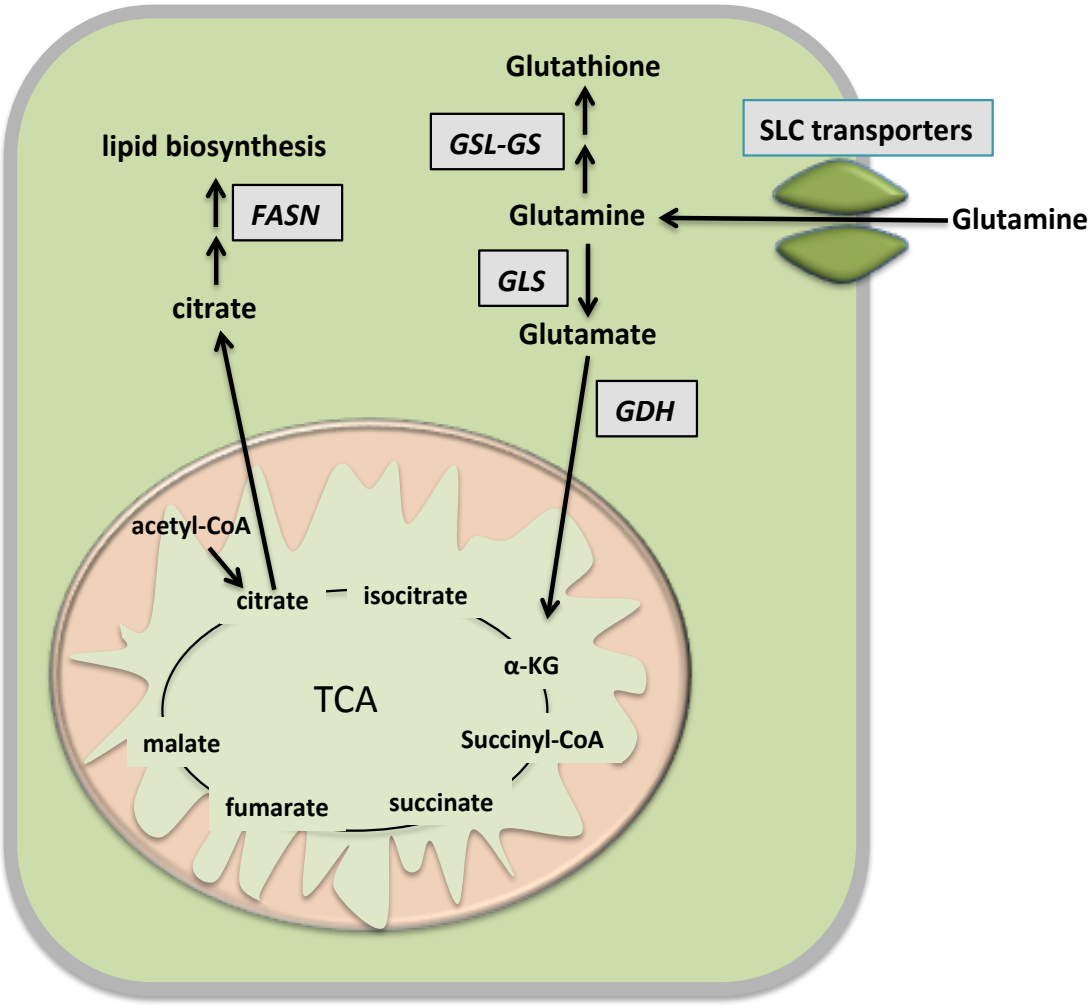

Figure 1.4 Glutamine metabolism in tumor cells. Simplified schematic diagram of glutamine undergoing glutaminolysis to generate alpha-Ketoglutarate (α-KG), a TCA cycle intermediate. This can give rise to elevated citrate generation, which serves as a precursor for lipid biosynthesis. By fatty acid synthase (FASN). Glutamine can also be converted to glutathione (GSH) in a 2-step reaction by glutamate cysteine ligase (GSL) and GSH synthase (GS).

metabolized to α-ketoglutarate (α-KG), a critical first step in generating cellular fuel and the building blocks for cell proliferation. This process can be separated into two distinct stages. First, glutamine is converted to glutamate by the enzyme glutaminase (GLS); and second, glutamine must be metabolized into the TCA substrate, α-KG. Furthermore, glutaminolysis is can also be controlled by glutamine

transport into the cell. Similar to GLUT transporters, these transporters are a critical first step in the metabolism of glutamine.

Glutamine transporters

Before glutamine can be converted to glutamate, glutamine transporters must first transport the amino acid into the cell. These glutamine transporters play a key role in glutamine metabolism by regulating intracellular and extracellular concentrations [60]. The most commonly studied glutamine transporters belong to the SLC1, SLC6, SLC7 and SLC38 families of amino acid transporters. SLC1 member, ASCT2 [61-63], and SLC7 member, LAT1 [64, 65], have recently been linked to several cancers, including breast, prostate and lung. Though the molecular mechanisms of regulation of these transporters remain largely unknown, recent studies have implicated roles for EGF [66], ERK [67], and insulin growth factor [68, 69] in the regulation of transporter expression and activity. Notably, the ASCT2 transporter can regulate mammalian target of rapamycin complex 1 (mTORC1) activity by controlling intracellular amino acid concentrations [70, 71]. Cumulative evidence has demonstrated a supportive role for amino acids in mTORC1 signaling [72, 73]; yet the discovery that inhibition of ASCT2 was sufficient to impair mTORC1 signaling and induce autophagy [71] further enhanced our understanding of mTORC1 regulation and glutamine metabolism.

Glutaminase

Once in the cell, glutamine undergoes the first stage of glutaminolysis where it is converted to glutamate by the aminohydrolase, glutaminase (GLS). Two isozymes of GLS, encoded by the human genes *GLS1* and *GLS2*, convert glutamine to glutamate [74]. GLS1 or the kidney-type isoform is reported to enhance malignancy and cell survival, and inhibition or silencing of this gene reduces tumor growth in multiple tumor models [75, 76]. For instance, Gross *et al.* inhibited GLS1 in triple-negative breast cancer cell lines identified as having enhanced glutamine metabolism and

observed significant anti-tumor activity both *in vitro* and *in vivo* [76]. As glutamine metabolism continues to present potential therapeutic targets, there has been increased investigation into the regulation of GLS1, particularly in malignant disease. Currently, MYC [77], mTOR [78] and RHO [79] have all been identified as indirect regulators of GLS1. As later discussed in Chapter 2, we also identify RHO as a positive regulator of glutaminolysis in breast cancer. In contrast to GLS1, the function of GLS2 appears to have dual roles that are dependent on context and tissue type. Some studies report GLS2 as a p53 target that reduces malignancy [80], while others demonstrate an oncogenic phenotype [81].

Generation of α-Ketoglutarate

In the second stage of glutaminolysis, glutamate undergoes oxidative deamination by glutamate dehydrogenase (GDH) in the mitochondrion or transamination by either glutamate pyruvate transaminase (GPT) or glutamate oxaloacetate transaminase (GOT) to generate α-KG. The byproduct of glutamate transamination is the generation of non-essential amino acids, and this pathway appears to be dominant during high rates of glucose metabolism. In events of inadequate glucose, GDH is a key pathway in the generation of α-KG. Recent studies by Jin *et al*. though, suggest that GDH is the primary enzyme in converting glutamate to α-KG, at least in the lung and breast cancer cell lines, H1299 and MDA-MB-231, respectfully [82]. They also demonstrated that silencing of GDH reduces tumor cell proliferation by decreasing the TCA intermediate, fumarate, which in turn prevents activation of the antioxidant, GPx [82]. Thus, in tumor cells that display glutamine addiction, GDH may play a greater role in α-KG generation.

The conversion of α-KG to other TCA cycle intermediates is a critical axis point for the final fate of glutamine. For instance, α-KG can be metabolized to citrate, which donates acetyl-coA groups for lipid biosynthesis. This pathway is used for *de novo* lipogenesis under hypoxic conditions and is linked to tumor cell proliferation,

motility, and survival [83]. As discussed above, α-KG can also generate the TCA intermediate, fumarate, which has been implicated in redox homeostasis [82]. The TCA intermediate, α-KG, once in the TCA cycle can also enhance oxidative phosphorylation for ATP generation in transformed cells [84]. This is most likely to compensate for depleted glucose-driven OXPHOS, as glycolysis is unregulated in tumor cells. Furthermore, it may be advantageous for cells to utilize glutamine as an OXPHOS substrate, since glutamine also promotes redox homeostasis that may counteract OXPHOS ROS generation. Though, other TCA intermediates exist, it is unclear whether they have a direct pathological link to cancer, at least at this point.

Glutathione

As mentioned above, the maintenance of cellular redox homeostasis plays a critical role in cell biology, and the dysregulation of this balance can directly contribute to tumorigenesis, motility and drug resistance. Glutathione, a downstream metabolite of glutamine, for decades has been a focal point in glutamine metabolism research due to its antioxidant properties. Glutathione has been implicated in cell survival and chemotherapeutic resistance by enhancing the antioxidant potential of the cell, thus scavenging apoptosis-inducing ROS. Glutathione is a multifunctional molecule and in normal physiology plays a key role in detoxification, ROS scavenging, protein thiol maintenance, and regulation of DNA synthesis. Glutathione is a tripeptide, γ-L-glutamyl-L-cysteinyl-glycine, that is synthesized in a two-step process:

1. L-glutamate + L-cysteine + ATP → γ-glutamyl-L-cysteine + ADP + Pi
2. γ-glutamyl-L-cysteine + L-glycine + ATP → GSH + ADP + Pi

The first reaction, considered the rate-limited step, is catalyzed by the enzyme, glutamate cysteine ligase (GSL). The second reaction is catalyzed by GSH synthase (GS). Though glutathione is present in all mammal organisms in two forms, it predominantly exists in the thiol-reduced (GSH) form, compared to the disulfide-oxidized form (GSSH) that makes up approximately 1% of total glutathione. Therefore, GSH is often referenced when discussing glutathione.

Though GSH is implicated in a number of physiological functions, in the context of cancer, the majority of investigations have focused on the role of GSH to confer growth and therapy resistance. GSH functions as an antioxidant or ROS scavenger by conjugating with electrophiles in a reaction mediated by the glutathione-*S*-transferase (GST) family of proteins. Cytotoxicity by enhancing ROS is the major mechanism of many chemotherapeutics, thus elevated levels of GSH and GST are indeed observed in many instances of chemoresistance [85-87]. Depletion of GSH or silencing of GST can modulate drug resistance by sensitizing tumor cells to anticancer agents [88, 89]. In addition, recent studies have further demonstrated that combining glutathione-targeting drugs with other antitumor agents may have a synergistic effect [90].

Lipid metabolism

In the 1950's Medes *et al.* observed that neoplastic tissue displayed lipid levels that were comparable to that of liver tissue, which has a high rate of fatty acid biosynthesis [91]. From these early studies, they concluded that *de novo* lipogenesis provides the majority of lipids required for cancer cell proliferation [91]. This aberrant lipogenesis has since been linked to several malignant pathologies including angiogenesis [92], signaling [93, 94] and metastasis[92, 95]. Glutamine metabolites have been demonstrated as positive regulators of lipid biosynthesis in tumor cells, and under hypoxic conditions glutamine becomes the major substrate for lipogenesis by enhancing the carbon-donating substrate, citrate [83, 96]. Citrate can be converted to acetyl-CoA by the enzyme ATP-citrate lyase (ACLY), which then generates malonyl-CoA by the enzyme, acetyl-CoA carboxylase (ACC). Acetyl-CoA and malonyl-CoA are then coupled to the acyl-carrier protein domain of the enzyme fatty acid synthase (FASN), a rate-limiting enzyme in *de novo* lipid synthesis [97]. FASN overexpression has been observed in breast carcinoma [98] and has been reported to undergo bi-directional regulation by the oncogene, HER2 [99, 100]. FASN expression can also be induced by transcription factor sterol regulatory

element-binding protein 1 (SREBP1), which binds to its promoter region [101]. Additionally, p53 family proteins [102]and the lipogenesis-related nuclear protein, SPOT14 [103], which is overexpressed in breast cancer, have also been implicated in FASN regulation. FASN may offer new therapeutic opportunities as several reports demonstrate reduced tumor activity upon its inhibition [104-109].

The role of oncogenic pathways in metabolic reprogramming

The discovery that oncogenes and tumor suppressors can play a major role in the metabolic reprogramming of cancer cells enhanced our understanding of tumor metabolism and provided additional targets for pharmacologic studies. These oncogenic controllers often interact with several branches of tumor metabolism including glycolysis, glutaminolysis, lipogenesis, and the pentose phosphate shunt and tend to regulate these pathways in a multifaceted manner (Figure 1.5). Though several pro-tumor proteins and pathways contribute to metabolic reprogramming, only a few are discussed below.

PI3K/AKT/mTOR pathway

Dysregulation of the PI3K/AKT pathway occurs at high frequency in human cancers and continues to be a center of focus in tumor biology [110]. The most characterized downstream effector of PI3K is the serine/threonine kinase, AKT (also referred to as Protein Kinase B or PKB). Upon stimulation, AKT can augment glycolysis by enhancing the membrane translocation and expression of GLUTs, and also through the phosphorylation and activation of the glycolytic enzymes, HK and PFK [19, 45, 111]. Additionally, AKT can activate mammalian target of rapamycin (mTOR), which indirectly regulates metabolic pathways through activation of HIF-1α. Though mTOR complexes have been reported to enhance glutamine metabolism, it is unclear whether this is via AKT activation and remains under investigation. mTOR is comprised of mTOR complex 1 (mTORC1) and mTOR complex 2 (mTORC2), and

though they have similar components, they have distinct binding partners [112]. Despite having divergent functions and signaling pathways in normal physiology [113], their functions in tumor metabolism appear to overlap, at least in the process of lipid biosynthesis. Both complexes have been implicated in activating the SREBP1 transcription factor, which in turn promotes ACC and FASN [114-116].

MYC

Oncogenic MYC is a transcription factor frequently overexpressed in human cancers that has been implicated in the regulation of cell metabolism, RNA, apoptosis, mitochondrial and ribosome biogenesis and cell cycle [117]. MYC directly enhances glycolysis by upregulating the expression of GLUT family transporters [118], LDH [55, 119], PKM2 [120] and PFK1 [118]. In addition to its role in glycolysis, MYC also augments glutamine metabolism by enhancing glutamine uptake and glutaminolysis [18]. MYC directly enhances glutamine uptake by inducing the expression of the glutamine transporters, SLC5A1 (ASCT2) and SLC7A1. Moreover, it has recently been documented that MYC can inhibit the microRNAs that target GLS1—microRNA-23A and microRNA-23B [77]. Thus in this capacity, MYC contributes to the conversion of glutamine to glutamate by indirectly stimulating the expression of GLS1.

RAS/MAPK

Oncogenic RAS mutations occur at high frequencies in human cancers and can drive the metabolic phenotype of cancer cells from OXPHOS toward aerobic glycolysis [121]. Ras can activate the PI3K/AKT/mTOR pathway and in this capacity augments glycolytic proteins to promote mitochondrial dysfunction and drive glycolysis in HEK293 cells [121]. Furthermore, mutated RAS has been reported to promote glucose uptake and flux and enhance biosynthesis pathways in pancreatic ductal adenocarcinoma (PDAC) [21]. Yin H *et al.* demonstrated in an inducible mutant KRAS mouse model of PDAC that KRAS was involved in driving the expression of genes in

several biosynthesis pathways, including steroid and pyrimidine biosynthesis that promote the pentose phosphate pathway [21]. KRAS also appeared to regulate glycolytic flux both at the gene expression and protein level but regulating GLUT1, HEK, and LDH [21]. Additional reports have implicated KRAS in aberrant glutamine metabolism. The conversion of glutamate to α-KG is canonically mediated by GDH, yet Son *et al*. observed that oncogenic KRAS rendered PDAC cells dependent on GOT1, the transaminase that converts glutamate to α-KG [22]. KRAS directed the process of reducing GDH gene expression and upregulating GOT1 expression, such that GOT1 became the dominant pathway. Interestingly, when GOT1 was dominant, PDAC cells obtained a higher antioxidant potential [22], suggesting that mutated RAS can also regulate redox homeostasis in tumors.

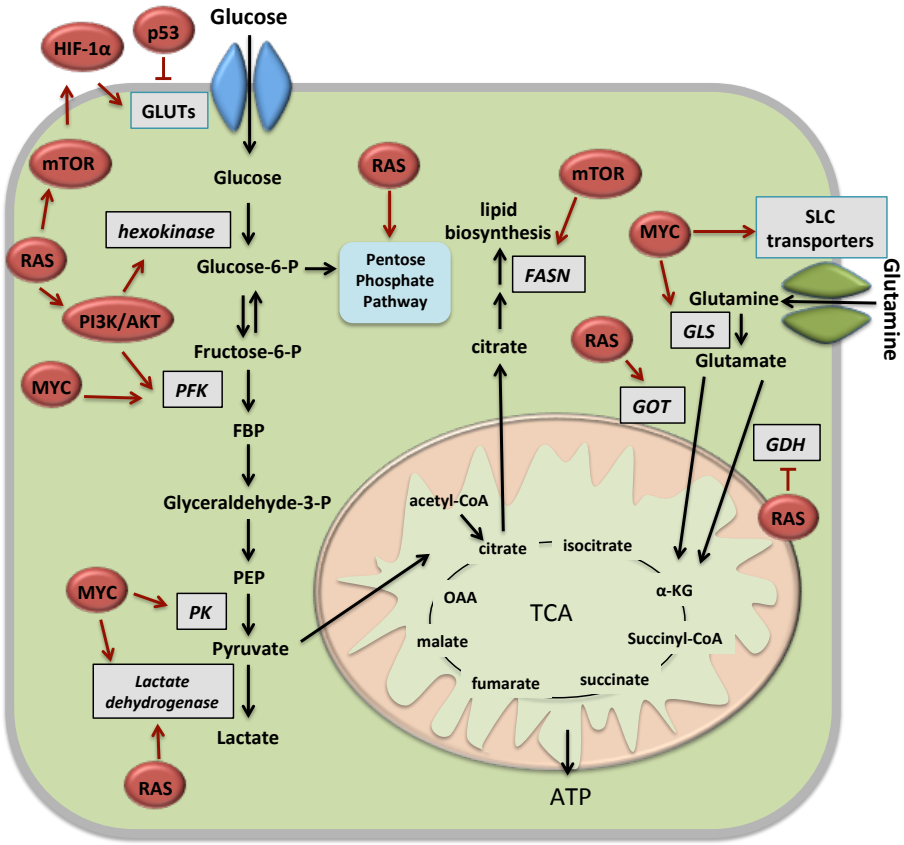

Figure 1.5 Oncogenes regulate metabolic reprogramming. Simplified schematic diagram showing common modes of oncogene regulation of tumor metabolism, as discussed in the text.

EPH receptors and ephrin ligands

The EPH receptor family is the largest known family of receptor tyrosine kinases and is comprised of 15 distinct members, 14 of which are encoded in the human genome (excluding EPH member, EPHA9) [122, 123]. They are further divided into the A-subclass or B-subclass based on their extracellular sequence homology and their affinity of binding to their ligands—the ephrins (EPH family interacting proteins). Ephrins ligands are also divided into an A-subclass and B-subclass where their primary distinction is in their membrane association. For instance, ephrin-A ligands are tethered to the cell membrane by a glycosylphosphatidlinositol (GPI) anchor, and the B-subclass contains a transmembrane domain followed by a short cytoplasmic region. Thus the A-subclass of EPH receptors typically promiscuously bind six ephrin-A ligands and the B-class receptors promiscuously bind three ephrin-B ligands (Table 1.2).

	EPH receptors	Ephrin ligands
A class	EPHA1	Ephrin-A1
	EPHA2	Ephrin-A2
	EPHA3	Ephrin-A3
	EPHA4	Ephrin-A4
	EPHA5	Ephrin-A5
	EPHA6	Ephrin-A6
	EPHA7	
	EPHA8	
	EPHA10	
B class	EPHB1	Ephrin-B1
	EPHB2	Ephrin-B2
	EPHB3	Ephrin-B3
	EPHB4	
	EPHB5	

Table 1.2 EPH receptor and ephrin ligand classification.

EPH receptors consist of an extracellular and intracellular portion. The extracellular region contains a highly conserved N-terminal ligand binding domain, a cysteine-rich region (including an epidermal growth factor-like motif), and two fibronectin type-III repeats. A transmembrane region connects to the intracellular portion which is composed of a tyrosine kinase domain, a sterile-α-motif (SAM) domain, and a PSD95/Dlg/ZO1 (PDZ)-binding motif [124] (Figure 1.6). Structural and crystal analyses of EPH-ephrin interactions have developed our understanding of EPH/ephrin complex assembly and signaling events [125].

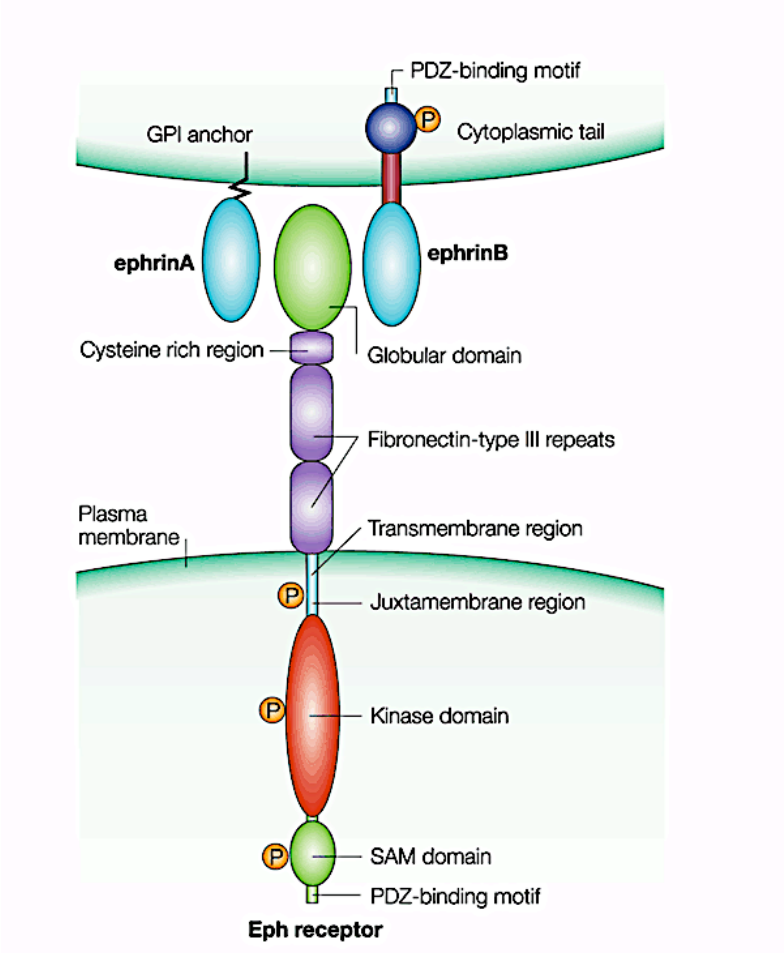

Figure 1.6 EPH receptor and ephrin ligand structure. Schematic diagram of EPH receptors and ephrin ligands. The top of the figure shows an ephrin expressing cell and the bottom half of the figure shows an EPH RTK expressing cell (Adapted from [126]).

Classically, ephrin binding with EPH receptors on juxtaposed cells occurs when the hydrophobic loop of ephrins is inserted in a newly arranged cleft on the N-terminal ephrin-binding domain of an EPH receptor [125]. This binding initiates the autophosphorylation of tyrosine residues on neighboring EPH receptors and confers oligomerization [127, 128]. Additionally, the binding of ephrin induces further conformational change in the cytoplasmic portion of the EPH receptor, which is facilitated by the phosphorylation of two highly conserved tyrosine residues in the juxtamembrane domain. This in turn exposes the kinase domain and established docking sites for signaling effector molecules with SRC homology 2 (SH2) domains [129]. This example of classic RTK forward signaling, however, is complicated by the ability of ephrins to engage in reverse signaling and the ability of EPH receptors to engage in crosstalk with other receptors [126].

Signaling Mechanisms

EPH receptor and ephrin ligand signaling has been implicated in a variety of normal developmental pathways and in several pathological diseases, including neoplastic formation and progression. Either through direct interaction or by indirect activation of proteins, EPH signaling has been reported to regulate cell morphology, motility, immunity, proliferation and synaptic plasticity [122]. As the field of EPH receptor signaling continues to expand, additional signaling pathways and cellular functions have been linked to EPH receptors, including, but not limited to apoptosis, neovascularization, and tumorigenesis [130-133]. Since EPH receptors can interact with such a wide spectrum of signaling molecules such as FAK, GRB2, p85, SHP2, SRC, VAV GEFs, EGFR, and HER2, it is no surprise their function has such broad functional implications [134-138]. Yet, EPH receptor and ephrin ligands display distinct signaling mechanisms that challenge the traditional signaling patterns of RTKs. In addition to engaging in bi-directional signaling, the receptors can also signal despite ligand activation [128].

Forward signaling vs. reverse signaling

One unique characteristic of EPH-ephrin complexes is their ability to transduce bidirectional signals through both the EPH receptor, referred to as 'forward' signaling, and through the ephrin ligand, referred to as 'reverse' signaling [123, 128]. The forward signaling mechanism occurs in the traditional manner of RTK signaling, in that ligand binding induces phosphorylation of tyrosine residues in the kinase domain of EPH receptors and sequential activation of effector signaling molecules. Some of the most notable signaling pathways regulated by EPH-forward signaling include PI3K/AKT/mTOR [130, 139], RAS/RAF/MAPK [138, 139], and RHO/RAC [137, 140-142] pathways. Although forward signaling can occur when membrane-bound ephrins bind to EPH receptors on adjacent cells, several studies have also demonstrated that ephrins can be cleaved and these soluble ephrins are also functionally active. Evidence exists that both ephrin classes are susceptible to protease cleavage, primarily by ADAMs (A Disintegrin And Metalloproteases) and matrix metalloproteases (MMPs), and this cleavage can play a major regulatory role in EPH-ephrin complex signaling [143].

The mechanism of reverse signaling or ligand-mediated signaling is highly dependent on the ephrin class. The A-subclass of ephrins is tethered by a GPI anchor and lacks the transmembrane region and cytoplasmic tail that is common to the B-subclass. The cytoplasmic region of B class ephrins serves as a key signaling mechanism. Engagement with EPHB receptors causes ephrin-B ligands to undergo tyrosine phosphorylation on their C-terminal tail [144] that is mediated by interactions with SRC family kinases [145], and by a variety of other RTKs [146]. Studies also demonstrate that ephrin-B ligands can initiate reverse signaling through PDZ-domain-mediated associations. For instance, the GTPase-activating protein, PDZ-RGS3, directly binds to the PDZ-binding motif on B-subclass ligands [147]. Ephrin-A ligands also engage in reverse signaling, however, due to the lack of a cytoplasmic region, the mechanisms surrounding this function remain obscure. It is thought that

upon engagement with EPHA receptors, ephrin-A ligands localize to distinct plasma membrane microdomains and mediate signal transduction through acquisition of signaling molecules, as this has been reported in other GPI-anchored proteins that have signaling responses [148]. Additional studies have further suggested that ephrin-A ligands transduce signaling through these microdomains in a manner that is dependent on FYN tyrosine kinase, and this signaling is functionally relevant in mediating cellular adhesion [149].

Ligand-dependent vs. ligand-independent signaling

EPH receptor signaling offers another layer of complexity in its ability to transduce signaling in both a ligand-dependent and ligand-independent manner. Ligand-dependent signaling is associated with tyrosine phosphorylation, and rapid internalization and degradation of EPH receptors [150]. Ligand-activated EPH RTKs have been linked with inhibition of EPH-related signaling pathways including integrins [135], RAS/MAPK [151], RHO/RAC [136] and PI3K/AKT/mTOR [152] pathways. Conversely, ligand-dependent signaling can also activate the ABL/CRK pathway [153]. Particularly in the context of cancer, ephrin-induced EPH activation is considered anti-mitogenic, as several of these pathways can regulate proliferation and motility.

EPH receptors also signal in a ligand-independent manner by engaging in crosstalk with other cellular proteins—a characteristic that extends to both classes. For instance, EPHA receptors are reported to interact with EGFR, HER2, and FGF receptors and EPHB receptos are associated with CXCR4 receptors. Individual EPH members and the proteins they crosstalk with are highlighted in TABLE 1.3.

The emerging concept that ligands can serve as a molecular switch to modulate EPH signaling outcomes is supported by recent reports that demonstrated the opposing signaling properties of EPH receptors. For example, EPHA2 has been shown to

EPH receptor	Crosstalk receptor	Signaling outcome	Reference
EPHA	CXCR4	CDC42 inhibition	[154]
EPHA	Integrins	Rac1 inhibition	[155]
EPHA2	EGFR and HER2	Cell motility regulation	[137, 156]
EPHA2	Claudin4	Claudin4 phosphorylation	[157]
EPHA2	Integrins	FAK inhibition	[135]
EPHA2	E-Cadherin	EPHA2 activation	[158]
EPHA4	Integrins	Integrin activation	[159]
EPHA4	FGFR	MAPK activation	[160]
EPHA4	EGFR	EGFR phosphorylation	[161]
EPHA8	Integrins	PI3K activation	[162]
EPHA4	NMDA receptor	NMDAR phosphorylation	[163]
EPHA8	E-Cadherin	E-Cadherin activation	[164]
EPHB2	Syndecan2	Syndecan2 phosphorylation	[165]
EPHB2	L1	L1 phosphorylation	[166]
EPHB2/B4	CXCR4 receptor	AKT activation	[167]
EPHB2/B3	RYK receptor	Tyrosine phosphorylation	[168]
EPHB6	T cell receptor	T cell activation	[169]

Table 1.3 Crosstalk between EPH RTKs and other receptors.

regulate integrin signaling both in a positive and negative manner [135, 170-172]. It was discovered that EPHA2, in the absence of ligand binding, could directly interact with FAK—a key regulator of integrin signaling—that would then promote integrin signaling [135]. Yet, in the presence of ephrin-A1, the preferential ligand for EPHA2, the phosphatase SHP2 is recruited to the EPHA2-FAK-integrin complex, where FAK is subsequently dephosphorylated and inactivated [135]. An additional example involves the interaction between EPHA2 and AKT. Ligand stimulated EPHA2 inhibits AKT phosphorylation as a downstream signaling effector, yet in the absence of ephrin-A1, the regulatory loop of AKT can directly phosphorylate EPHA2 at site S897 in turn regulating the receptor's activity [152]. The basis for the regulation of this ligand dependent "switch" in signaling remains elusive and is most likely multifold.

Current evidence suggests a variety of factors, such as receptor composition, concentration and clustering abilities may all contribute the diverse signaling pathways.

EPH receptors as tumor promoters or tumor suppressors

Genome-wide expression analyses have revealed that EPH RTKs are overexpressed in several malignant tissue types as compared to adjacent normal tissue [133]. "A" class EPH RTKs (EPHA2, EPHA4, and EPHA7) and B class RTKs (EPHB4 and EPHB6) have been demonstrated to negatively correlate with survival in breast cancer patients [173] (FIGURE 1.7). Though several EPH receptors have been implicated in cancer, EPHA2 has emerged as a focus of study as its overexpression has been linked to poor prognosis in a wide spectrum of human cancers including breast [173], lung [174, 175], pancreatic [176], ovarian [177] and esophageal [178]. The tumorigenic potential of EPHA2 has further been demonstrated *in vitro* by the malignant transformation of the human mammary epithelial cell line, MCF-10A, by EPHA2 overexpression [179]. To further test the effects of EPHA2 overexpression on tumor potential *in vivo*, Lu *et al.* stably transfected EPHA2 into a poorly invasive ovarian cancer cell line and observed that the overexpression of EPHA2 enhanced tumor growth and metastatic potential [180]. EPH RTK overexpression not only enhances tumor activity, but may also be a major mechanism of conferring drug resistance in tumors. Several studies have demonstrated that EPHA2 becomes overexpressed in drug resistant cells as observed in trastuzumab resistant breast cancer cells [181], tamoxifen insensitive breast cancer cells [182] vemurafenib resistant melanoma cells [183] and erlotinib resistant lung cancer cells [184].

The role of EPH RTKs as a tumor promoter is further evidenced by studies that block the function of EPH RTKs using *in vitro* and *in vivo* techniques to demonstrate a decrease in tumor activity. In addition to the substantial amount of work that has used RNAi-mediated silencing of EPH RTKs to impair tumor growth [137, 184-187],

animal models have significantly contributed to our understanding of EPH RTKs in growth regulation. For instance, genetic deletion of EPHA2 in mice that express the oncogenic promoters, MMTV-Neu or $KRAS^{G12D}$ decreased tumor burden and progression compared to mice with functional EPHA2 [130, 137]. In contrast, EPHB4 overexpressing mice when crossed with mice that express MMTV-Neu had enhanced tumor development and progression [187].

Though there is a clear role for EPH RTKs in tumorigenesis, their functions are multifold and extend beyond their intrinsic roles in tumor cells. EPH RTK

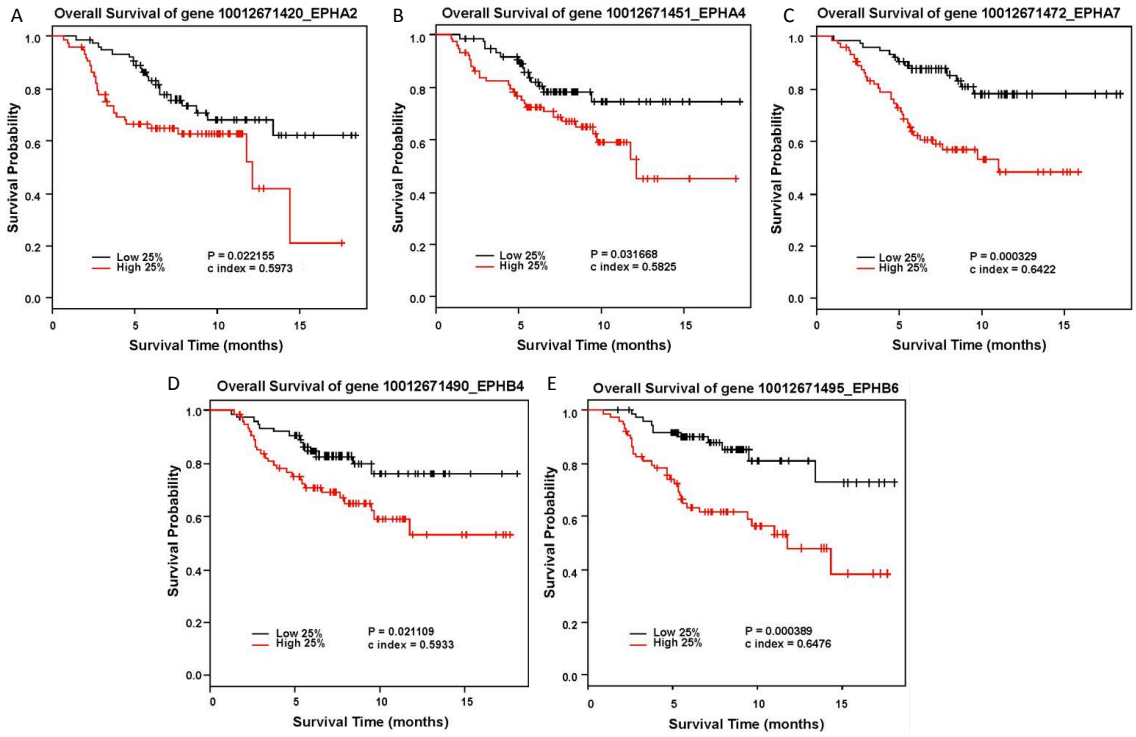

Figure 1.7 Expression of EPHA2, EPHA4, EPHA7, EPHB4, and EPHB6 negatively correlates with overall survival in human breast cancer. Kaplan-Meier analyses of the van der Vijver dataset, of 295 human breast tumors and associated clinical data. The impact of elevated *EPHhA2* (A), *EPHhA4* (B), *EPHA7* (C), *EPHB4* (D), and *EPHB6* (E) expression on overall survival (Adapted from [173]).

overexpression can also enhance tumor angiogenesis to promote tumor growth and dissemination [188, 189]. Tumor cells require a blood supply to gain access to oxygen and vital nutrients for sustained proliferation and growth [188]. To obtain this blood supply, tumor cells secrete stimulatory angiogenic factors, such as vascular endothelial growth factor (VEGF) to drive vascular remodeling and growth [190]. Indeed, some EPH receptors and ephrin ligands play a critical role in this vessel recruitment, and inhibition of EPHA2 [191] and ephrinB2 [192] have been demonstrated to reduce tumor vessel density and tumor volume.

A fundamental factor that contributes to EPH RTKs being able to function as tumor promoters exists in their ability to engage in ligand-independent signaling. As discussed above, ligand engagement can induce EPH tyrosine phosphorylation and degradation in some tissue to inhibit mitogenic pathways [150]. Thus the ability of EPH receptors to function as tumor promoters or tumor suppressors may highly rely on the presence of ephrin ligands, their ability to bind their receptor, and the downstream pathway affected by its tyrosine phosphorylation, at least in some EPH RTK members. EPHA2 and EPHB4 have both been reported as overexpressed in breast cancer and this overexpression is often coupled with low expression levels or impaired binding to ephrin-A1 and ephrin-B2, their preferential ligands, respectfully. This is evidenced by the mutually exclusive IHC staining of EPHA2 or ephrin-A1 in human breast cancer samples [173][Chapter 2], and decreased levels of tyrosine phosphorylation of EPHB2 in breast cancer cell lines despite elevated expression [153]. Previous studies demonstrated that breast cancer cells overexpressing EPHB4 displayed decreased expression of ephrinB4 and impaired EPHB4 tyrosine phosphorylation levels, yet the delivery of soluble ephrinB2-f/c activated EPHB4 tyrosine phosphorylation and the ABL-CRK pathway attenuated tumor growth in a xenograft model [153]. Thus in this capacity, EPHB4 when activated by its ligand, ephrin-B2, functioned as a tumor suppressor. EPHA2 also exhibits tumor-suppressing capabilities when stimulated by ephrin-A1 ligand at least in breast

cancer cells [Chapter 2]. However, not all cancers exhibit differential expression of EPH RTKs and ephrin ligands. For instance, EPHA2 and ephrin-A1 were co-expressed in ovarian cancer and the overexpression of both proteins correlated with poor prognosis [193]. A plethora of evidence exists that supports pro-tumor and antitumor functions of EPH RTKs and their ligands. Together, it can be concluded that individual EPH RTK members can have diverse functions, EPH/ephrin signaling may be tissue specific, outcomes may depend on molecular makeup of the individual cancer, and whether cell adhesions are impaired.

Thesis Project

Breast cancer continues to be a major health concern for women worldwide. Early diagnoses and the use of targeted therapies have aided in reduced mortality, however, approximately 40,000 deaths per year still occur in the United States. Thus is it necessary to investigate the mechanisms that promote breast cancer development, maintenance and metastatic spread as means to identify new therapeutic targets and improve patient outcome. The EPH family of receptor tyrosine kinases has long been implicated in cancer with the EPHA2 receptor correlating with poor prognosis in many tumor types including breast. Despite elevated EPHA2 levels in breast cancer samples, the expression of its preferential ligand, ephrin-A1, is often lost or reduced. In the absence of ephrin-A1, EPHA2 can engage in ligand-independent signaling and activate several oncogenic pathways to augment breast cancer growth, thus the loss of eprin-A1 may give these tumors a growth benefit. Furthermore, the dysregulation of cell metabolism also contributes to malignant growth and progression in breast cancer. Interestingly, several downstream effectors of EPHA2 have been implicated in the regulation of tumor cell metabolism, yet whether EPHA2 and ephrin-A1 could modulate tumor metabolism remained unexplored. This dissertation set out to further investigate the EPH/ephrin signaling paradox and dissect the mechanisms in which EPHA2 and

ephrin-A1 regulate breast cancer growth and to determine whether aberrant tumor metabolism is a mode of EPHA2/ephrin-A1-regulated growth. We specifically performed this this study in a HER2-positive breast cancer, since it was already established that EPHA2 could regulate growth in this model. We generated an ephrin-A1 knockout mouse that also expressed an activated form of the Neu/HER2 oncogene. Not only did this model recapitulate EPHA2 and ephrin-A1 expression patterns in human tissue samples (low ephrin-A1), but also enhanced tumor growth compared to mice expressing functional ephrin-A1. This demonstrated that the presence of ephrin-A1 combated tumorigenesis in these mice, potentially as a molecular switch of EPHA2, in that ephrin-A1 may cause EPHA2 to function as a tumor suppressor. We further integrated RNAi-mediated silencing techniques, data mining of microarray datasets, global metabolic analyses of mammary tumors, pharmacologic treatments, and staining of breast cancer patient tissue to systematically investigate the function of EPHA2 and ephrin-A1 in breast cancer and tumor metabolism. This thesis work generated several significant and novel findings. We were the first to use a genetic mouse model to demonstrate that the deletion of membrane-bound ephrin-A1 enhanced tumorigenesis in Neu/HER2 expressing mice. We further demonstrated that loss of ephrin-A1 enhanced EPHA2 protein expression as a mechanism to drive tumor cell growth, and that either tyrosine phosphorylation of EPHA2 or phosphorylation of serine 897 could promote this growth in breast cancer cells. We also revealed the first evidence linking EPHA2/ephrinA1 signaling to tumor metabolism as evidenced by augmented glutaminolysis in ephrin-A1 knockout tumors compared to wild type tumors. Furthermore, we discovered that this elevated glutaminolysis occurred as a result of increased GLS activity and inhibition of GLS reduced tumor growth *in vivo* despite overexpression of EPHA2 or inhibited ephrin-A1. We also showed that EPHA2/ephrin-A1 signaling regulated lipogenesis and this enhanced lipid content promoted cell growth. Mechanistically, we determined that EPHA2/ephrin-A1 increased RHO-GTPase activity to mediate this enhanced tumor metabolism. Finally,

we demonstrated that low ephrin-A1 levels correlated with poor outcome in breast cancer patients, thus ephrin-A1 may serve as a prognostic marker in some types of breast cancer. These findings invite exciting questions about the role of EPHA2/ephrinA1 signaling in other breast cancer subtypes and malignancies that display elevated glutaminolysis or EPHA2 expression.

CHAPTER II

THE EPHRIN-A1/EPHA2 SIGNALING AXIS REGULATES GLUTAMINE METABOLISM IN HER2-POSITIVE BREAST CANCER.

The work presented in this chapter is currently accepted for publication with the same title in Cancer Research, 2016.

Abstract

Dysregulation of receptor tyrosine kinases (RTKs) contributes to cellular transformation and cancer progression by disrupting key metabolic signaling pathways. The EPHA2 RTK is overexpressed in aggressive forms of breast cancer, including the HER2+ subtype, and correlates with poor prognosis. However, the role of EPHA2 in tumor metabolism remains unexplored. In this study, we used in vivo and in vitro models of HER2-overexpressing breast cancer to investigate the mechanisms by which EPHA2 ligand-independent signaling promotes tumorigenesis in the absence of its prototypic ligand, ephrin-A1. We demonstrate ephrin-A1 loss leads to upregulated glutamine metabolism and lipid accumulation that enhanced tumor growth. Global metabolic profiling of ephrin-A1-null, HER2-overexpressing mammary tumors revealed a significant increase in glutaminolysis, a critical metabolic pathway that generates intermediates for lipogenesis. Pharmacologic inhibition of glutaminase activity reduced tumor growth in both ephrin-A1-depleted and EPHA2-overexpressing tumor allografts in vivo. Mechanistically, we show that the enhanced proliferation and glutaminolysis in the absence of ephrin-A1 was attributed to increased RhoA-dependent glutaminase activity. EPHA2 depletion or pharmacologic inhibition of Rho, glutaminase, or fatty acid synthase abrogated the increased lipid content and proliferative effects of ephrin-A1 knockdown. Together,

these findings highlight a novel, unsuspected connection between the EPHA2/ephrin-A1 signaling axis and tumor metabolism, and suggest potential new therapeutic targets in cancer subtypes exhibiting glutamine dependency.

Introduction

Receptor tyrosine kinases (RTKs) are key regulators of signal transduction pathways that promote cell growth, survival, and motility during malignant progression of solid tumors. Recent advances in the analysis of tumor genomes revealed that EPHA2 RTK is frequently overexpressed in aggressive human breast cancers and correlates with poor patient survival and resistance to therapeutic agents [133, 137, 173, 181]. EPHA2 belongs to the Eph family of RTKs, which contain distinct regions for ligand binding, receptor clustering, and signaling. Though receptor clustering and activation occur upon Eph receptor binding to their ligands, known as ephrins, Eph receptors can also be activated by other cell-surface receptors, such as EGFR and ERBB2 [137, 156]. Thus, cumulative evidence in breast cancer supports two modes for EPHA2 signaling. In the ligand-dependent mode, EphA2 can engage in ligand-dependent forward signaling that suppresses tumor cell proliferation and invasiveness [152, 194]. In the second mode, EphA2 can signal in a ligand-independent manner that promotes tumor malignancy—a mechanism highly dependent upon phosphorylation of S897 (6). This model, however, has not been directly tested in a transgenic mammary tumor model, and the mechanism by which ephrin-A1 exerts its tumor-suppressive role has yet to be fully elucidated.

In this study, we demonstrate a novel role for ephrin-A1 as a regulator of mammary tumor growth and tumor metabolism. Gene deletion of *ephrin-A1* (*Efna1*) increased the growth of endogenous mammary tumors in a mouse model of breast cancer driven by activated ErbB2 (MMTV-*NeuT*). RNAi-mediated silencing of ephrin-A1 increased lipid accumulation and cell proliferation in both mouse and human breast

cancer models. Furthermore, metabolic profiling of tumors revealed increased glutaminolysis in ephrin-A1-null tumors. Mechanisticaly, we identified a signaling pathway involving EPHA2-RhoA-glutaminase that mediates ephrin-A1-dependent suppression of glutaminolysis and lipid accumulation in tumor cells. Collectively, these studies provide *in vivo* evidence for a tumor suppressive role of ephrin-A1 in breast cancer, and uncover a novel function of ephrin-A1 and EPHA2 in the regulation of tumor metabolism.

Materials and Methods

Animal models and *in vivo* studies

Animals were housed under pathogen-free conditions, and experiments were performed in accordance with AAALAC guidelines and with Vanderbilt University Institutional Animal Care and Use Committee approval. *Ephrin-A1*$^{-/-}$ mice were crossed with MMTV-*NeuT* mice. MMTV-*NeuT*-positive mice that were EphrinA1$^{+/+}$ or Ephrin-A1$^{-/-}$ were identified by PCR analysis of genomic DNA using the following primers: Ephrin-A1 forward primer (5'-CCCAACAAAAACAAACAGCCG-3') and two allele specific reverse primers, WT (5'-GAGGTGGAGGAAGGGAAAAAGAC-3') and KO (5'-TGGATG TGGAATGTGTGCGAGG-3'). The *NeuT* transgene was detected by PCR using the following primers: *NeuT* forward (5'-CATGGCCAGACAGTCTCCGT-3') and reverse (5'- TGAGCTGTTTTGAGGCTGACA-3').

Allograft experiments were performed in FVB mice. For ephrin-A1 gain of function experiments, MMTV-*Neu* cells were treated with Adeno-virus ephrin-A1 or with Adeno-virus LacZ as a control. For EPHA2 overexpression experiments, MMTV-*Neu* cells were treated with Adeno-virus EPHA2 or Adeno-virus GFP as a control. Ephrin-A1 knockdown experiments were carried out by generating stable *EFNA1* knockdown cells lines created by lentiviral transduction of a pGIPZ vector containing *EFNA1* specific mouse shRNA constructs (sh*EFNA1* mature antisense 3'-

GTAGTAGTAGCTGTGTCCT-5') (clone ID: V3LMM_511961). Ephrin-A1 knockdown was confirmed by qRT-PCR. Cells (1×10^6) were injected into the mammary glands of 6 to 8-week-old FVB mice. Tumors were measured at the described time points using digital calipers. Volumes were calculated using the following formula: volume = length × width^2 × 0.52. Where indicated, BPTES (10mg/kg) or vehicle (VEH) was delivered by intraperitoneal injection every other day starting on day 3. Statistical significance was determined by two-way ANOVA using GraphPad Prism software. Error bars represent standard error the mean (SEM) and a *P*-value <0.05 is considered significant.

Analysis of human breast cancer tissue microarray and expression profiling datasets

Immunohistochemical staining was performed on a human Metastatic Breast Cancer Tissue Array from Cybrdi (Rockville, MD; Cat# CS08-10-001) for ephrin-A1 and phosphorylated EPHA2 (pS897). The scoring system is as follows: 0-10% + tumor epithelium = 0; 10-25%+ tumor epithelium = 1; 25-50%+ tumor epithelium = 2; >50%+ tumor epithelium = 3. Samples were subdivided by scores of 0-1 as low/negative and scores of 2-3 as high. Statistical significance was determined using Chi Square Analysis. Survival analyses were performed as previously described [195]. *EPHA2* and *EFNA1* gene expression data was downloaded from GEO (Affymetrix HGU133A, accession# GPL96, and HGU133 Plus 2.0, accession# GPL570) and recurrence-free survival information was analyzed using the online software package, Kaplan–Meier Plotter (http://kmplot.com). The packages 'recurrence-free survival' and 'automatic cutoff' were used to calculate and plot Kaplan–Meier survival curves for 936-patients with lymph node-positive breast cancer. Tumors were ranked according to gene expression values of *EPHA2* and *EFNA1*, scored as high or low. Statistical significance was determined by logrank *P*-value and hazard ratios with 95% confidence intervals are displayed.

Cell culture

Human cell lines were purchased from the ATCC and maintained as described (3, 4). BT474 cell lines were authenticated by the ATCC cell authentication services utilizing short tandem repeat profiling. Other cell lines were used at low passage and were not authenticated. The mouse MMTV-*Neu* cell line was generated and provided by Rebecca Cook (Vanderbilt University). These cells were maintained in DMEM/F12 media supplemented with estrogen (5ng/ml), progesterone (5ng/ml), insulin (0.5µg/mL), EGF (5ng/ml), L-glutamine (2 mM), penicillin (100U/ml) and streptomycin (100U/ml) and 10% fetal bovine serum.

Generation of stable cell lines

Stable *EFNA1* knockdown cells lines were created by lentiviral transduction of a pLKO.1 vector containing *EFNA1* specific shRNA constructs (sh*EFNA1* no. 1 mature antisense 3'- TTTCTTTGGCTTAAAGGCAGG -5' or sh*EFNA1* no. 2 mature antisense 3'-TTTGAACTGTTCCAGAAGACG -5') and were maintained in 1 to 2 µg/ml of puromycin-containing complete media. Stable BT474 cells overexpressing GFP or *EFNA1* were created by lentiviral transduction. pCW-Cas9, a gift from Eric Lander and David Sabatini (Addgene plasmid # 50661), was linearized through restriction digestion by NheI and BamHI. Full-length GFP or human EFNA1 cDNA were subcloned into pCW using NEBuilder Assembly Kit (NEB). Cells were maintained in 1µg/mL doxycycline as indicated. Stable EPHA2 wild-type and mutant containing cell lines were generated by lentiviral transduction of the pCDH-CMV-MCS-EF1-Puro vector containing either full length human wild-type EPHA2, EPHA2^{S897A}, or EPHA2^{D739N}.

Antibodies and immunoblotting

The following antibodies were used: EPHA2 (D7, mouse monoclonal, 1:1000, Millipore), EPHA2 (XP rabbit monoclonal, 1:500, Cell Signaling), EPHA2 phospho-S897 (rabbit, 1:1000, Cell Application, Inc.), EPHA2 phospho-Y588 (mouse monoclonal, 1:2000, Cell Signaling), Ephrin-A1 (mouse monoclonal, 1:1,000), Rho

(mouse monoclonal 1:1000, Millipore), EPHA4 rabbit polyclonal, 1:250, Abnova), EPHB6 (rabbit polyclonal, 1:500, Abgent), α-actin (I-19, goat polyclonal, 1:1,000, Santa Cruz) and β-tubulin (mouse monoclonal, 1:2,000, Sigma-Aldrich). Secondary antibodies include: HRP-conjugated or IRDye®-conjugated anti-mouse or anti-rabbit antibodies. For immunoblotting, cells were washed with PBS and lysed on ice with RIPA buffer supplemented with a protease inhibitor cocktail (P8340) (Sigma-Aldrich) and phosphatase inhibitors (Roche Diagnostics). Lysates underwent SDS/PAGE (Invitrogen) followed by blotting with the indicated antibodies. Clarity Western ECL substrate (Bio-Rad), SuperSignal West Femto Maximum Sensitivity Substrate (Thermo Scientific), or LI-COR Odyssey were used for signal detection.

Metabolomic profiling in tumors

The mass spectrometer platforms, sample extraction and preparation, instrument settings and conditions, and data handling have been previously described in detail [196]. Briefly, the sample preparation process was carried out using the automated MicroLab STAR® system (Hamilton, Reno, NV). Recovery standards were added prior to the first step in the extraction process for QC purposes. Homogenized tumor samples were extracted using 5µL methanol per mg tissue. The resulting extract was divided into three fractions for untargeted metabolic profiling and randomized for analysis. Samples were characterized using three independent platforms: ultrahigh-performance liquid chromatography/tandem mass spectrometry (UHPLC-MS/MS) in the negative ion mode, UHPLC-MS/MS in the positive ion mode and gas chromatography-mass spectrometry (GC-MS) after siaylation. The reproducibility of the extraction protocol was assessed by the recovery of the xenobiotic compounds spiked in every sample prior to extraction. Extracts were analyzed using a platform consisting of a Waters ACQUITY UHPLC (Waters Corporation, Milford, MA, USA) and a Thermo-Finnigan LTQ mass spectrometer (Thermo Fisher Scientific Inc., Waltham, MA. USA). Compounds were identified by comparison to library entries of purified standards or recurrent unknown entities. Identification of known chemical entities

was based on comparison to metabolomic library entries of purified standards based on chromatographic properties and mass spectra. All statistical analyses were performed in R version 2.14.2. Welsh's two sample t-test was employed to identify statistically significant metabolite differences between tumor groups. For all analyses, missing values (if any) were imputed with the observed minimum for that particular compound (imputed values were added after block-normalization). The statistical analyses were performed on natural log-transformed data to reduce the effect of any potential outliers in the data.

Metabolite assays

Intracellular glutamate concentrations were determined using the enzymatic assay, Glutamate Assay Kit (Sigma), according to the manufacturer's protocol. MCF-10A-HER2 or MMTV-*Neu* cells (10^6) were cultured in glutamine-free DMEM/F12 base media for 24 hours. Cells were stimulated with 5% serum, EGF (5ng/mL), and 2mMol of glutamine. Briefly, after treatment, cells were washed with PBS and collected with the provided glutamate assay buffer. Lysates were centrifuged and the supernatants were further centrifuged in 10kDa ultrafiltration spin columns. The concentrated samples were plated in 96-well plates with the supplied glutamate enzyme mix. Absorbance was measured at 450nm. Concentrations were determined from the standard curve. Statistical significance was determined using ANOVA analysis on GraphPad Prism software; a *P*-value <0.05 is considered significant.

BrdU proliferation assay

BrdU incorporation was determined using a BrdU cell proliferation colorimetric assay kit (Cell Signaling) according to the manufacturer's protocol. Cells ($5x10^3$) were plated in 96-well tissue culture plates with serum/EGF-free media and were treated with CT04 Rho inhibitor (1ug/mL), 968 (10μM), BPTES (10μM), or Orlistat (20 μM) for 18 hours where indicated. Cells were then stimulated with a 5% serum, EGF

(5ng/ML), and BrdU solution for 2 hours (MCF-10A-HER2 and MMTV-Neu cells) or 5% serum and BrdU solution for 1 hour (BT474 cells). Briefly, media was removed and cells were fixed with the provided fixing/denaturing solution. Cells were incubated with the detection antibody followed by the HRP-conjugated secondary antibody solution. Colorimetric reaction was visualized upon addition of the TMB substrate and absorbance was measured at 450nm. BrdU incorporation is expressed as absorbance (nm) or are normalized to the control and are represented as percent change. Statistical significance was determined using unpaired Student's t-test or one way ANOVA, as indicated. Error bars represent SEM and a *P*-value<0.05 is considered significant.

Three-dimensional spheroid cultures

Eight-well chamber slides were coated with Matrigel™ (BD Biosciences). Cells ($5x10^3$) were cultured in media with 2% serum, 5ng/ml EGF and 2.5% Matrigel™. Inducible stable cells were treated with PBS or 1 µg/mL Doxycycline (Sigma-Aldrich) for three days prior to seeding and were maintained in drug for the duration of the assay. On day 12, spheroids were imaged and Image J software was used to measure the surface area of spheroids (at least 3 fields/chamber; 3 biological replicates). All other spheroid assays were imaged after 8 days of culture. Surface area is expressed in arbitrary units and statistical significance was determined by unpaired student's t-test or one-way ANOVA, as indicated. Error bars represent SEM and a *P*-value <0.05 is considered significant.

Oil-red-O staining

Cells were plated in 24-well chamber tissue culture plates and were permitted to grow to confluence in full growth media, unless otherwise stated. Cells were treated with CT04 Rho inhibitor (1ug/mL) (Cytoskeleton, Inc.), 968 (10µM) or Orlistat (20 µM) for 24 hours, followed by washing with cold PBS and fixation with 10% formalin for at least 1 hour. Cells were subsequently washed with distilled water, incubated

with 60% isopropanol and dried under a fan. Cells were then incubated in Oil-Red-O working solution for 20 minutes. Working solution was made by diluting 6mL of a 10mM stock of Oil-Red-O (dissolved in isopropanol) with 4mL distilled water and subsequent filtration with a 0.2µm filter. Cells were then immediately washed with distilled water and images were acquired by microscopy. Phase contrast microscopy (Olympus 1X71, Olympus DP72 camera) was used to ensure equal cell confluence among images. Image J software was used to measure the area coverage of Oil-Red-O-stain (at least 3 fields/well). Stained area is expressed in arbitrary units and statistical significance was determined by unpaired student's t-test or ANOVA, as indicated. Error bars represent SEM and a *P*-value <0.05 is considered significant.

Immunohistochemistry and immunofluorescence

Tumors were harvested at the indicated time points, fixed in 10% buffered formalin (Fisher) and embedded in paraffin. Immunohistochemical or immunofluorescent staining for ephrin-A1, PCNA and Von Willebrand (vWF) was performed as described previously [197, 198]. A proliferative index was calculated as the number of PCNA+ nuclei relative to total nuclei. vWF protein area was quantified using Image J software. Statistical significance was determined by unpaired Student's t-test, and a P-value <0.05 is considered significant. Antibodies against Ephrin-A1, phospho-S897-EPHA2, PCNA (BD Biosciences), biotin goat anti-rabbit (BD Pharmingen), and anti-rabbit Cy3 (Jackson ImmunoResearch) were used for protein detection. In addition, retrievagen A (pH 6.0) (BD Pharmingen), streptavidin peroxidase reagents (BD Pharmingen), and the liquid 3,3'-diaminobenzidine tetrahydrochloride substrate kit (Zymed Laboratories) were used for antigen retrieval, and visualization of the protein, respectively. Cytoseal XYL was used to mount slides. Additionally, the antibody against vWF (Dako Cytomation) and the Alexa Fluor 488 secondary antibody (Invitrogen) were used for vWF detection within tumor sections. Prolong® Gold antifade reagent with DAPI (Molecular Probes) was used to mount slides. Images were taking on Olympus BX60 microscope with an Olympus DP72 camera.

RNAi studies

EFNA1 ON-TARGETplus Human SMARTpool siRNA (M-006369-01-005), *EFNA1* ON-TARGETplus Human siRNA #1 and #2 (J-006369-07 and J-006369-08), *GLS1* ON-TARGETplus Human SMARTpool siRNA (M-004548-01-0005), *GLS1* ON-TARGETplus Human siRNA #1 and #2 (J-004548-09 and J-004548-11), *GLS2* ON-TARGETplus Human SMARTpool siRNA (M-012500-00-0005), *GLS2* ON-TARGETplus Human siRNA #1 and # 2 (J-012500-09 and J-012500-09), *EPHA2* Silencer® siRNA (siEPHA2 #1 – AM51331; ID# 520) (Life Technologies/Ambion), *EPHA2* ON-Targetplus Human siRNA #2 (J-003116-09), *EPHA2* ON-Targetplus Human SMARTpool siRNA (L-003116-00-0005) and ON-TARGETplus Non-Targeting pool siRNA (D-001810-10-05) were purchased from Dharmacon/Thermo Scientific, unless otherwise noted, and were used at a concentration on of 12.5-25nM in combination with Lipofectamine RNAiMAX transfection reagent (Invitrogen). Experiments were carried out after 72 hours.

RT-PCR

Total RNA were extracted from cell lysates using RNeasy Mini Kit (Qiagen) according to the manufacture's protocol. cDNA was synthesized from 2µg of total RNA using qScript cDNA Synthesis SuperMix (Quanta BioSciences) as recommended by the manufacturer. Quantitative RT-PCR was carried out using the StepOnePlus RT-PCR system (Applied Biosystems). Reactions were run in triplicate in at least 2 independent biological experiments. Human GAPDH and mouse Actin (Applied Biosystems) were used as housekeeping genes accordingly.

Rho activity assay

Cells (2×10^6) were EGF-starved and serum-starved for 24 hours followed by 2.5 minutes of stimulation with 5% horse serum and EGF (0.5ng/mL). Cells were lysed on ice with RIPA buffer and incubated with Rhotekin-binding domain-GST beads (Millipore) as previously described [141].

Results

Ephrin-A1 inhibits mammary tumor growth in MMTV-*NeuT* transgenic mice and in human breast cancer cell lines.

Ephrin-A1-null mice are viable, fertile, and do not exhibit overt phenotypes in a pathogen-free animal facility [199]. Previous experimental data in breast cancer cell lines suggest a model in which the oncogenic role of EPHA2 is largely ligand-independent, whereas ephrin-A1, the prototypic ligand of EPHA2, transduces inhibitory signaling that blocks tumor cell proliferation and invasiveness [137, 152, 200]. To test this hypothesis *in vivo* in a clinically relevant transgenic mammary tumor model, we crossed *ephrin-A1*-deficient mice with MMTV-*NeuT* transgenic animals [201] to determine whether loss of ephrin-A1 enhanced breast cancer tumorigenesis and progression. MMTV-*NeuT*/*Efna1*$^{-/-}$ mice developed larger tumors compared to MMTV-*NeuT*/*Efna1*$^{+/+}$ littermates (Figure 2.1A). PCNA staining revealed that ephrin-A1 null tumors had an elevated proliferative index compared to wild-type tumors (Figure 2.1B). However, vWF staining, an endothelial cell marker, was not significantly different (Figure 2.2A), suggesting that tumor vasculature is not markedly affected by loss of ephrin-A1 in this model. These results suggest that Ephrin-A1 inhibits mammary tumor growth within its native environment, as genetic deletion of ephrin-A1 enhanced tumor growth in this aggressive breast cancer model.

To assess whether our data in this animal model is applicable to human disease, we tested whether loss of ephrin-A1 augmented growth in MCF-10A-HER2 cells, a human breast cell line overexpressing HER2. We used two independent shRNA sequences to stably knockdown ephrin-A1 in MCF-10A-HER2 cells and performed 3-

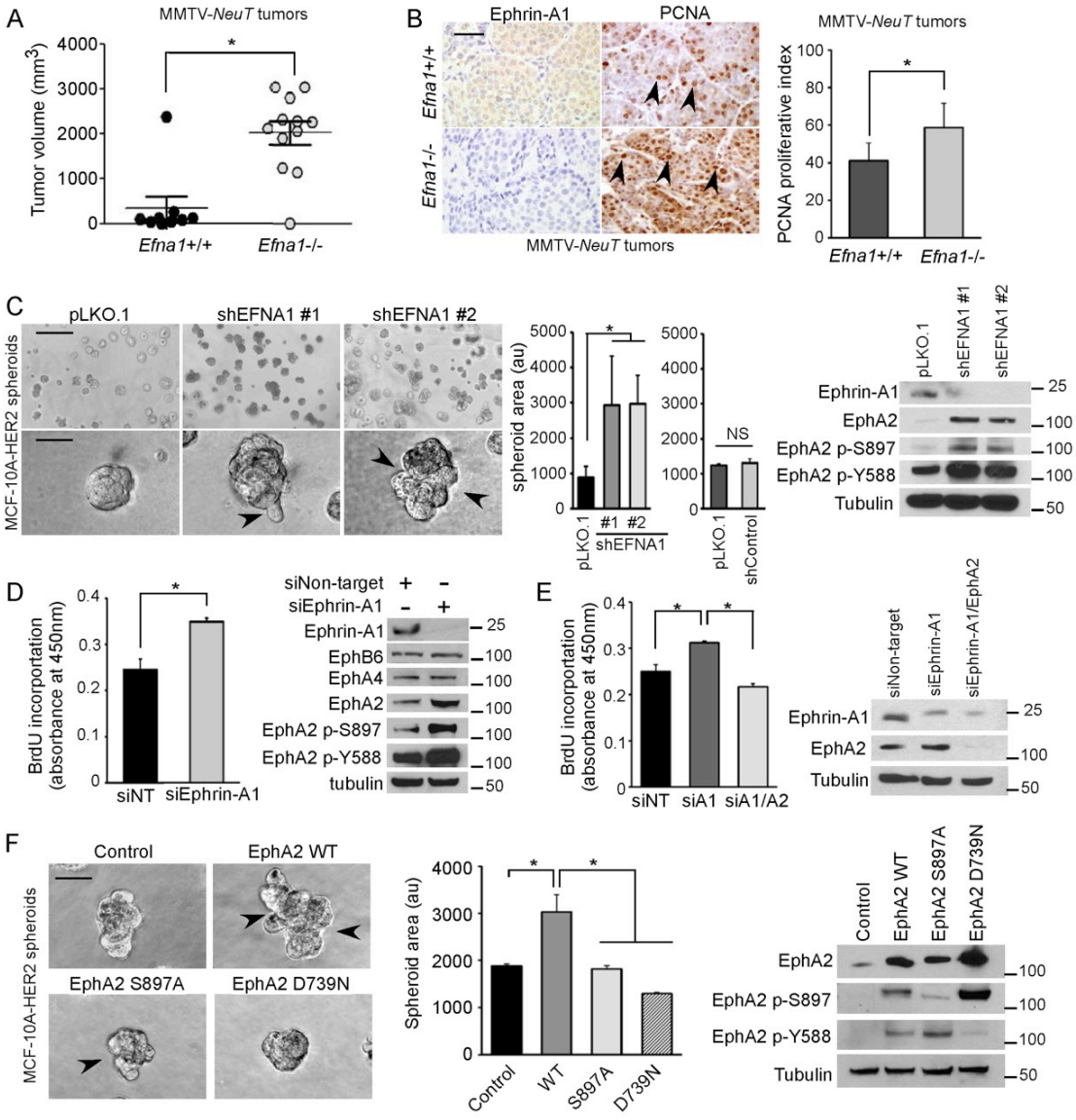

Figure 2.1 Loss of ephrin-A1 enhances breast cancer growth. (A) Tumor volume from 22-week old MMTV-*NeuT*/*Efna1*$^{+/+}$ and MMTV-*NeuT*/*Efna1*$^{-/-}$ mice. **P*<0.05, Student's t-test. **(B)** Immunohistochemistry of ephrin-A1 and PCNA in MMTV-*NeuT* tumors. Arrowhead indicates PCNA+ nuclei. **P*<0.05, Student's t-test. Scale bar 200µm. **(C)** 3D-spheroids expressing shRNAs targeting ephrin-A1 or pLKO.1 vector control at day 8. Average spheroid area is presented as arbitrary units (au) ± SEM. **P*<0.05, one-way ANOVA. Arrowheads indicate protrusions in the spheroids. Scale bars (top) 500µm; (bottom) 100µm. **(D)** BrdU incorporation assay in MCF-10A-HER2 cells transfected with control siNT or ephrin-A1 siRNA. Data expressed as mean ± SEM. **P*<0.05, one-way ANOVA. **(E)** BrdU incorporation assay in MCF-10A-HER2 cells transfected with control (siNT), siRNA targeting ephrin-A1 (siA1) or ephrin-A1 and EPHA2 (siA1/A2). Data expressed as mean ± SEM. **P*<0.05, one-way ANOVA. **(F)** 3D-spheroids expressing vector control, wild-type EPHA2, EPHA2^{S897A}, or EPHA2^{D739N} (kinase dead) at day 8. Average spheroid area is presented as arbitrary units (au)

± SEM. *P<0.05, one-way ANOVA, Scale bar 100μm. *In vitro* data are representative of 2-5 biological replicates.

dimensional (3D) spheroid growth assays. MCF-10A-HER2 cells treated with shEphrin-A1 developed significantly larger spheroids that displayed protrusive properties compared to control cells (Figure 2.1C). To directly evaluate proliferation, MCF-10A-HER2 cells were treated with siRNAs targeting ephrin-A1 or a non-targeting control and BrdU incorporation was measured. Knockdown of ephrin-A1 significantly enhanced proliferation (Figure 2.1D and Figure 2.2B), which is accompanied by an increase in EPHA2 protein expression and phosphorylation of EPHA2 at Y588 and S897, markers of kinase activity and ligand-independent signaling, respectively. However, there were no discernable changes in the expression of EPHA4 or EPHB6, in which high expression levels were shown to correlate with poor patient survival in human breast cancer (2) (Figure 2.1D).

To test whether ephrin-A1-induced growth suppression requires EPHA2, we silenced EPHA2 and ephrin-A1 simultaneously. Knockdown of EPHA2 in MCF-10A-HER2 cells inhibited the elevated cell proliferation in ephrin-A1-deficient cells (Figure 2.1E), suggesting that EPHA2 is the receptor for ephrin-A1 that links this ligand to tumor suppression in breast cancer. To investigate whether EPHA2 kinase activity or phosphorylation of S897 is required for ligand-independent signaling, we expressed wild-type EPHA2, EPHA2^{S897A}, or EPHA2^{D739N} (kinase dead) in MCF-10A-HER2 cells and evaluated spheroid growth. We found that both S897 phosphorylation and kinase activity are required for the EPHA2-dependent increase in cell growth (Figure 2.1F), suggesting that EPHA2 receptor forward signaling is important in this process.

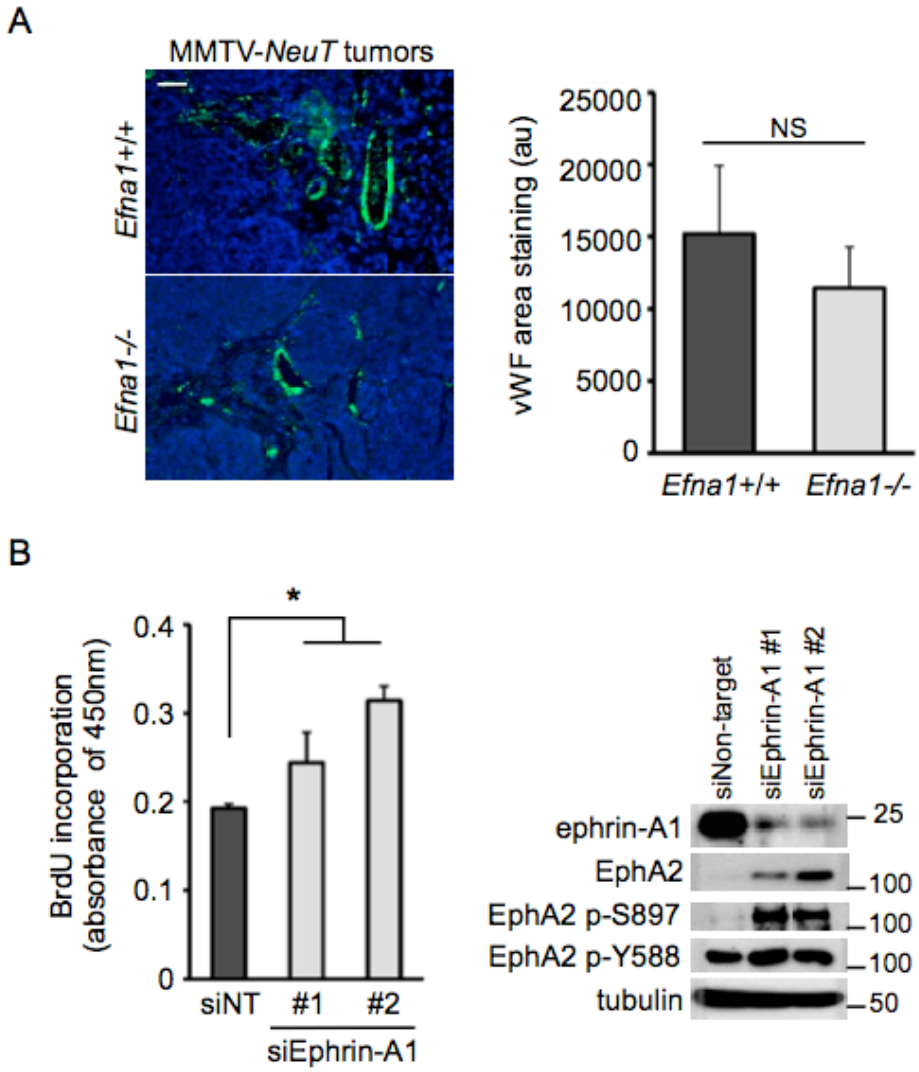

Figure 2.2 Vessel density from tumor sections and EPHA2 activity in ephrin-A1 knockdown MCF-10A-HER2 cells. (A) Immunofluorescence of vWF (green) in tumors from MMTV-*NeuT* mice. vWF area was determined using Image J software. Sections were counterstained with DAPI (blue) to visualize nuclei. Error bars represent SD. Scale bar 50µm. NS, not significant. **(B)** BrdU incorporation colorimetric assay in MCF-10A-HER2 cells transfected with non-targeting (siNT), or two independent ephrin-A1 targeted siRNAs (siEphrin-A1). Data are expressed as mean + SEM. *P<0.05, Student's t-test. Expression levels of ephrin-A1, EPHA2, p-S897 and p-Y588 EPHA2 were measured by western blot analysis.

To complement loss-of-function studies, we determined whether overexpression of ephrin-A1 could inhibit growth and proliferation of breast cancer cells *in vivo*. MMTV-*Neu* cells overexpressing ephrin-A1 or control LacZ protein were transplanted into mammary fat pads of recipient mice and tumor volume was measured. Overexpression of ephrin-A1 significantly reduced tumor volume relative to controls (Figure 2.3A). Analyses of PCNA expression in these tumor allografts revealed that tumor cell proliferation was significantly lower in MMTV-*Neu* tumors expressing ephrin-A1 compared with that of MMTV-*Neu* tumors expressing the control LacZ protein (Figure 2.3B). We next evaluated the effect of ephrin-A1 overexpression in the HER2-dependent human breast cancer cell line, BT474. Overexpression of ephrin-A1 by either an adenoviral delivery or a lentiviral doxycycline-inducible system reduced EPHA2 expression, spheroid size and BrdU incorporation compared to control cells expressing GFP (Figure 2.3, C-E). Collectively, our findings support the model in which ephrin-A1 acts as a molecular switch to modify EPHA2 receptor signaling output, such that loss of ephrin-A1 enhances tumor cell growth.

Low ephrin-A1 or high EPHA2 expression is associated with poor survival in lymph node positive breast cancer patients.

We previously reported that *EPHA2* overexpression is linked to poor prognosis in breast cancer patients [173, 181]. To investigate whether high EPHA2 expression correlates with ligand-independent signaling, we analyzed the level of phospho-S897 EPHA2, a marker for ligand-independent activation [152], and ephrin-A1 expression in adjacent sections of tumor samples in a human breast cancer tissue microarray (TMA). As shown in Figures 2.4A and 2.4B, 75% of pS897-EPHA2-positive samples were negative for ephrin-A1 in primary tumors, and 74% of pS897-EPHA2 positive lymph node metastases were negative for ephrin-A1 (n= 20 and 27 for primary and metastatic tumors, respectively; $p<0.05$), suggesting that high levels of ligand-independent EPHA2 signaling in human breast cancer are associated with low levels

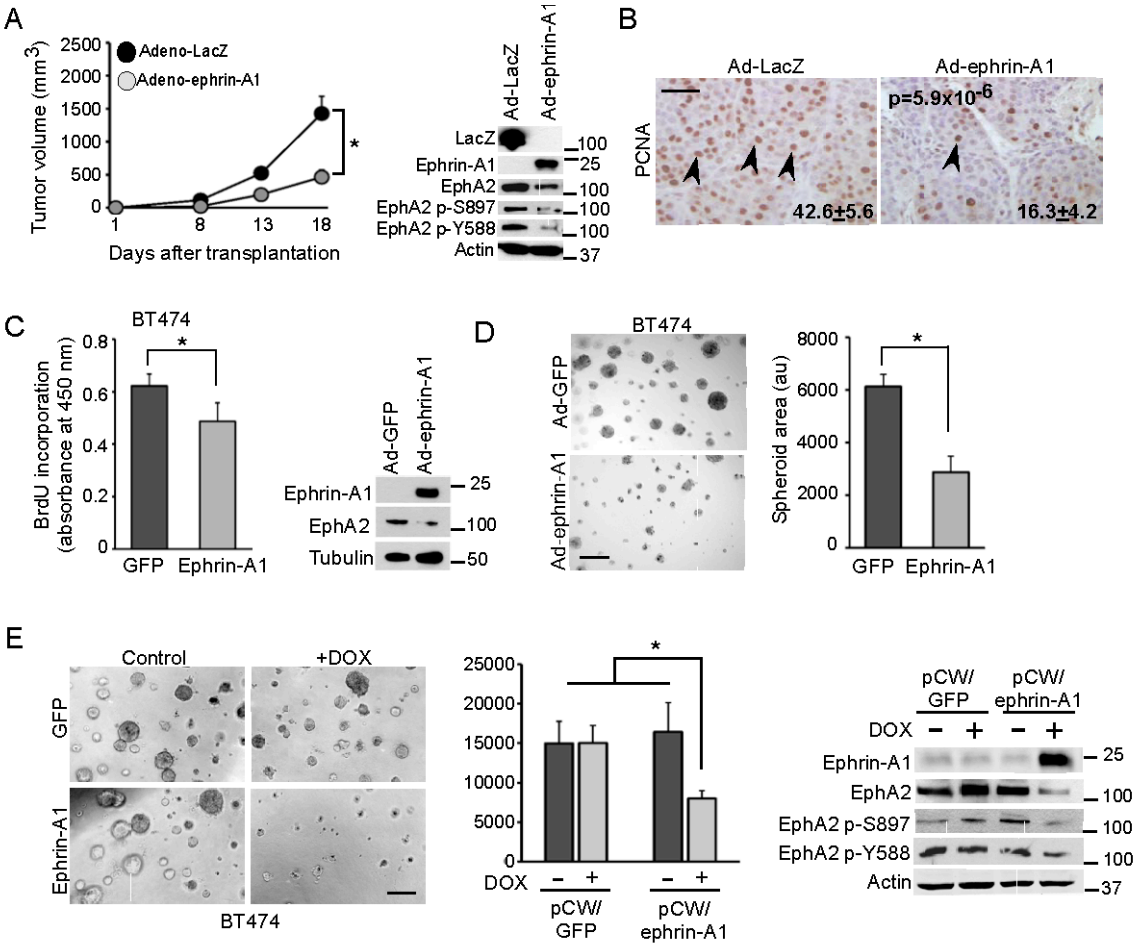

Figure 2.3 Overexpression of ephrin-A1 inhibits breast cancer growth. (A) MMTV-*Neu* cells (10^6) expressing LacZ or ephrin-A1 were injected into mammary fat pads of mice. Tumor volume was recorded over a time course. Data are presented as average tumor volume ± SEM; *n*=6 per group. **P* <0.05, two-way ANOVA repeated measures. **(B)** Immunohistochemistry of PCNA in tumor sections. Arrowhead indicates PCNA+ nuclei. **P*<0.05, Student's t-test. Scale bar 200µm. **(C)** BrdU incorporation in BT474 cells expressing GFP or ephrin-A1. Data expressed as mean ± SEM. **P*<0.05, t-test. **(D)** 3D-spheroids with BT474 cells expressing GFP control or ephrin-A1 at day 8. Average spheroid area is presented as arbitrary units (au) ± SEM. **P*<0.05, Student's t-test. Scale bar 500µm **(E)** 3D-spheroids with BT474 cells expressing inducible GFP or EFNA1 in the presence of PBS or 1 µg/mL doxycycline (DOX) at day 12. Average spheroid area is presented as arbitrary units (au) ± SEM. **P*<0.05, one-way ANOVA. Scale bar 500µm. *In vitro* experiments represent 2-4 biological replicates.

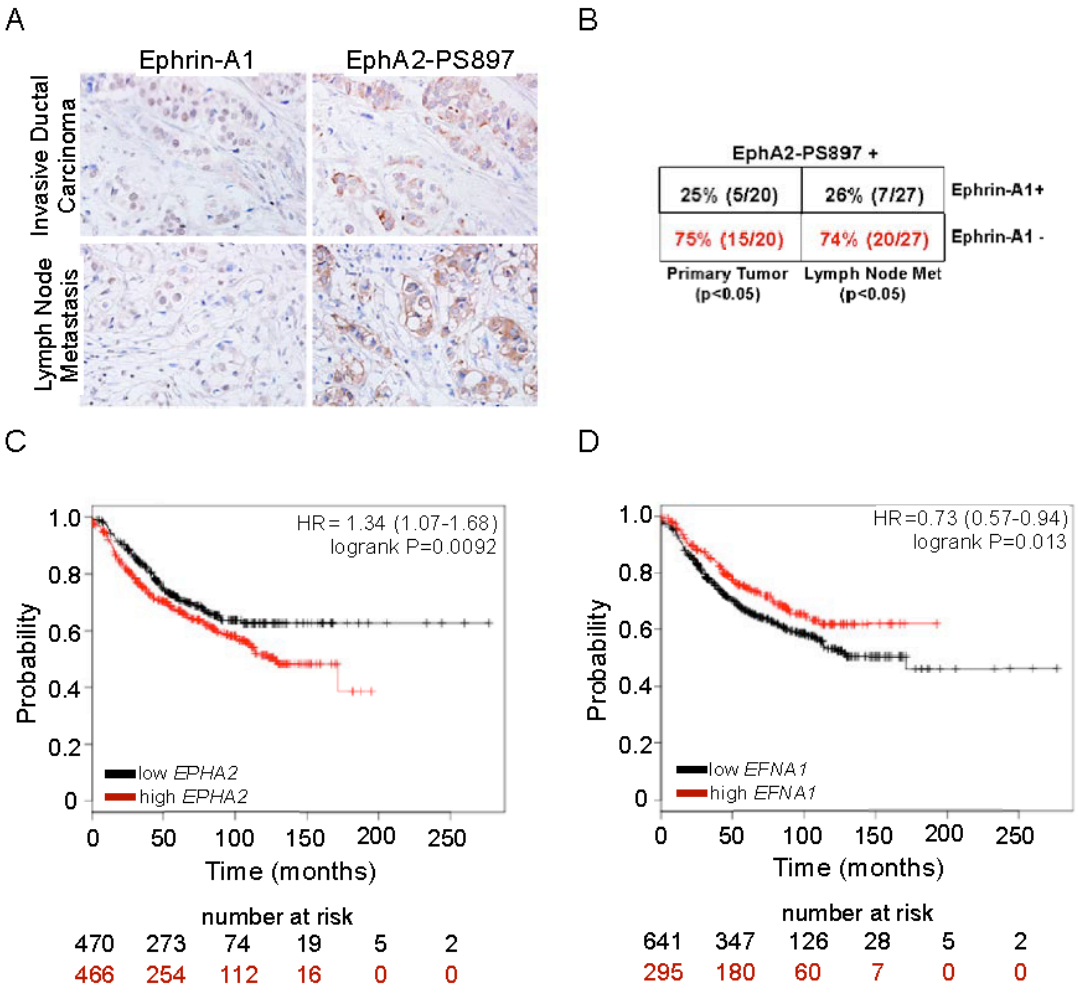

Figure 2.4 Low ephrin-A1 expression is linked to poor prognosis in lymph node positive breast cancer patients. (A) Immunohistochemistry of human breast cancer tissue microarrays for ephrin-A1 and EPHA2 phospho-S897 (pS897). **(B)** The percentage of tumors staining positive for EPHA2-phospho-S897 in ephrin-A1-positive and ephrin-A1 negative samples are summarized (*n*= 20 and *n*=27 for primary and metastatic tumors). **P*<0.05, Chi Square test. **(C,D)** Kaplan-Meier analysis from NCBI GEO datasets of recurrence-free survival for 936-patients with lymph node-positive breast cancers. Tumors were ranked according to gene expression values of *EPHA2* and *EFNA1* scored as high (red) or low (black). Hazard ratios with a 95% confidence interval are displayed and statistical significance (*P*<0.05) was determined by log rank test [195].

of ephrin-A1 expression. To investigate whether the expression level of *ephrin-A1* is associated with clinical outcomes, we mined datasets from the NCBI Gene Expression Omnibus [GEO; [195]; Figure 2.4, C and D]. We found no correlation between ephrin ligand expression and clinical outcome in overall breast cancer samples. However, high *EFNA1* expression was associated with increased probability of 20-year recurrence-free survival in lymph node-positive breast cancer patients (n=936, $p<0.05$), whereas high *EPHA2* expression is associated with decreased survival ($p<0.01$). Collectively, these data support a tumor-suppressive role for ephrin-A1 in metastatic malignant human breast cancer.

Ephrin-A1 regulates lipid accumulation in breast cancer cells

Reprogramming of energy metabolism is a hallmark of cancer that confers growth and survival advantages to tumor cells [202, 203]. We discovered that knockdown of ephrin-A1 leads to accumulation of vacuole-like structures in MCF10A-HER2 cells (Figure 2.5A, arrowhead). To investigate whether these vacuole-like structures represented lipid droplets, we stained cells with the lipid soluble dye, Oil-Red-O. As shown in Figure 2.5B, the Oil-Red-O positive area was significantly increased in ephrin-A1 knockdown cells compared to control cells. As fatty acid synthase (FASN) is a key enzyme for *de novo* fatty acid synthesis, we tested whether inhibition of FASN could rescue increased lipid deposits in ephrin-A1-deficient cells. Orlistat, an irreversible inhibitor of FASN [105, 204], suppressed lipid accumulation in ephrin-A1 knockdown cells (Figure 2.5C) and inhibited the proliferative phenotype observed in *ephrin-A1*-deficient MCF-10A-HER2 cells (Figure 2.5D).

Since EPHA2 is the primary receptor for ephrin-A1 (Figure 2.5E), we reasoned that overexpression of EPHA2 should produce a similar lipid accumulation phenotype as ephrin-A1 knockdown cells. Indeed, overexpression of wild-type EPHA2, but not

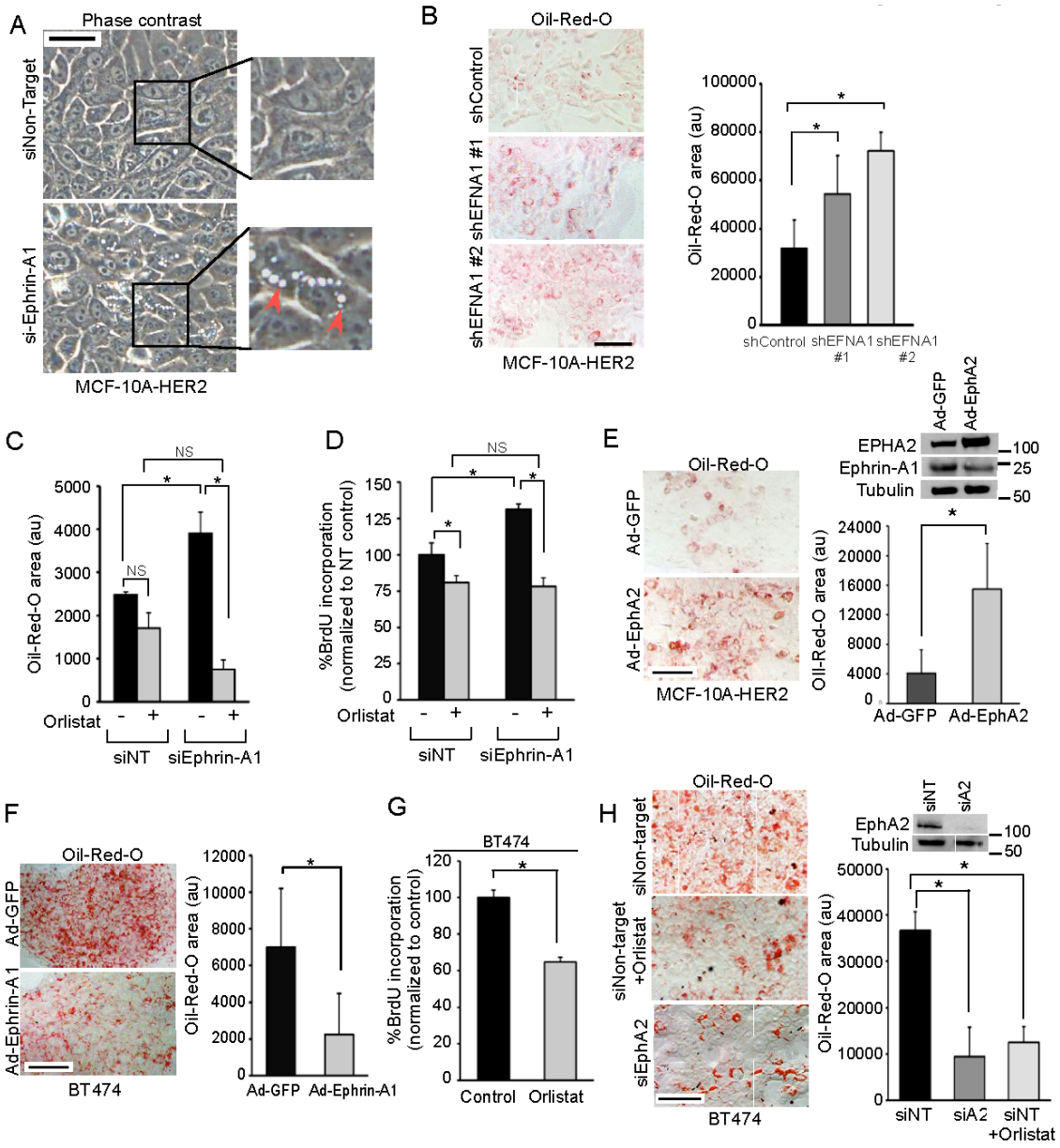

Figure 2.5 Ephrin-A1 regulates lipid accumulation in breast cancer cells. (A) Phase contrast microscopy images of MCF-10A-HER2 cells transfected with non-targeting or ephrin-A1 siRNAs. Scale bar 50µm. Arrows (red) show vacuole-like structures. **(B)** Oil-Red-O staining in control and ephrin-A1 shRNA knockdown cells. Data are presented as average Oil-Red-O area in arbitrary units (au). **P*<0.05, one-way ANOVA. Scale bar 100µm. **(C)** Oil-Red-O staining in siNon-Targeting (siNT) and siEphrin-A1 MCF-10A-HER2 cells treated with DMSO or Orlistat (20µM) for 24 hrs. **P*<0.05, one-way ANOVA. **(D)** BrdU incorporation in siNT and siEphrin-A1 MCF-10A-HER2 cells treated with DMSO or Orlistat (20µM) for 18 hrs. Data normalized to siNT control. **P*<0.05, one-way ANOVA. **(E)** Oil-Red-O staining in cells overexpressing EPHA2 or control GFP. **P*<0.05, Student's t-test. Scale bar 100µm. **(F)** Oil-Red-O staining in BT474 cells expressing GFP or ephrin-A1. **P*<0.05, Student's t-test. Scale bar 200µm. **(G)** BrdU incorporation in BT474 cells treated with Control (DMSO) or Orlistat

(20μM). Data normalized to the siNT control. *P<0.05 by Student's t-test. **(H)** Oil-red-O staining in BT474 cells treated with Control (DMSO) or Orlistat (20μM) for 24 hrs or transfected with non-targeting siRNA or EPHA2 siRNA. *P<0.05, one-way ANOVA. Scale bar 100μm. All experiments represent 2-5 biological replicates. Error bars represent SEM. NS, not significant.

EPHA2^{S897A} or EPHA2^{D739N} mutants, enhanced lipid content in MCF-10A-HER2 cells (Figure 2.5E, Figure 2.6A). In contrast, overexpression of ephrin-A1 significantly reduced lipid deposits in BT474 cells, which have high endogenous levels of lipids (Figure 2.5F). Orlistat treatment inhibited proliferation and lipid accumulation in BT474 cells, and EPHA2 silencing also reduced lipid content (Figure 2.5G and H, Figure 2.6B). Collectively, Orlistat-induced inhibition of lipid content and a reduction in tumor cell proliferation suggests a link between increased lipogenesis and tumor cell growth upon loss of ephrin-A1 or overexpression of EPHA2.

Ephrin-A1 regulates glutamine metabolism through modulation of glutaminase activity

To globally assess tumor metabolite profiles, tumors from MMTV-*NeuT*/*Efna1*$^{+/+}$ and MMTV-*NeuT*/*Efna1*$^{-/-}$ were analyzed by mass spectrometry. We observed no consistent pattern of metabolite profile differences related to glucose metabolism. However, there were marked increases in metabolites associated with glutamine metabolism in MMTV-*NeuT*/*Efna1*$^{-/-}$ tumors relative to wild-type control tumors (Figure 2.7A and B, Figure 2.8), suggesting that ephrin-A1 may regulate glutaminolysis.

A decrease in glutamine coupled with an increase in glutamate (Figure 2.7B) in ephrin-A1-null tumors suggests enhanced glutamine consumption by glutaminase (GLS), a key rate-limiting enzyme in glutaminolysis. To directly test whether ephrin-A1 regulates the activity of GLS, MMTV-*Neu* cells treated with shEphrin-A1 or

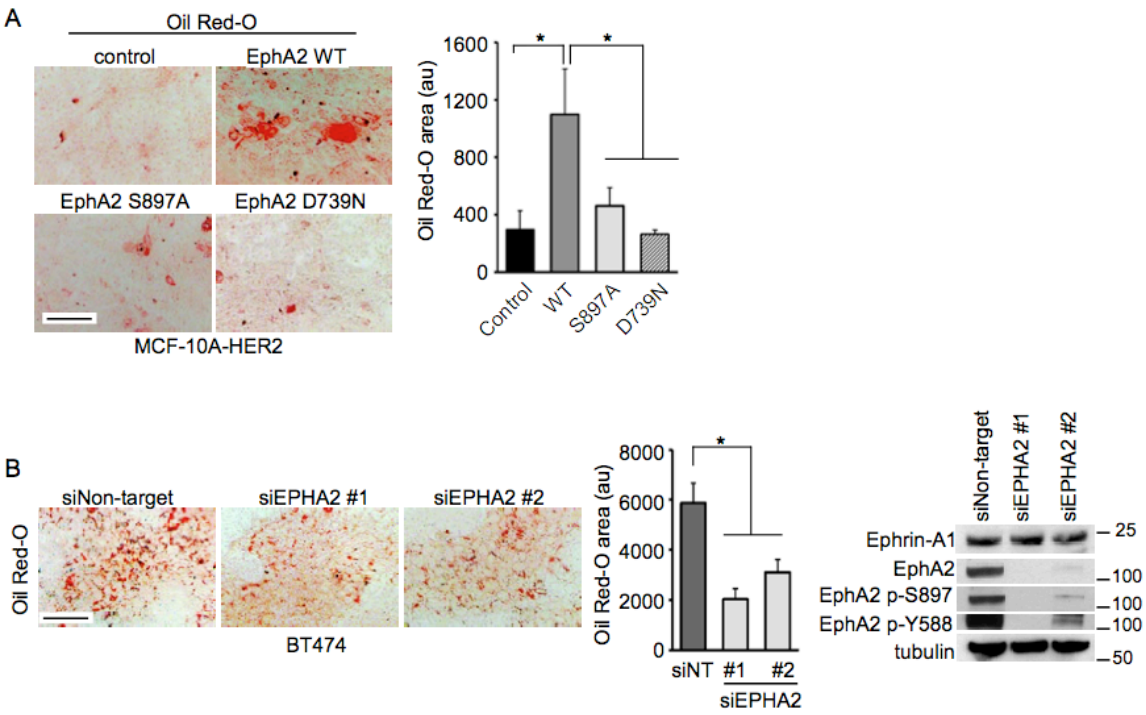

Figure 2.6 Inhibition of EPHA2 inhibits lipid accumulation. (A) Oil-Red-O staining of MCF-10A-HER2 cells expressing vector control, wild- type EPHA2, EPHA2^{S897A} or EPHA2 ^{D739N} mutants. Data are presented as the average Oil-Red-O area and expressed in arbitrary units (au). Error bars represent SEM. **P*<0.05, One-way ANOVA. Scale bar, 100µm. **(B)** Oil-Red-O staining in BT474 cells transfected with siControl, siEPHA2 #1, and siEPHA2 #2. Data are presented as the average Oil-Red-O area and expressed in arbitrary units (au). Error bars represent SEM. **P*<0.05, One-way ANOVA. Scale bar, 100µm.

shControl were glutamine-starved, stimulated by fresh glutamine, and intracellular glutamate was measured. Figure 2.7C shows that intracellular glutamate steadily accumulated after addition of fresh glutamine in the media; however, there were higher glutamate levels in ephrin-A1 knockdown cells relative to control cells, and this increase was blocked by the treatment of GLS inhibitors, 968 or BPTES (Figure 2.7D). Because loss of ephrin-A1 promoted growth in both *in vitro* and *in vivo* models and enhanced GLS activity, we sought to determine whether GLS plays a direct role in tumor cell proliferation. Ephrin-A1 knockdown and control MMTV-*Neu* cells were treated with glutaminase inhibitors, 968 or BPTES, and BrdU incorporation was assessed. As expected, knockdown of ephrin-A1 enhanced proliferation in

MMTV-*Neu* cells, and 968 or BPTES was able to inhibit the elevated BrdU incorporation in ephrin-A1-deficient cells (Figure 2.7E). To test the effects of GLS inhibition on tumor growth *in vivo*, shEphrin-A1 and shControl MMTV-*Neu* cells were transplanted into contralateral mammary fat pads of recipient mice and treated with either BPTES (10mg/kg) or vehicle control every other day by intraperitoneal (IP) injection. Ephrin-A1 knockdown tumors were significantly larger than the shControl tumors (Figure 2.7F). BPTES treatment significantly reduced the volume of ephrin-A1 knockdown tumors, whereas BPTES appeared to have no significant effect on shControl tumors at the indicated dose (Figure 2.7F).

To complement ephrin-A1 knockdown studies, we tested the effects of EPHA2 overexpression on GLS activity and tumor volume. We reasoned, since ephrin-A1 is the prototypic ligand of EPHA2 receptor and loss of ephrin-A1 can augment EPHA2 activity, that EPHA2 overexpression should have a similar effect on GLS activity and tumor cell growth as ephrin-A1 deficiency. Indeed, we observed that MMTV-*Neu* cells overexpressing EPHA2 had enhanced GLS activity compared to control cells (Figure 2.7G) and this increase could be blocked by GLS inhibitors, 968 or BPTES (Figure 2.7H). EPHA2 overexpression also enhanced BrdU incorporation, which was inhibited by 968 or BPTES (Figure 2.7I). Furthermore, EPHA2 overexpression enhanced tumor growth *in vivo*, and BPTES significantly decreased tumor volume to a level similar as control tumors (Figure 2.7J). Together, these data show that inhibition of GLS activity can impair proliferation and tumor growth, suggesting that enhanced glutaminolysis is, at least in part, the mechanism for the enhanced tumor growth in EphA2 overexpressing or ephrin-A1-deficient tumors.

We next tested whether ephrin-A1 also regulates GLS activity in the human cell line MCF-10A-HER2. Similar to MMTV-*Neu* cells, knockdown of ephrin-A1 in MCF-10A-

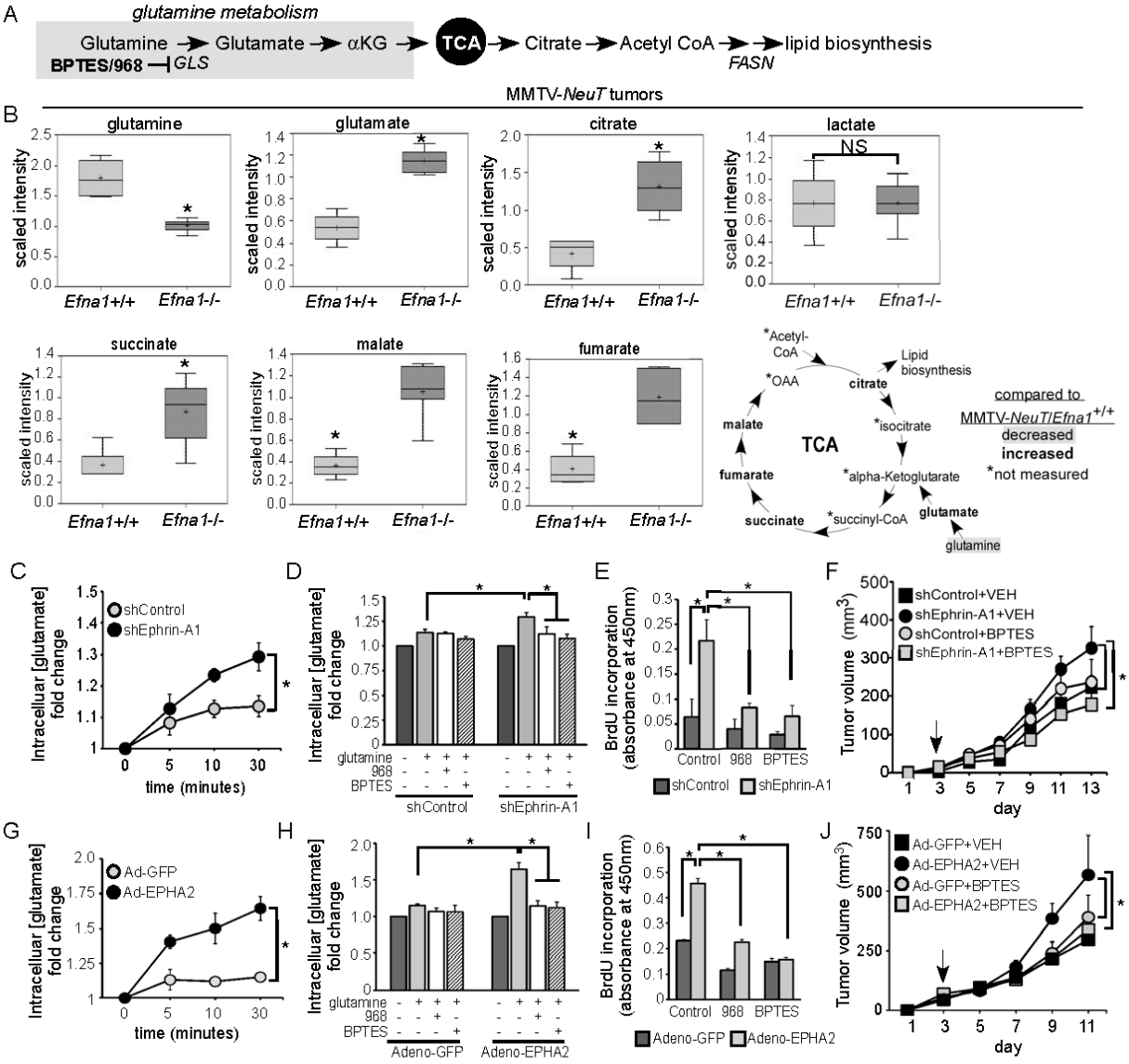

Figure 2.7 Loss of ephrin-A1 augments glutamine metabolism. **(A)** A schematic diagram of glutamine metabolism pathway. **(B)** LC/GC-MS derived relative metabolites abundance from MMTV-*NeuT*/*Efna1*$^{+/+}$ and MMTV-*NeuT*/*Efna1*$^{-/-}$ tumors. TCA schematic depicts relative changes (increase, bolded; decrease, shaded) from tumors. **P*<0.05, Welsh's two sample t-test. **(C,G)** Glutaminase activity was measured by intracellular glutamate concentrations upon 2mM glutamine and 5 ng/ml EGF stimulation in MMTV-*Neu* cells over a time course. **P*<0.05, two-way ANOVA repeated measures/randomized block. **(D,H)** Intracellular glutamate was measured upon addition of 2mM glutamine and 5ng/ml EGF. Cells were treated with 968 (10μM) or BPTES (10μM) and were normalized to baseline. **P*<0.05, one-way ANOVA. **(E,I)** BrdU incorporation in MMTV-*Neu* cells treated with vehicle Control, 968 (10μM) or BPTES (10μM). **P*<0.05, one-way ANOVA. **(F)** shControl or shEphrin-A1 MMTV-*Neu* cells were transplanted into mammary fat pads of mice. BPTES (10mg/kg) or vehicle (VEH) was delivered by IP injection every other day starting on day 3 (arrow). *n*=8 per group.

*P <0.05, two-way ANOVA repeated measures. **(J)** MMTV-*Neu* cells overexpressing GFP or EPHA2 were transplanted into mammary fat pads of mice. BPTES (10mg/kg) or VEH was delivered by IP injection every other day starting on day 3 (arrow). n=5 per group. *P <0.05, two-way ANOVA repeated measures. All *in vitro* experiments represent 2-4 biological replicates. Data are expressed as mean ± SEM.

HER2 cells enhanced GLS activity compared to control cells (Figure 2.9A), and inhibition of GLS rescued the pro-proliferative phenotype induced by ephrin-A1 knockdown (Figure 2.9B). We reasoned, if ephrin-A1 regulates cell proliferation through modulation of GLS, supplementing with downstream metabolites such as α-ketogluterate (αKG) should rescue the proliferative phenotype induced by the GLS inhibitor. We observed that addition of dimethyl-αKG (DM-αKG), the soluble form of αKG, restored proliferation inhibited by 968 in ephrin-A1 knockdown cells (Figure 2.9B). Additionally, overexpression of wild-type EPHA2, but not S897A and D739N mutants, enhanced glutamine metabolism (Figure 2.10D), suggesting that both EphA2 kinase activity and phosphorylation of S897 are required for EphA2-dependent regulation of glutamine metabolism.

Glutaminase exists in two isoforms, GLS1 and GLS2, or kidney-type isoform and liver-type isoform, respectively [74]. To determine which isoform regulates glutamine levels in ephrin-A1 knockdown cells, we silenced these distinct enzymes with siRNAs. Knockdown of GLS1 rescued the elevated glutaminase activity in *ephrin-A1*-deficient cells (Figure 2.9C and D, Figure 2.10A-C), suggesting that ephrin-A1 regulates glutaminolysis through inhibition of GLS1. It remains to be determined if GLS2 is also important in ephrin-A1-dependent glutaminolysis (Figure 2.9C and E).

Regulation of glutaminase activity by ephrin-A1 is mediated through RhoA GTPase

GLS, the biologic target of compound 968, was previously shown to be regulated by Rho family GTPases [79]. Inhibition of GLS or aminotransferase (AT) has been shown to suppress Rho GTPase-induced transformation and inhibit tumor growth in breast

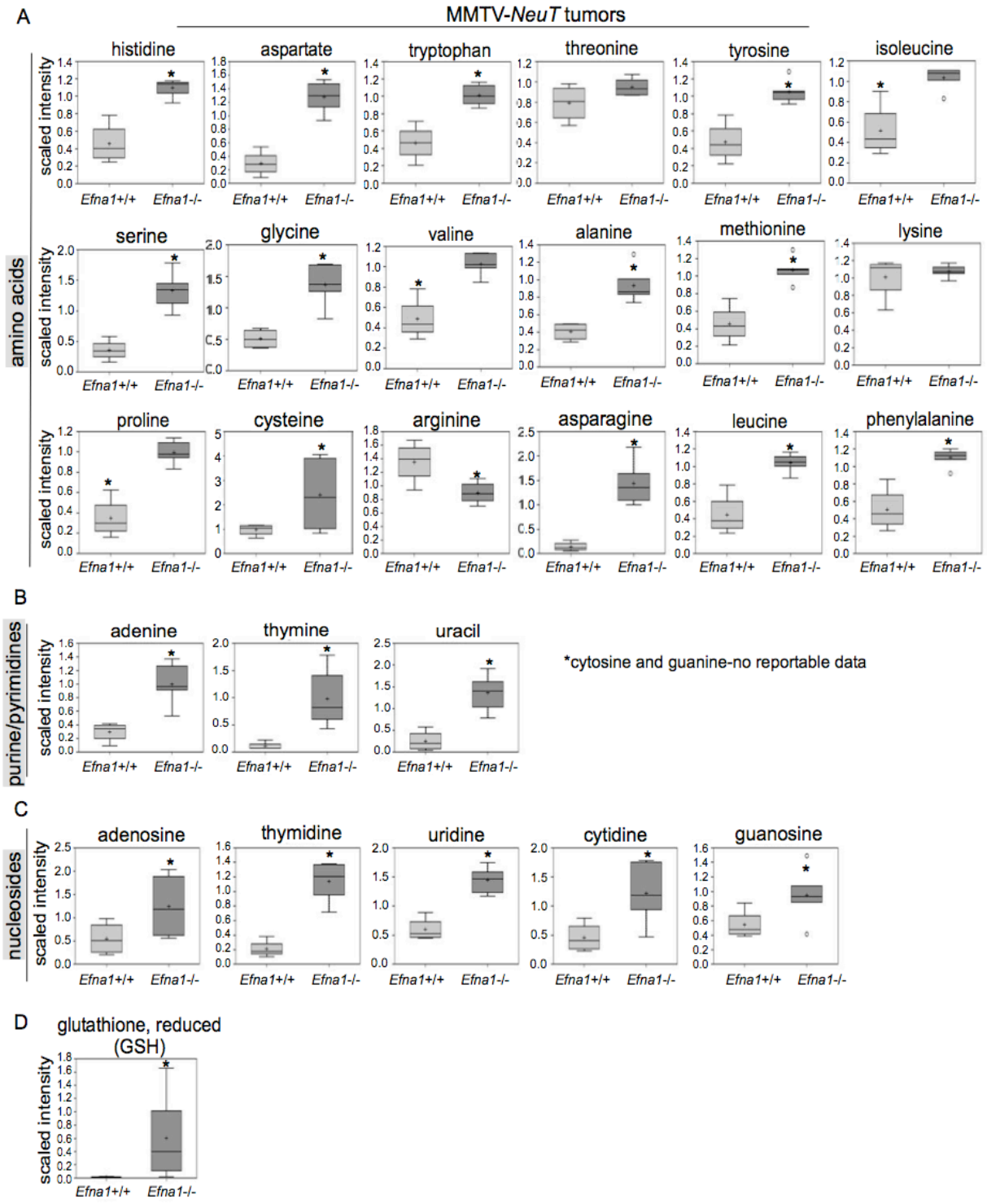

Figure 2.8 LC/GC-MS derived relative metabolite abundance from MMTV-Neu- T/efna1+/+ and MMTV-Neu-T/efna1-/- tumors. (A) Relative amino acid abundance; **(B)** relative purine and pyrimidine abundance; **(C)** relative nucleoside abundance; **(D)** relative reduced glutathione (GSH) abundance. Data underwent natural log-transformation. **P*<0.05, Welsh's two sample t-test.

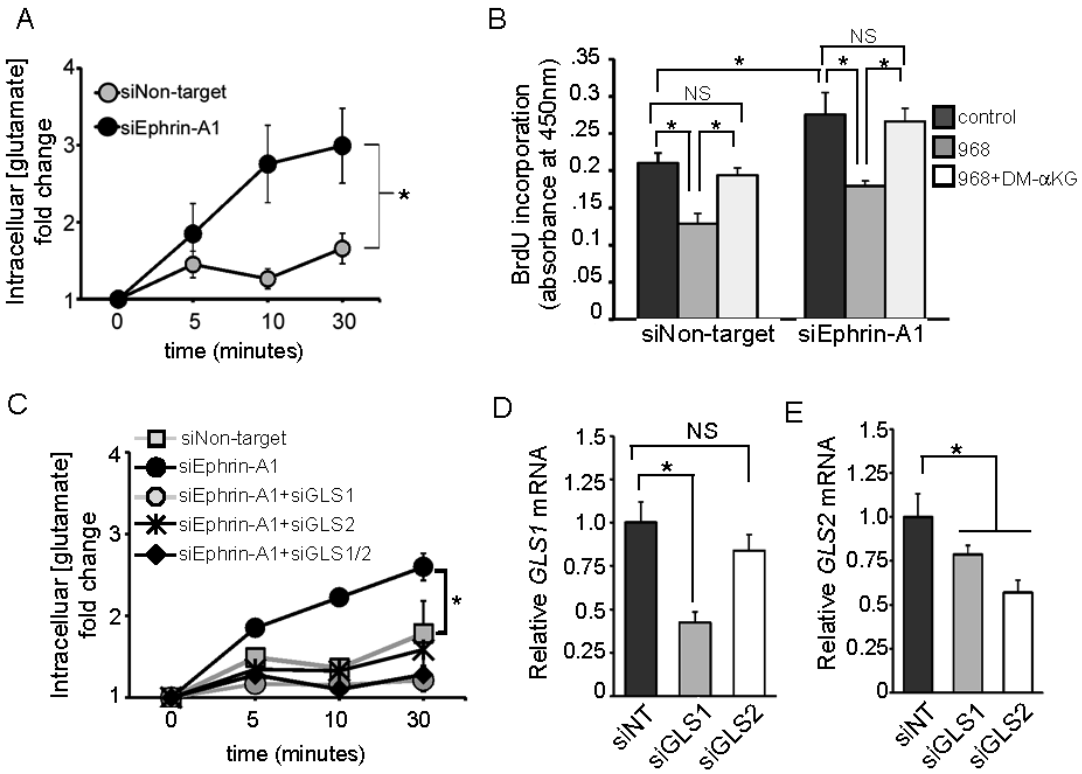

Figure 2.9 Knockdown of either GSL1 or GSL2 restored glutaminase activity in ephrin-A1-difficient cells (A) Glutaminase activity was measured by intracellular glutamate concentrations upon 2 mM glutamine and 5 ng/ml EGF stimulation in MCF-10A-HER2 cells over a time course; expressed as fold change ± SEM. **P*<0.05, two-way ANOVA repeated measures/randomized block. **(B)** BrdU incorporation in MCF-10A-HER2 cells after 968 or 968+DMαKG treatment. **P*<0.05, one-way ANOVA. **(C)** Intracellular glutamate in siNon-target, siEphrin-A1, siEphrin-A1+siGLS1, siEphrin-A1-siGLS2 and siEphrin-A1+siGLS1+siGLS2 MCF-10A-HER2 cells upon 2 mM glutamine and 5 ng/ml EGF stimulation. **P*<0.05, two-way ANOVA repeated measures/randomized block. **(D,E)** Relative mRNA levels of *GLS1* and *GLS2* were measured by real-time qRT-PCR to confirm knockdown. **P*<0.05, one-way ANOVA. All experiments represent 2-5 biological replicates. Error bars represent SEM. NS, not significant.

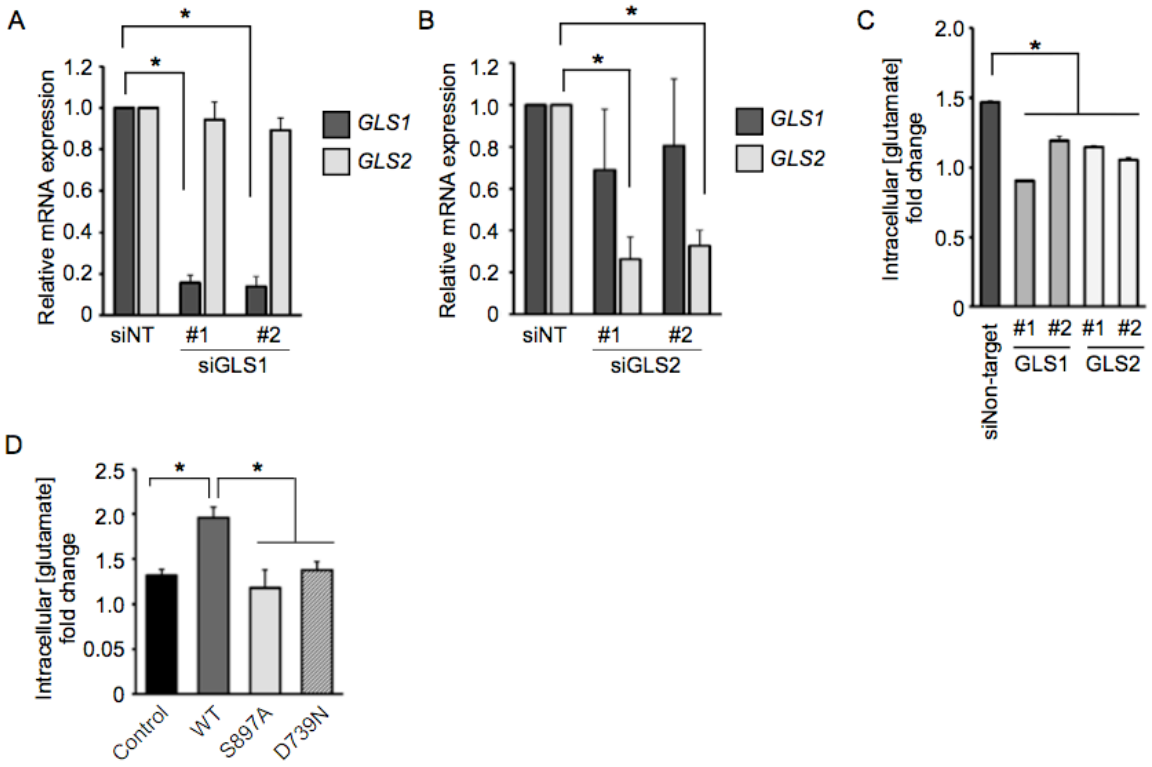

Figure 2.10 Inhibition of GLS1, GLS2, and EPHA2 impairs the conversion of glutamine to intracellular glutamate. (A &B) Relative mRNA expressions of *GLS1* and *GLS2* in MCF-10A-HER2 cells transfected with non-targeting (siNT), two independent glutaminase 1 targeted siRNAs (siGLS1), or two independent glutaminase 2 targeted siRNAs (siGLS2). Error bars represent SEM. **P*<0.05, one-way ANOVA. **(C)** Intracellular glutamate concentrations in MCF-10A-HER2 cells transfected with non- targeting (siNT), two separate glutaminase 1 targeted siRNAs (siGLS1), or two separate glutaminase 2 targeted siRNAs (siGLS2) upon 2 mM glutamine and 5 ng/ml EGF stimulation for 30 minutes; expressed as fold change. **P*<0.05, one-way ANOVA; error bars represent SEM. **(D)** Intracellular glutamate concentrations in MCF-10A-HER2 cells expressing vector control, wild-type EPHA2, $EPHA2^{S897A}$ or $EPHA2^{D739N}$ upon 2 mM glutamine and 5 ng/ml EGF stimulation for 30 minutes; expressed as fold change. **P*<0.05, one-way ANOVA; error bars represent SEM. All experiments represent 2 to 3 biological replicates.

adenocarcinoma xenografts, respectively [79, 205]. Since overexpression of EPHA2 receptor can activate RhoA activity [137, 142, 206], we tested whether the GLS activity induced by ephrin-A1 depletion could be mediated through RhoA signaling. RNAi-mediated silencing of ephrin-A1 increased the levels of active GTP-bound RhoA, relative to non-targeting siRNA controls (Figure 2.11A). CT04, a cell permeable Rho inhibitor, inhibited RhoA-GTP levels and decreased GLS activity in ephrin-A1 knockdown cells (Figure 2.11B and C). Furthermore, inhibition of RhoA, GLS, or FASN decreased elevated Oil-Red-O staining and cellular proliferation induced by knockdown of ephrin-A1 (Figure 2.11D and E), suggesting that inhibition of tumor cell growth by ephrin-A1 is mediated through RhoA and glutaminase.

Discussion

RTK signaling is critical to cell growth and survival in normal epithelial cells. Dysregulation of RTKs by mutations, amplification, or overexpression can increase kinase activity, leading to oncogenic transformation and malignant progression. Yet, recent studies have discovered dual roles for Eph receptors in both promoting and inhibiting tumor initiation and metastatic progression [179, 182, 194, 207, 208] based on *in vitro* and allograft studies using mammary epithelial and cancer cell lines. Ephrin-A1 overexpressing xenograft models and intratumoral delivery of Ad-ephrinA1-Fc both reduced tumor volume [209]. In breast cancer cell lines, ligand-induced EPHA2 signaling inhibits proliferation, whereas ligand-independent crosstalk between EPHA2 and other oncogene pathways results in tumor promotion [137, 181]. These data suggest ephrin-A1 can act as a molecular switch in breast cancers, such that loss of ligand-dependent signaling switches EPHA2 to function as a tumor promoter. Herein, we provide functional evidence in a transgenic MMTV-*NeuT* mouse model that genetic deletion of *Ephrin-A1* enhances tumor cell proliferation and mammary tumor growth. The role of ephrin-A1 in suppression of tumor malignancy is also supported by human breast cancer data in which lower *ephrin-A1*

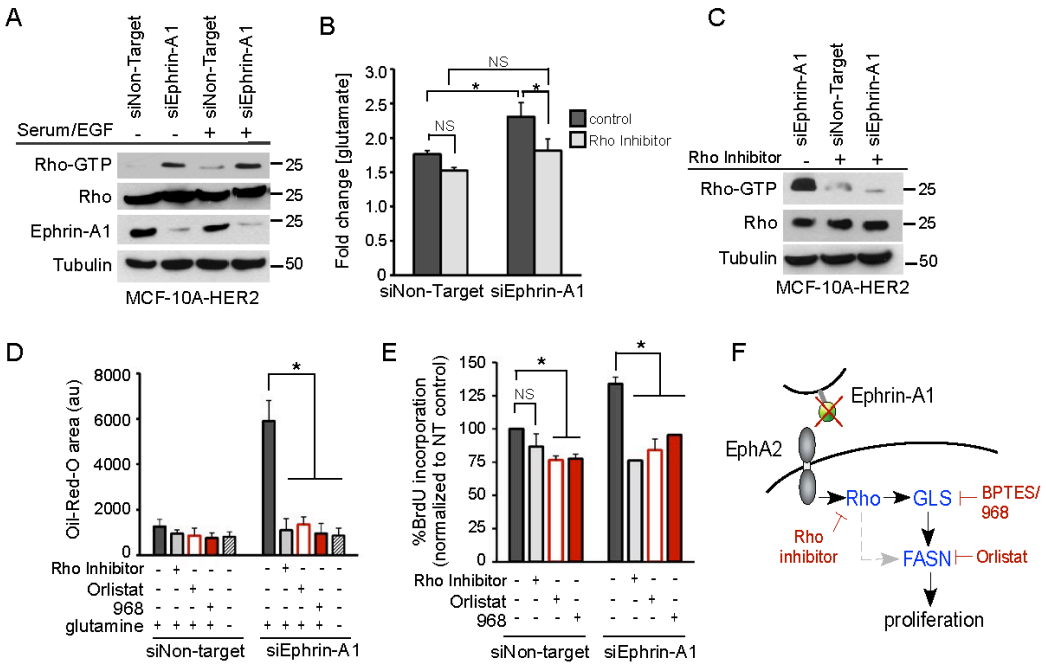

Figure 2.11 Ephrin-A1 regulates glutamine metabolism in a Rho-dependent manner. (A) Rhotekin-GST effector pull-down activity assay in MCF-10A-HER2 cells. **(B)** Glutaminase activity assay in the presence or absence of Rho inhibitor CT04 (1µg/mL) for 18 hours. Data expressed as the fold change normalized to siNT control + SEM. *P<0.05, one-way ANOVA. **(C)** Rho-GTP levels were measured by Rhotekin-GST effector pull-down assay. Shown are representative western blots with indicated antibodies. **(D)** Oil-red-O staining in MCF-10A-HER2 cells with treatments of Rho inhibitor CT04 (1µg/mL), glutaminase inhibitor 968 (10uM), FASN inhibitor Orlistat (20uM), or glutamine (glut) withdrawal for 24 hours. Data presented as average Oil-Red-O area and expressed in arbitrary units (au). *P<0.05, one-way ANOVA. **(E)** BrdU incorporation in MCF-10A-HER2 cells after treatment with CT04 Rho inhibitor (1µg/mL), 968 (10uM), or Orlistat (20uM) for 18 hours. Data are normalized to the siNT control; error bars represent SEM. *P<0.05, one-way ANOVA. NS, not significant. **(F)** A working model of ephrin-A1 regulation of tumor metabolism in breast cancer cells.

(*EFNA1*) gene expression is associated with poor survival in lymph node-positive patients, thus demonstrating clinical relevance.

Our previous studies in the 4T1 model showed knockdown of ephrin-A1 had no effect on tumor volume, but resulted in decreased tumor angiogenesis and lung metastasis [198]. Consistent with our previous studies, orthotopic transplantation of

wild-type 4T1 tumors into ephrin-A1-deficient hosts resulted in marked decrease of vWF staining in tumor sections (data not shown), suggesting that host ephrin-A1 deficiency affects tumor neovascularization. However, global knockout of ephrin-A1 in our MMTV-*NeuT* model displayed no significant changes in tumor vascular density. Lack of significant changes in tumor vessels in this model could be due to an inhibitory effect of ephrin-A1 on tumor cells that override the angiogenesis promoting effects.

Studies in this report unequivocally demonstrate a role of ephrin-A1 in regulating cell proliferation in the HER2/Neu model. The differential effects of ephrin-A1 deficiency on tumor growth between the 4T1 and the HER2/Neu models may at least be in part due to the differences in breast cancer subtype, as 4T1 cells are mesenchymal without normal cell-cell contacts. Thus, even if ephrin-A1 was expressed in these cells, it may not bind to EPHA2 on neighboring cells to inhibit its function, whereas ephrin-A1 in MMTV-*Neu* cells may interact with EPHA2 on adjacent tumor cells more effectively to exert its inhibitory role. It is currently unknown whether ephrin-A1 affects metastasis in this model. However, in view of the potential role of ephrin-A1 in angiogenesis and metastasis, inhibiting EPHA2 receptor, rather than focusing on overexpressing ephrin-A1, may improve future targeting strategies.

Metabolic reprogramming is a hallmark of cancer that confers growth and survival [210]. While RTKs are known to regulate tumor metabolism through modulation of signaling pathways such as AKT and mTOR, the connection between EPH RTKs and tumor metabolism remained unexplored. The discovery that ephrin-A1 regulates lipid and glutamine metabolism suggests ephrin-A1 is capable of inhibiting tumor growth by modulation of key metabolic enzymes. One rate-limiting enzyme for neoplastic lipogenesis, FASN, has been shown to be induced by RTKs via the SREBP1 transcription factor and promotes proliferation in breast cancer cells [211, 212].

Alternatively, both glucose and glutamine can be metabolized to provide citrate that supports acetyl-coA production for *de novo* lipid biosynthesis [213, 214]. We did not observe significant changes in FASN or SREBP1 expression in human breast cancer cells. Interestingly, our global metabolic study revealed glutaminolysis, but not glycolysis, is increased in ephrin-A1-null tumors compared to wild-type tumors. These findings are consistent with recent reports that during hypoxia, glutaminolysis is the predominant pathway for *de novo* lipogenesis [96]. Thus, our data support a model in which EPHA2 ligand-independent signaling through down-regulation of ligand levels, EPHA2 overexpression, and/or failed engagement of endogenous ligand-receptor on adjacent cells, promotes tumor cell growth and progression by elevating glutaminolysis.

While most cancers depend on a high rate of aerobic glycolysis, some cancers also display glutamine addiction [16, 215], including breast [216]. Glutamine metabolism has been shown to be regulated by a number of signaling pathways including Rho family GTPases. Compound 968, a small molecular inhibitor of glutaminase, suppressed oncogenic transformation induced by Rho GTPases [79]. We found that this pathway is repressed by ephrin-A1. First, EPHA2 RTK is known to regulate RhoA activity [137, 142]. Second, RhoA-GTP levels are substantially elevated in ephrin-A1 knockdown cells. Third, inhibition of Rho activity significantly decreased intracellular glutamate levels in ephrin-A1 knockdown cells. Finally, inhibition of Rho, GLS, or FASN suppressed proliferation induced by depletion of ephrin-A1. These results demonstrate that ephrin-A1 regulates glutaminolysis and support a model in which ephrin-A1 inhibition of glutaminase activity is, at least in part, through Eph receptor-dependent activation of RhoA GTPases (Figure 2.11F).

Although our work emphasizes the role of ephrin-A1 in glutamine metabolism and lipid biogenesis, other glutamine metabolism pathways may also be important in ephrin-A1-induced growth inhibition. For example, glutamine contributes to *de*

novo synthesis of the major cellular antioxidant glutathione (GSH), nucleic acids, and certain amino acids. Indeed, we observed increases in GSH, nucleosides, and amino acid levels in ephrin-A1-null tumors relative to control wild-type tumors (Figure 2.8). Accordingly, future investigations will reveal whether these branches of glutamine metabolism are also critical in ephrin-A1-mediated inhibition of cell proliferation.

The identification that ephrin-A1 and EPHA2 are linked to tumor metabolism opens up exciting new questions in tumor biology. Although ephrin-A1 inhibits both glutamine metabolism and accumulation of lipids, it is unclear whether increased lipids are due to augmented glutaminolysis in ephrin-A1 knockdown cells, or occur as an independent event. In addition to Rho GTPase, glutamine metabolism is also regulated by other signaling molecules relevant to breast cancer, such as c-Myc and PKC-delta [16]. Future studies will focus on whether ephrin-A1/EPHA2 regulation of glutaminolysis is also modulated by c-Myc or PKC and whether these molecules operate in the same linear pathway or in different parallel pathways as Rho. Furthermore, the results presented in this study have significant translational potential. Ephrin-A1 may be used as a biomarker, as decreased ephrin-A1 expression may predict poor clinical outcome in metastatic breast cancer. Finally, glutamine addiction in breast cancer is associated with elevated EPHA2 receptor levels in subtypes of disease that are refractory to current therapies, such as drug-resistant HER2-positive tumors. Since EPHA2 kinase activity is required for its regulation of glutamine metabolism, selective EPHA2 kinase inhibitors [130, 217] and/or inhibitors of key metabolic enzymes may provide more effective cancer therapeutics in these difficult to treat subtypes.

CHAPTER III

Conclusions and Future Directions

Conclusions

In the early 1900's several bodies of work emerged that documented the observation that tumor cells exhibited a metabolic phenotype drastically different from non-malignant cells. These works launched a century's worth of research dedicated to understanding the mechanisms that drive metabolic reprogramming and the contributions that this reprogramming has on tumor development, maintenance and progression. This aberrant metabolism observed in tumor cells confers growth by providing the energy and biomass requirements needed to sustain viability and support rapid cell division. As breast cancer persists as one of the deadliest cancers diagnosed in women, it re-enforces the need to continue studying the mechanisms that support its growth, such as metabolic reprogramming. Previous genome wide analyses identified the EPH family of RTKs as dysregulated in several cancers, including breast. Several studies have since been conducted to determine the role of EPH RTKs in malignant growth and the mechanisms surrounding their functions. The EPHA2 receptor, in particular, has emerged as a key regulator of mammary tumor growth and its overexpression correlates with poor prognosis in breast cancer patients. Several studies have also demonstrated that EPHA2 can enhance malignant growth by activating several signaling pathways that are also linked to tumor metabolism; yet, whether EPHA2 influenced metabolic reprogramming remained unexplored. This thesis sought out to determine whether EPHA2 enhanced tumor growth by regulating tumor metabolism. Additionally, a unique characteristic of EPHA2 is that it exhibits pro- and anti-tumor activity depending on whether is it bound to its preferential ligand, ephrin-A1. Therefore, a secondary goal of this thesis was to further characterize the

role of ephrin-A1 as a molecular switch of EPHA2. The data presented in this thesis contribute to our understanding of the mechanisms that promote the dysregulation of tumor metabolism and the role of glutaminolysis in augmenting breast cancer growth. We integrated *in vitro* and *in vivo* techniques to demonstrate the first functional evidence that EPHA2 signaling augments glutamine metabolism to promote tumor growth and furthermore, that ephrin-A1 acts as a molecular switch of EPHA2 in controlling these metabolic and proliferative phenotypes. Together, our findings have provided genetic, molecular and pharmacologic evidence that define EPHA2/ephrin-A1 as a regulator of tumor metabolism. Lastly, this work provides the foundation for additional investigations into the mechanisms in which EPHA2/ephrin-A1 signaling regulates tumor metabolism and whether this phenotype is observed across other human cancers.

Future Directions

The completion of the work described in this thesis has contributed to defining EPHA2/ephrin-A1 signaling as a modulator of tumor metabolism in HER2-positive breast cancer. Simultaneously, it has invited additional and exciting questions regarding the role of EPHA2/ephrin-A1 in other branches of tumor metabolism and other molecular subtypes of breast cancer. Some of these questions will be discussed as potential starting points for future investigations.

<u>Does EphA2/ephrin-A1 signaling contribute to aberrant metabolism in the early stages of tumor development?</u>

Dysregulation of cellular metabolism is a hallmark of cancer and a driving force in the early stages of cell transformation and hyperplastic growth [218]. Consistent with previous reports that EPHA2 can transform mammary epithelial cells [179], preliminary analyses from our laboratory of mammary gland development revealed that ephrin-A1-deficient animals display elevated EPHA2 expression and mammary epithelial hyperplasia at 20 weeks of age (Figure 3.1A). This is further evidenced by

the observation that ephrin-A1-deficient mammary epithelia have a higher proliferative index compared to wild type littermates (Figure 3.1B). To evaluate this growth phenotype *in vitro*, we isolated primary mammary epithelial cells and performed confocal analysis of mammary organoid cultures, which demonstrated that loss of ephrin-A1 enhanced glandular branching (Figure 3.1C). Mammary epithelial lysates from these mice also exhibited increased expression of EphA2, phosphorylated ERK and phosphorylated AKT compared to WT lysates (Figure 3.1D).

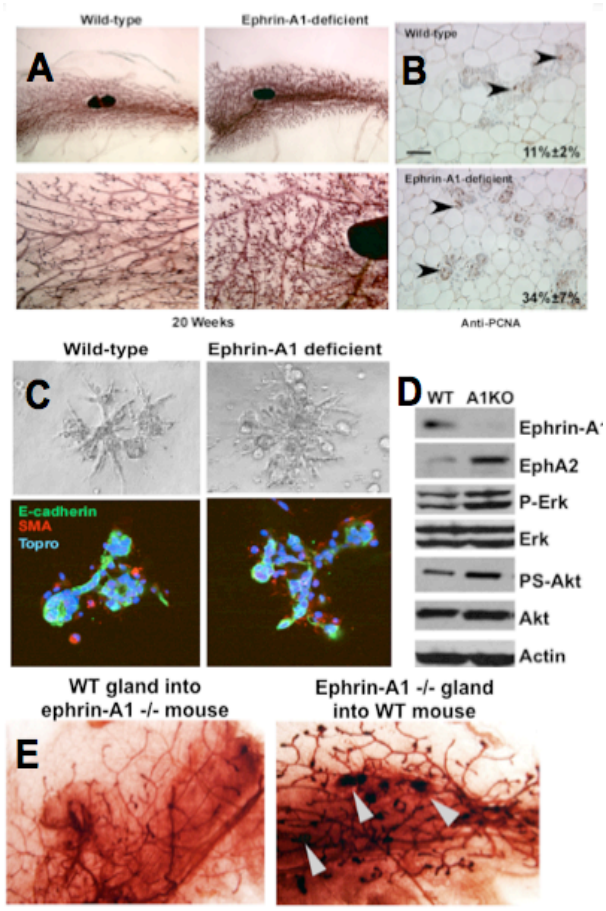

Figure 3.1 Hyperplastic phenotype in ephrin-A1 deficient mammary glands and epithelium. (A) Mammary gland whole mounts from wild-type and ephrin-A1 knockout mice at 20 weeks; **(B)** PCNA staining of sectioned mammary glands; **(C)** Mammary epithelium organoid cultures; **(D)** Western blot analysis of signaling pathways; **(E)** Mammary glands were transplanted into mice of opposite genotype. (Experiments performed by Dana Brantley-Sieders; Vanderbilt University.)

Lastly, to determine whether this phenotype is epithelial cell-intrinsic or influenced by the stroma microenvironment, 20 week-old WT or ephrin-A1-/- mammary tissue was transplanted reciprocally into pre-cleared fat pads of either ephrin-A1-/- or WT 3 week-old recipient female mice. As shown in Figure 3.1E, only ephrin-A1-/- mammary glands grown in WT hosts developed hyperplasia. These data suggest the hyperplastic phenotype is due, at least in part to, the loss of ephrin-A1 in the epithelium and is likely not dependent on the stromal tissue and microenvironment.

Since EPHA2/Ephrin-A1 signaling regulated glutaminolysis and growth in our breast cancer tumor model, these mechanisms may also be relevant in the early hyperplastic stages in the presence or absence of an oncogene. In addition, other branches of metabolism may also be upregulated due to the loss of ephrin-A1 compared to the wild type tissue. For instance, we observed an increase in phosphorylated AKT, a known activator of glycolysis in transforming cells [111]. It is possible that loss of ephrin-A1 activates EPHA2 pro-tumor activity, which in turn induces the upregulation of metabolic pathways to support hyperplasic and malignant growth. If this were indeed the mechanism, it would be expected that several of the regulatory proteins of tumor metabolism, as discussed in Chapter 1, would be upregulated in the hyperplastic tissue from ephrin-A1 knockout mice. Furthermore, if inhibition of these pathways rescued reduced mammary hyperplasia, this would suggest that enhanced aberrant metabolism was a potential mechanism and may warrant further investigation.

How does EPHA2 does confer drug resistance?

Resistance to chemotherapies and targeted therapies persists as a major concern in the treatments of breast cancer. Less than half of breast cancer patients have a complete response to chemotherapies regardless of molecular subtype [219] and a significant portion of patients with HER2 type breast cancer that receive the targeted therapy, trastuzumab, adjuvant to chemotherapy also exhibit innate and

acquired resistance [220, 221]. This ultimately results in decreased patient survival, thus highlighting the importance of investigating the mechanisms that surround this resistance. Interestingly, previous studies have demonstrated that EPHA2 overexpression mediated resistance to trastuzumab [181]. As evidenced in Figure 3.2, when Zhuang *et al.* overexpressed constitutively activated EPHA2 in MCF-10A-HER2 cells, these cells developed an impaired response to trastuzumab that was restored by knocking down EPHA2. Furthermore, these studies also demonstrated that derived trastuzumab resistant human breast cancer cells exhibited enhanced EPHA2 expression compared to the drug-sensitive parent cells, yet inhibiting EPHA2 was able to restore trastuzumab sensitivity *in vitro* and *in vivo.*

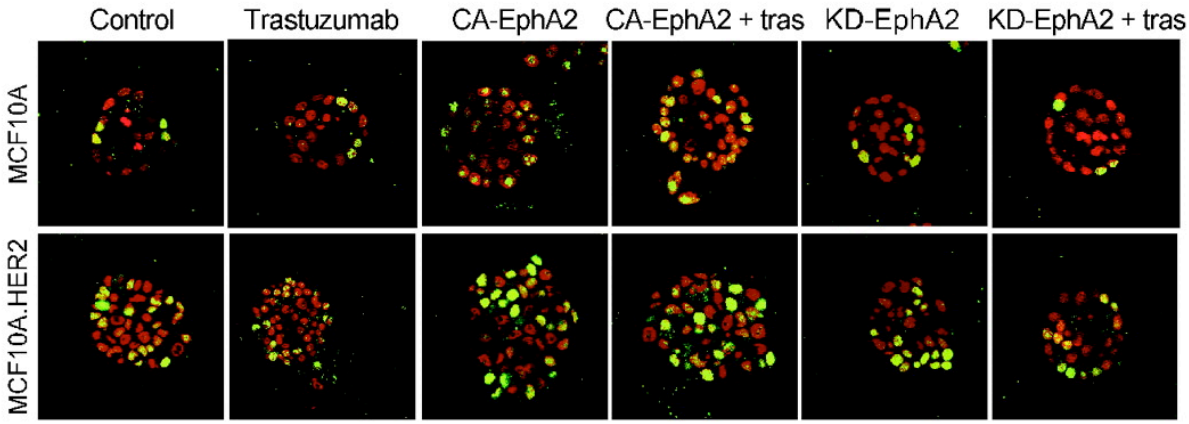

Figure 3.2 EphA2 overexpression confers cellular intrinsic resistance to trastuzumab Constitutively activated (CA-EphA2) or kinase dead (KD-EphA2) EphA2 receptor were introduced into MCF10A or MCF10A.HER2 cells by retroviral transduction. Pooled G418-resistant cell populations were cultured in 3-dimensional Matrigel and stained for Ki67 (green) to assess proliferation and counter-stained for To-Pro-3 (red) to visualize nuclei. Overexpression of CA-EphA2, but not KD-EphA2, desensitizes MCF10A.HER2 cells to trastuzumab (Adapted from [181].

The ability of a tumor cell to scavenge apoptosis-inducing ROS is a mechanism that tumor cells use to overcome the cytotoxic effects of chemotherapy. Glutathione (GSH), as discussed in Chapter 1, can play a critical role in tumor cell viability by

acting as a potent anti-oxidant when it conjugates with electrophiles in a reaction mediated by GST [86]. Notably, tumors from MMTV-*NeuT*/*Efna1*$^{-/-}$ mice displayed significantly increased levels of GSH compared to tumors with functional ephrin-A1 (Chapter 2, Figure 2.8D). Though these tumors had enhanced GSH, and GSH can accumulate as a result of enhanced glutamine metabolism, we did not directly evaluate GSH concentrations or its antioxidant potential in tissue culture experiments upon loss of ephrin-A1 or overexpression of EPHA2. Since separate experiments have demonstrated that EPHA2 overexpression can mediate drug resistance and can enhance glutamine metabolism, it may be valuable to determine whether elevated glutamine metabolism and GSH generation is a mechanism of EPHA2-induced drug resistance. Recent studies have also implicated EPHA2 in regulating sensitivity to the chemoagent, paclitaxel in ovarian [222], prostate[223], and nasopharyngeal [224] cancer. Thus it may also be of interest to determine whether EPHA2 is able to mediate chemoresistance in breast cancer cells that are not HER2 type and whether this is mediated by EPHA2-induced metabolic changes. Furthermore, monitoring tumor cells using optics metabolic imaging may also provide longitudinal insight of the metabolic adaptive response of these cells as they become resistant to certain chemo-agents.

<u>What is the role of EPHA2/ephrin-A1-induced metabolism in tumor cell motility and metastatic spread?</u>

A major question raised from our studies in Chapter 2, is whether aberrant glutamine metabolism contributes to metastatic disease in breast cancer patients. Low *EFNA1* (ephrin-A1) expression correlated with poor survival in lymph-node positive breast cancer patients (Chapter 2), suggesting that ephrin-A1 might serve as a prognostic marker in more aggressive forms of breast cancer, however we did not further investigate the role of ephrin-A1 and EPHA2 signaling on tumor progression or whether glutamine metabolism could impact progression or tumor motility. Only a few studies have addressed whether glutaminolysis can directly regulate cell

migration. Wang *et al.* treated a variety of tumor cells with the GLS inhibitor, 968, and observed a significant reduction in cell migration [79]. Supplementation of the downstream product of GLS, α-KG, was able to restore growth to these cells, suggesting that these cells had impaired migration rather than had suffered from cytotoxicity [79]. Though we did not specifically test invasiveness or migration in this study, overwhelming data from our laboratory and others have demonstrated that EPHA2 contributes to tumor dissemination [137, 141, 152, 185, 225, 226]. However, it is unknown whether metabolic perturbations induced by EPHA2 may be a mechanism of cancer progression. Other studies, however, have demonstrated that other branches of tumor metabolism can promote tumor metastasis [227, 228]. Of particular interest is the discovery that FASN, a rate-limiting enzyme of *de novo* lipogenesis, has been implicated as a regulator of tumor metastases and motility [229, 230]. We observed that either loss of ephrin-A1 or overexpression of EPHA2 was able to enhance the presence of lipid deposits and proliferation, yet inhibition of FASN inhibited both lipid accumulation and growth (Chapter 2). Interestingly, in preliminary studies, we have detected elevated FASN protein in both human breast cancer samples and in MMTV-*NeuT* tumors that inversely correlates with ephrin-A1 protein expression (Figure 3.3). Therefore, future investigations may warrant the interrogation of the regulatory mechanisms surrounding FASN and whether this may be a mode of enhancing metastatic disease in EPHA2 overexpressing tumors.

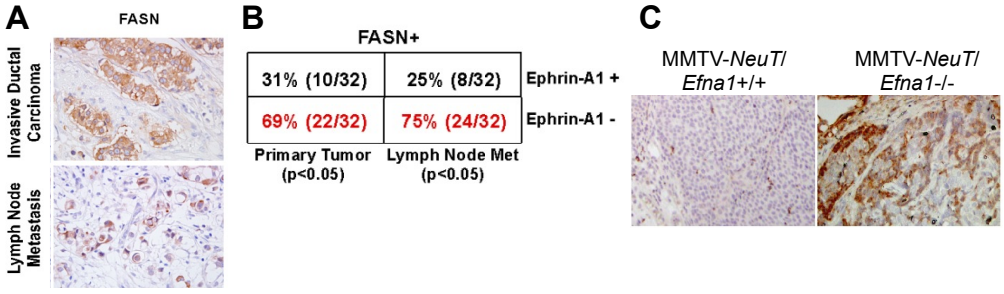

Figure 3.3. FASN protein expression inversely correlates with ephrin-A1. IHC analysis of FASN in human breast cancer tissue microarrays **(A,B)**; and in MMTV-*NeuT* tumors from mice **(C) .**

Does EPHA2 regulate tumor metabolism in other breast cancer molecular subtypes?

Our data unequivocally demonstrate a role for EPHA2 and ephrin-A1 in governing tumor metabolism in a HER2-positive model of breast cancer (Chapter 2). However, we did not investigate whether this phenotype was a mechanism among other molecular subtypes of breast cancer, particularly in triple negative breast (TNBC), as it has been reported that this subtype has enhanced glutaminolysis [231, 232]. However, recent preliminary studies from our laboratory have demonstrated that inhibition of EPHA2 *in vitro* impaired glutaminolysis in TNBC cells lines and inhibited proliferation (data not shown). These data suggest a role for EPHA2 in regulating glutaminolysis in other molecular subtypes, however the mechanisms surrounding this regulation still remain unclear. Furthermore, these recent findings provide further basis to investigate whether Luminal A and Luminal B subtypes have a metabolic phenotype regulated by EPHA2 signaling. Though we observed EPHA2/ephrin-A1 signaling regulated glutaminolysis, it is conceivable that this signaling also regulates glycolysis as the two processes are closely related.

Additionally, ER-negative breast cancers have recently been found to have enhanced glutaminolysis [232]. Interestingly, previous studies that evaluated EPHA2 expression in a comprehensive selection of breast cancer cell lines, identified EPHA2 as having the greatest expression in ER-negative tissue [233]. This study also demonstrated ephrin-A1 as a binary molecular switch that activated EPHA2 anti-tumor activity [233]. Further evaluation of the metabolic phenotype of these cell lines in response to EPHA2 signaling may provide further insight into the role of EPHA2/ephrin-A1 signaling in tumor metabolism.

Do other EPH RTKs regulate tumor metabolism?

In addition to EPHA2, several other EPH RTKs (EPHA4, EPHA7, and EPHB4 and EPHB6) have been identified as overexpressed in breast cancer patients and have been linked with poor prognosis [173]. Under physiologic conditions, ephrin ligands

interact with EPH RTKS at cell-cell junctions to inhibit the Ras-Raf-MAPK, PI3K-Akt and Abl-Crk pathways, as a critical regulatory mechanism for development and tissue homeostasis. Yet in malignant tissue, this signaling is dysregulated and ephrin expression is often loss or cell-cell junctions are disrupted thus preventing ephrins from binding their EPH receptors. In the absence of ligand, some EPH RTKS engage in ligand-independent signaling and obtain pro-tumor functions. As discovered in this thesis, one consequence of this pro-tumor activity is the upregulation of glutamine metabolism in breast cancer cells. Since other EPH RTK are reported as having oncogenic potential, investigating whether their downstream signaling impacts metabolic pathways may provide insight into additional EPH functions.

Concluding remarks

The results reported in this thesis represent a significant advancement in the understanding of the functional and mechanistic contributions of EPHA2/ephrin-A1 signaling in regulating breast cancer growth. Yet, much work still remains in the understanding of how this receptor and ligand regulate growth in other molecular subtypes of breast cancer and the mechanisms in which this signaling controls metastatic disease and chemoresistance. Because EPHA2 has already demonstrated to have such an impact in breast cancer, the future investigation of these questions will surely be addressed.

Appendix A

Elevated Slit2 Activity Impairs VEGF-induced Angiogenesis and Tumor Neovascularization in EPHA2-deficient Endothelium.

The work presented in Appendix A is published with the same title in Molecular Cancer Research, March 2015 [[Volume 13, Number 3].

Abstract

Angiogenic remodeling during embryonic development and in adult tissue homeostasis is orchestrated by cooperative signaling between several distinct molecular pathways, which are often exploited by tumors. Indeed, tumors upregulate pro-angiogenic molecules while simultaneously suppressing angiostatic pathways in order to recruit blood vessels for growth, survival, and metastatic spread. Understanding how cancers exploit pro- and anti-angiogenic signals is a key step in developing new, molecularly targeted anti-angiogenic therapies. While EPHA2, a receptor tyrosine kinase (RTK), is required for vascular endothelial growth factor (VEGF)-induced angiogenesis, the mechanism through which these pathways intersect remains unclear. Slit2 expression is elevated in EPHA2-deficient endothelium, and here it is reported that inhibiting Slit activity rescues VEGF-induced angiogenesis in cell culture and *in vivo*, as well as VEGF-dependent tumor angiogenesis, in EPHA2-deficient endothelial cells and animals. Moreover, blocking Slit activity or Slit2 expression in EPHA2-deficient endothelial cells restores VEGF-induced activation of Src and Rac, both of which are required for VEGF-mediated angiogenesis. These data suggest that EPHA2 suppression of Slit2 expression and Slit angiostatic activity enables VEGF-induced angiogenesis *in vitro* and *in vivo*, providing a plausible mechanism for impaired endothelial responses to VEGF in the absence of EPHA2 function.

Implications

Modulation of angiostatic factor Slit2 by EPHA2 receptor regulates endothelial responses to VEGF-mediated angiogenesis and tumor neovascularization.

Introduction

Angiogenic remodeling, which generates new vessel sprouts from pre-existing vessels, is essential for proper embryonic development, normal tissue homeostasis, and contributes to the pathogenesis and progression of cancer. Proper vessel formation requires a balance between angiogenic stimuli, which regulate endothelial cell invasion and migration, proliferation, and tubulogenesis, and angiostatic factors that terminate or inhibit these processes upon vessel maturation to promote vascular stability (Reviewed in [234]). Vascular endothelial growth factor (VEGF), the best-characterized pro-angiogenic factor, is a key regulator of physiologic angiogenesis and tumor neovascularization (Reviewed in [235, 236]). In addition to VEGF, the Eph family of receptor tyrosine kinases (RTKs) and their cell surface membrane-bound ephrin ligands also regulate physiologic and pathologic angiogenesis. Specifically, EPHA2 and its primary ligand, ephrin-A1, have become the targets of intensive investigation due to their functions in tumorigenesis and neovascularization (Reviewed in [191, 237-239]).

Though VEGF regulates endothelial cell activation, proliferation, migration, and morphogenesis, this factor does not act in isolation. Indeed, coordinated signaling between VEGF and a plethora of other factors, such as Notch, transforming growth factor b (TGF-b), angiopoietins, platelet derived growth factors (PDGF), and ephrins/Eph RTKs, is essential for normal physiologic angiogenesis (Reviewed in [240, 241]). Previous studies from our laboratory and others demonstrated that the VEGF pathway also cooperates with ephrin/Eph signaling to regulate angiogenesis. Specifically, soluble EphA receptors, EPHA2-deficiency, or antibodies targeting

EPHA2 impair VEGF-induced angiogenesis, as well as angiogenic responses induced by ephrins [198, 242-246]. The mechanism through which blocking EPHA2 function interferes with VEGF-mediated angiogenesis remains unclear.

Members of the Slit/roundabout (Robo) gene family also regulate vascular remodeling and homeostasis (Reviewed in [247]). The three Slit proteins (Slit1-3) identified in vertebrates interact with receptors of the Robo family (Robo1-4), Robo1 and Robo4 being most highly expressed in endothelial cells [248]. The role of Slit proteins in regulation of angiogenesis remains controversial, however, with reported pro- [249-253] and anti-angiogenic activities [254-258]. Recent investigations clearly demonstrated that Slit2 inhibits VEGF-induced vascular remodeling [254-257, 259].

In a previous study, we reported elevated *slit2* mRNA expression in EPHA2-deficient endothelial cells relative to wild-type controls, and determined that Slit functioned as an inhibitory angiocrine factor. Inhibition of Slit function in conditioned media harvested from EPHA2-deficient endothelium alleviated repression of mammary tumor cell growth and motility in culture and *in vivo* [260], consistent with the chemorepulsive, growth inhibitory, and tumor suppressive function of Slit2 in mammary epithelium and breast cancer [261-268]. These data suggest that elevated Slit2 expression in EPHA2-deficient endothelium contributes to reduced tumor growth in EPHA2-deficient mice.

We previously reported that the pro-angiogenic effects of ephrin-A1 were suppressed in the presence of Slit2 [269], suggesting cross-talk between EphA receptor signaling and the Slit-Robo pathway may also regulate angiogenesis. Because Slit2 expression is significantly elevated in EPHA2-deficient endothelium, we hypothesized that overexpression of this angiostatic factor could account for impaired VEGF-induced angiogenesis in the absence of EPHA2. To test this

hypothesis, we blocked Slit activity in EPHA2-deficient endothelium using soluble Robo1-Fc receptor as a ligand trap. Inhibiting Slit function in EPHA2-deficient endothelium rescued VEGF-induced endothelial cell assembly and migration in culture, as well as subcutaneous vessel remodeling *in vivo*. Stable knockdown of Slit2 in EPHA2-deficient endothelium rescued VEGF-mediated assembly and migration as well, whereas EPHA2 overexpression reduced Slit2 expression. Lastly, inhibiting Slit function rescued VEGF-dependent tumor angiogenesis *in vivo*, and restored VEGF-induced activation of Src and Rac, both of which are required for VEGF-mediated angiogenesis. Thus, elevated Slit2 in the absence of EPHA2 appears to be one mechanism that renders endothelium resistant to VEGF-induced vascular remodeling.

Materials and Methods

Reagents

Antibodies against the following proteins were used: Src, phospho-Src family (Tyr416; Cell Signaling Technology, Boston, MA); Rac (BD Biosciences, San Jose, CA); EPHA2 (SC-924), Robo4 (SC-67057), phosphotyrosine (PY99, SC-7020; PY20, SC-508) and actin (SC-1616; Santa Cruz Biotechnology, Santa Cruz, CA); von Willebrand factor (vWF; Zymed Laboratories, South San Francisco, CA); tubulin (Sigma Aldrich, St. Louise, MO). Pak-PBD agarose Rac assay reagent was purchased from Millipore (Billerica, MA). Recombinant mouse VEGF 164, rat Robo1-Fc, human IgG, and recombinant Slit2 were purchased from R&D Systems (Minneapolis, MN). Gelfoam absorbable gelatin sponges (Pharmacia) were obtained from the Vanderbilt University Hospital Pharmacy. TRITC-dextran, FITC-dextran, and 4',6-diamidino-2 phenylindole dihydrochloride (DAPI) were purchased from Sigma-Aldrich. Growth factor-reduced Matrigel was purchased from BD Biosciences. Arf6 activity assay kits were purchased from Cytoskeleton, Inc. (Denver, CO). Calbiochem SecinH3 Arf inhibitor was purchased from Millipore. Transwells were obtained from Corning, Inc.

(Corning, NY). Mouse Slit2 ELISA kit was purchased from Novatein Biosciences (Woburn, MA). 4T1 tumor cells were purchased from the American Type Culture Collection (ATCC, Manassas, VA) and maintained in Gibco DMEM Media (Life Technologies, Carlsbad, CA) supplemented with penicillin-streptomycin (Cellgro/Mediatech) and 10% fetal bovine serum (Hyclone, Logan, UT). Adenoviruses harboring wild-type EPHA2, kinase dead W42 mutant EPHA2 [141], and control LacZ were generated as described previously [270].

Endothelial cell culture

Immortalized murine pulmonary microvascular endothelial cells (MPMEC) were isolated from three month old wild-type or EPHA2-deficient H-2KB-tsA58 transgenic "Immorto-mice" [271, 272] as described previously [273]. Cells were maintained in EGM-2 medium (Lonza, Walkersville, MD) supplemented with penicillin-streptomycin and 10% fetal bovine serum. Cells were maintained at 33 °C in EGM-2 medium supplemented with interferon-g (10 ng/mL; Millipore), a permissive condition that allows the expression of the temperature sensitive SV40 T-antigen (Tag) transgene. The cells were incubated at 37 °C for at least 3 days in the absence of interferon-g to downregulate TAg expression and revert the cells to a non-immortalized state prior to experimental manipulation. Human primary retinal microvascular endothelial cells (HRMEC) were purchased from Cell Systems (Kirkland, WA) and maintained in EGM-2 medium as described above.

RT-PCR and ELISA

To generate conditioned medium (CM) from tumor cells and endothelial cells, 1 x 10^6 cells were plated in 10 cm dishes and grown to approximately 75% confluence in normal growth medium, then incubated in 3 mL of serum-free Opti-MEM medium for 48-hours. CM was collected and filtered in (0.2 mm syringe filters, VWR International, Radnor, PA) prior to use as described previously [260].

For Real Time PCR analyses, total RNA from triplicate sets of endothelial cells was isolated using Trizol (Invitrogen) as per the manufacturer's protocol. For some experiments, endothelial cells were incubated with CM from 4T1 tumor cells for 24-hours prior to RNA isolation. Expression of murine *slit2* or *robo1-4* mRNA in endothelial cells was validated by qRT-PCR analysis as described previously [260], using the following primers: Slit2 Fwd (20mer) 5'-agg gaa gat gag tgg cat tg-3' (240>259; NM_178804.2); Slit2 Rev (20mer) 5'-gtg cct gag acc agc aaa at-3' (486>467; NM_178804.2), and control 18S ribosomal RNA primers: Fwd (20mer) 5'-caa ctt tcg atg gta gtc gc-3'; Rev (21mer) 5'-cgc tat tgg agc tgg aat tac-3'. Primers for murine Robo1, 2, and 4 and endogenous control were purchased from Taqman (Mm00437762_m1 for B2m control; Mm00803879_m1 for Robo1; Mm00620713_m1 for Robo2; Mm00452963_m1 for Robo4). Expression of human *slit2* mRNA in HRMEC and *gapdh* control was scored using the TaqMan Gene Expression Assay (Life technologies): SLIT2 - Hs00191193_m1, GAPDH – Hs02758991_m1. Real Time PCR was performed using a StepOnePlus Real-Time PCR System from Applied Biosciences (Foster City, CA) with iQ SYBR supermix from BioRad. We used a two-step amplification procedure (40 cycles of 95C, 15sec 60C, 30sec followed by melting temperature determination stage) and quantified relative changes in gene expression using the DDCt method as per manufacturer's instructions.

Slit2 protein expression in undiluted endothelial CM was quantified by ELISA as per manufacturer's protocol. Plates were read using a BioTek Synergy HT (Winooski, VT) plate reader and associated software and data exported to Microsoft Excel for quantification and statistical analyses.

Stable shRNA-mediated Slit2 and Robo1 knockdown in endothelial cells

pGIPZ based shRNA vectors to knockdown mouse Slit2 and Robo1 were purchased from Open Biosystems (Slit2 V2LMM_92930, V3LMM_471050; Robo1

V2LMM_195374, V2LMM_83507; Thermo Fisher Scientific, Pittsburgh, PA), and the viruses were produced in 293T cells for infection with Cell Biolabs 2nd generation lentivirus packaging system (San Diego, CA) as per supplier's instructions. Infected EPHA2-deficient MPMEC were selected in 2 μg/mL puromycin and pooled clones tested in assembly and migration assays as described below. We confirmed diminished Slit2 protein expression by ELISA analysis of CM from knockdown clones versus vector control, and diminished expression of Robo1 mRNA by Real-Time qRT-PCR, as described above.

Transient siRNA-mediated EPHA2 knockdown in human endothelial cells

Human EPHA2-targeting and control siRNAs were purchased from and transfected into HRMEC. *EPHA2* ON-TARGETplus Human SMARTpool siRNA (L-003116-00-0005) and ON-TARGETplus Non-Targeting pool siRNA (D-001810-10-05) (Dharmacon/Thermo Scientific) were used at a concentration of 12.5 nM in conjunction with Lipofectamine RNAiMAX transfection reagent (Invitrogen) according to the manufacturer's protocol as described previously [130]. Assembly assays were performed 48 hours post-transfection. Knockdown was confirmed by immunoblot analysis as described below.

***In vitro* angiogenesis assays**

In vitro vascular assembly assays were performed as described previously [270, 273].Briefly, 12-well plates were coated with 100 mL of growth factor reduced Matrigel (BD Biosciences). After 24 hour starvation in Opti-MEM, 25,000 MPMEC or HRMEC were plated in wells in the presence or absence of VEGF (50 ng/mL) plus or minus Slit2 (100 ng/mL), Robo1-Fc (1 mg/mL) or control IgG (1 mg/mL) and photographed after 24-hours. For some studies, assays were performed in the presence of SecinH3 Arf inhibitor (5 mM) or DMSO vehicle control. Images were acquired using an Olympus CK40 inverted microscope through an Optronics DEI-750C CCD video camera using CellSens capture software. Adjustments were applied

to the entire image using Adobe Photoshop (CS6) software and were consistent between experimental and control images. The degree of assembly was quantified by measuring branch length, the distance from branching point to the tip of assembled cells. The branch length in assembled endothelial cell networks was expressed as arbitrary units per 10X field in four random fields from each well, with triplicate samples per condition, using Scion Image version 1.62c software. For some experiments, endothelial cells were transduced with recombinant adenoviruses (10^8 pfu/mL) or transfected with siRNAs 48 hours prior to assembly assay.

For migration assays, endothelial cells were serum-starved for 24-hours in Opti-MEM medium. Transwells were coated with growth factor reduced Matrigel (1:20 dilution with Opti-MEM) for 30 minutes and blocked with 1% bovine serum albumin solution for an additional 30 minutes. One hundred thousand cells were plated in the upper chamber of the transwells, and 600 mL of Opti-MEM medium containing VEGF (50 ng/mL) plus or minus Slit2 (100 ng/mL), Robo1-Fc (1 mg/mL) or control IgG was added to the lower chamber. After 5-hours, cells were fixed and stained with crystal violet to visualize endothelial cells. Cells that migrated to the lower surface of transwell filters were counted in four random fields from each well, with triplicate samples per condition as described previously [270, 273].

***In vivo* sponge assays for angiogenesis**

Sponge assays for angiogenesis were performed as described previously [270, 274]. Briefly, gel foam sponges were cut into small pieces (2.5 to 3 mm wide by 5 mm long) and soaked with 100 mL of phosphate-buffered saline containing 100 ng of VEGF plus or minus Slit2 (100 ng), Robo1-Fc (2.5 mg) or control IgG. The sponges were then implanted into the subcutaneous dorsal flank of three-month-old female Balb/c wild-type or EPHA2-deficient recipient female mice. Each recipient received one pro-angiogenic factor impregnated sponge and one relevant control factor impregnated sponge implanted in the opposite flank. After 7 days, the mice were

injected with a 2% tetramethyl rhodamine isothiocyanate (TRITC)-dextran-phosphate-buffered saline solution or 2% fluorescein isothiocyanate (FITC)-dextran-phosphate-buffered saline solution to label host blood vessels [270, 274], and the sponges were collected and analyzed. Whole-mount images were acquired on an Olympus CK40 inverted microscope through an Optronics DEI-750C charge-coupled-device video camera using CellSens capture software. Density of blood vessels within the sponges was quantified by fluorescence intensity (10X magnification) of TRITC-dextran or FITC-dextran using Scion Image software, version 1.62c. Data are a representation of results from five independent sponges under each condition. Statistical significance was determined by a two-tailed, paired Student's t test. Vessel identity was confirmed in paraffin sections prepared from sponges and counterstained with DAPI and/or co-stained with the endothelial cell marker von Willebrand Factor (vWF) as described previously [131, 194, 275].

Tumor-endothelial cell co-culture migration assays

For co-culture experiments, transwells were coated with growth factor-reduced Matrigel (1:20 dilution) and 1 x 10^5 4T1-GFP cells were plated on the lower surface of the transwell filter. Wild-type or EPHA2-deficient endothelial cells (1 x 10^5) labeled with CellTracker Orange CMTMR dye (Molecular Probes/Life Technologies) were added to upper transwell chambers in the presence or absence of Slit2 (100 ng/mL), Robo1-Fc (1 mg/mL), or control IgG (100 ng/mL to 1 mg/mL). After 5 h, cells were removed from the upper surface of the transwell filter using a cotton swab, and endothelial cells on the lower surface of the filter quantified. Similar experiments were performed comparing EPHA2-deficient endothelial cells expressing control versus Slit2 shRNAs. Data are a representation of six to nine independent samples per condition with standard deviation, and statistical significance was assessed by two-tailed, paired Student's t test.

Cutaneous window chamber assay

Window assays were performed as described previously [197, 276]. Briefly, a 5 mm diameter flap of skin was dissected away from the dorsal skin flap of anesthetized recipient wild-type or EPHA2-deficient three month old Balb/c female mice, leaving a fascial plane with associated vasculature. A gelfoam sponge (approximately 1 mm in diameter) impregnated with 1 mg of Slit2, Robo1-Fc, or control IgG in 50% Matrigel/PBS was implanted in the window chamber adjacent to a portion of 4T1 tumor (approximately 0.7 mm in diameter) isolated from a donor mouse. The chambers were sealed with glass coverslips and photographed on 1 day following implantation to measure initial tumor size and baseline vascular morphology. 7 days after implantation, FITC-conjugated dextran (2% in PBS, Sigma-Aldrich) was injected intravenously, and tumors in window chambers were photodocumented using an Olympus BX60 microscope and digital camera. Branches from host blood vessels within the window chambers were enumerated in at least three independent fields per mouse, and statistical significance was determined by two-tailed, paired Student's t-test. Data are a representation of 6-8 independent samples per condition with standard error of the mean, and statistical significance was assessed by two-tailed, paired Student's t-test.

Orthotopic tumor transplantation

4T1 tumor cells (1×10^5) were resuspended in growth-factor reduced Matrigel plus or minus IgG (1 mg), Slit2 (100 ng), or Robo1-Fc (1 mg) and orthotopically transplanted in the mammary glands of recipient wild-type (IgG or Slit2) or EPHA2-deficient (IgG or Robo1-Fc) three month old Balb/c female mice as described previously [131]. Tumors were harvested after 7 days, measured by digital caliper, and volume was calculated [length x width^2 x 0.52]. Tumor sections were stained for the endothelial marker vWF factor and microvascular density quantified based on pixel density as described previously [131, 194, 275].

Immunoblot analyses

Endothelial cells were serum-starved for 24-hours in Opti-MEM + 2% FCS. For EPHA2-deficient cells, 1 mg/mL Robo1-Fc or control IgG was added to the starvation medium. Rac activation in approximately 500 mg endothelial cell lysate was assessed by Pak-PBD agarose Rac assay reagent as described previously [270, 273]. Arf6 activation was assessed by GGA3-PBD effector pulldown assay as per supplier's protocol (Cytoskeleton, Inc.). For some assays, cells were pre-treated with SecinH3 Arf inhibitor (5 mM) or DMSO vehicle for one hour prior to stimulation. For analysis of Src phosphorylation and expression, approximately 50 mg of endothelial cell lysates were collected and processed as per antibody supplier's protocol (Cell Signaling Technologies). For all experiments, cells were stimulated with VEGF (50 ng/mL) plus or minus Slit2 (100 ng/mL), Robo1-Fc (1 mg/mL) or control IgG for 5 (Rac, Arf6) to 10 (Src) minutes, or for 16 hours with Robo1-Fc (1 mg/mL) to score rescue of basal Rac activity. The blots were stripped and re-probed with anti-actin or tubulin antibodies to confirm uniform loading and anti-EPHA2 antibodies to confirm EPHA2-deficiency in knockout cell lines. Data are a representation of three to five independent experiments.

Ethics Statement

All animals were housed under pathogen-free conditions, and experiments were performed in accordance with AAALAC guidelines and with Vanderbilt University Institutional Animal Care and Use Committee approval. The laboratory animal care program of Vanderbilt University (PHS Assurance #A3227-01) has been accredited by AAALAC International since 1967 (File #000020). The AAALAC Council on Accreditation's most recent review of VU's program was done in 2011 and resulted in "Continued Full Accreditation." EPHA2-deficient Balb/C congenics were generated, genotyped, and maintained as described previously [131].

Cell Line Statement

4T1-GFP cells generated in the laboratory of Mark Dewhirst (Duke University) were obtained from Dr. Charles Lin, where they were authenticated for tumor formation Balb/C mice *in vivo* [277], and were expanded and frozen upon receipt. Vials used in this study were passaged in our laboratory for fewer than six months after resuscitation.

Results

Slit2 expression is elevated in EPHA2-deficient endothelial cells and affects signaling downstream of VEGF

Recent studies demonstrated that *slit2* mRNA was significantly increased in EPHA2 deficient endothelium relative to wild-type controls [260]. Immunofluorescence staining suggested that protein levels were also higher in knockout cells, though these data were more qualitative. In this study, we quantified protein expression in endothelial cell conditioned medium by ELISA, which revealed significantly higher levels of Slit2 in EPHA2-deficient endothelial cells relative to wild-type controls (Figure 4.1A), consistent with our previous microarray and Real Time PCR studies [260].

Our previous studies compared Slit2 expression in normal endothelial cells harvested from wild-type and EPHA2-deficient animals and cultured in endothelial cell growth medium. To determine if overexpression persisted in knockout cells in the context of tumor angiogenesis, we repeated our analyses in endothelial cells treated with conditioned medium from 4T1 mouse mammary tumor cells. Treatment with tumor conditioned medium reduced levels of Slit2 relative to what

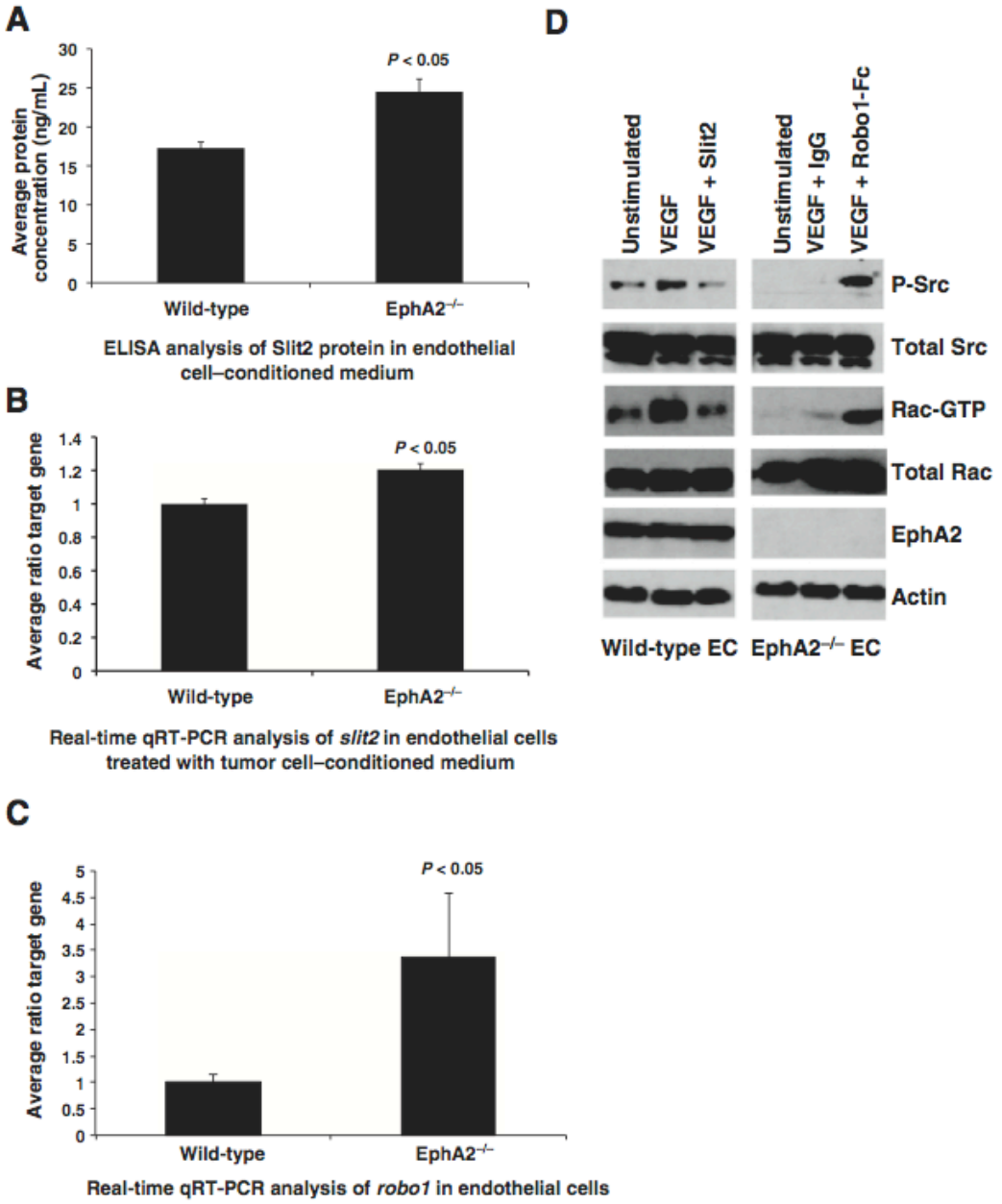

Figure 4.1 Slit2 expression is elevated in EPHA2-deficient endothelial cells and affects signaling downstream of VEGF. (A) Endothelial cells were grown in EGM-2 for 24-hours. Growth medium was replaced with 3 mL of serum-free media and cells incubated for 48-hours to generate conditioned medium. Conditioned medium was harvested and protein expression of secreted murine Slit2 quantified by ELISA. Levels of secreted Slit2 were significantly higher in EPHA2-deficient endothelial cells relative to wild-type endothelial cells. **(B)** Endothelial cells were grown in EGM-2 for 24-hours. Growth medium was replaced with 3 mL of conditioned medium from 4T1 mouse mammary tumor cells and cells incubated for 48-hours. RNA was harvested and subjected to Real-Time PCR to quantify *slit2* mRNA expression. Expression of *slit2* mRNA was significantly elevated in EPHA2-deficient endothelial cells relative to wild-type endothelial cells. **(C)** Real-Time PCR analysis confirmed

significantly elevated levels of *robo1* mRNA in EPHA2-deficient endothelial cells relative to wild-type controls. **(D)** Slit2 inhibited VEGF-induced activation of the intracellular serine/threonine kinase Src, as measured by phosphorylation, as well as activation of Rac-GTPase, as measured by detection of GTP-bound (active) Rac, in wild-type endothelial cells. Addition of soluble Robo1-Fc receptor, a Slit ligand trap, partially rescued VEGF-induced Src and Rac activity in EPHA2-deficient endothelial cells. Data are a representation of three independent wild-type versus three independent EPHA2-deficient immortalized endothelial cell lines/genotype from two independent experiments, with average +/- standard deviation. Statistical significance was assessed by two-tailed, paired Student's t-test.

we previously observed in normal endothelial cells, as expected based on the reported tumor suppressive role for Slit2 [260]. Still, elevated expression of *slit2* persisted in EPHA2-deficient endothelial cells relative to wild-type control endothelial cells upon treatment with tumor-conditioned medium (Figure 4.1B). These data suggest that Slit2 overexpression in the absence of EPHA2 may affect both normal physiologic and tumor angiogenesis. While we did not detect high expression levels of *robo2* or *robo4* in our lung microvascular endothelial cell lines (data not shown), *robo1* levels were significantly elevated in EPHA2-null endothelial cells relative to wild-type cells (Figure 4.1C).

We next assessed activation of signaling pathways downstream of Slit-Robo in wild-type versus EPHA2-deficient endothelium. Previous studies reported that Slit2 co-stimulation impairs VEGF-induced activation of Src and Rac, two major downstream signaling mediators through which VEGF stimulates angiogenic remodeling [255, 257]. As EPHA2-deficient endothelial cells are resistant to VEGF-induced angiogenesis [198, 242-246], we compared Src phosphorylation and levels of active, GTP-bound Rac in wild type cells treated with VEGF plus exogenous Slit2 to levels in EPHA2-deficient endothelial cells treated with VEGF in the presence of Robo1-Fc, a ligand trap for available Slit proteins. We confirmed inhibition of Src and Rac activities in wild-type endothelial cells stimulated with VEGF in the presence of recombinant Slit2 (Figure 4.1D). VEGF-induced activation of Src and Rac were

markedly reduced in EPHA2-deficient cells, consistent with elevated expression of Slit2 in these cells. Pre-treatment with Robo1-Fc rescued activation of Src and Rac in response to VEGF in EPHA2-deficient endothelial cells (Fig. 1d). These data suggest that elevated Slit2 levels in EPHA2-deficient endothelium may promote resistance to VEGF-mediated angiogenesis through its angiostatic function.

Inhibiting Slit activity rescues VEGF-induced vascular assembly and migration in EPHA2-deficient endothelial cells.

EPHA2-deficiency not only impairs angiogenic remodeling in response to ephrins, but also in response to VEGF (Figure 4.2; [198, 242-246]). As Slit2 has also been reported to inhibit angiogenesis induced by VEGF [254-257], we hypothesized that Slit2 overexpression in EPHA2-deficient endothelium might account for this defect. To test this hypothesis, we scored endothelial assembly on Matrigel and migration through transwells, comparing wild-type cells treated with VEGF to EPHA2-deficient cells treated with VEGF in the presence or absence of Robo1-Fc ligand trap. Wild-type endothelial cells assembled into interconnected structures resembling a primitive capillary plexus when plated on a thin layer of Matrigel in the presence of VEGF (Figure 4.2A). While VEGF stimulation in the presence of control IgG failed to induce a robust assembly response in EPHA2-deficient cells, pre-treatment with soluble Robo1-Fc partially rescued assembly (Figure 4.2A). Robo1-Fc treatment also partially rescued VEGF-induced migration of EPHA2-deficient endothelial cells (Figure 4.2B).

Co-stimulation of wild-type endothelial cells with Slit2 and VEGF inhibits angiogenic remodeling ([255, 257]; Figure 4.2C). Previous studies have linked Slit2 and VEGF to inhibitory modulation of ADP ribosylation factor 6 (Arf6) GTPase [255, 257], an upstream regulator of Rac activity [278]. Therefore, we assessed levels of active, GTP-bound Arf6 in wild-type endothelial cells treated with VEGF versus VEGF plus Slit2. Surprisingly, co-stimulation resulted in activation of Arf6 relative to untreated

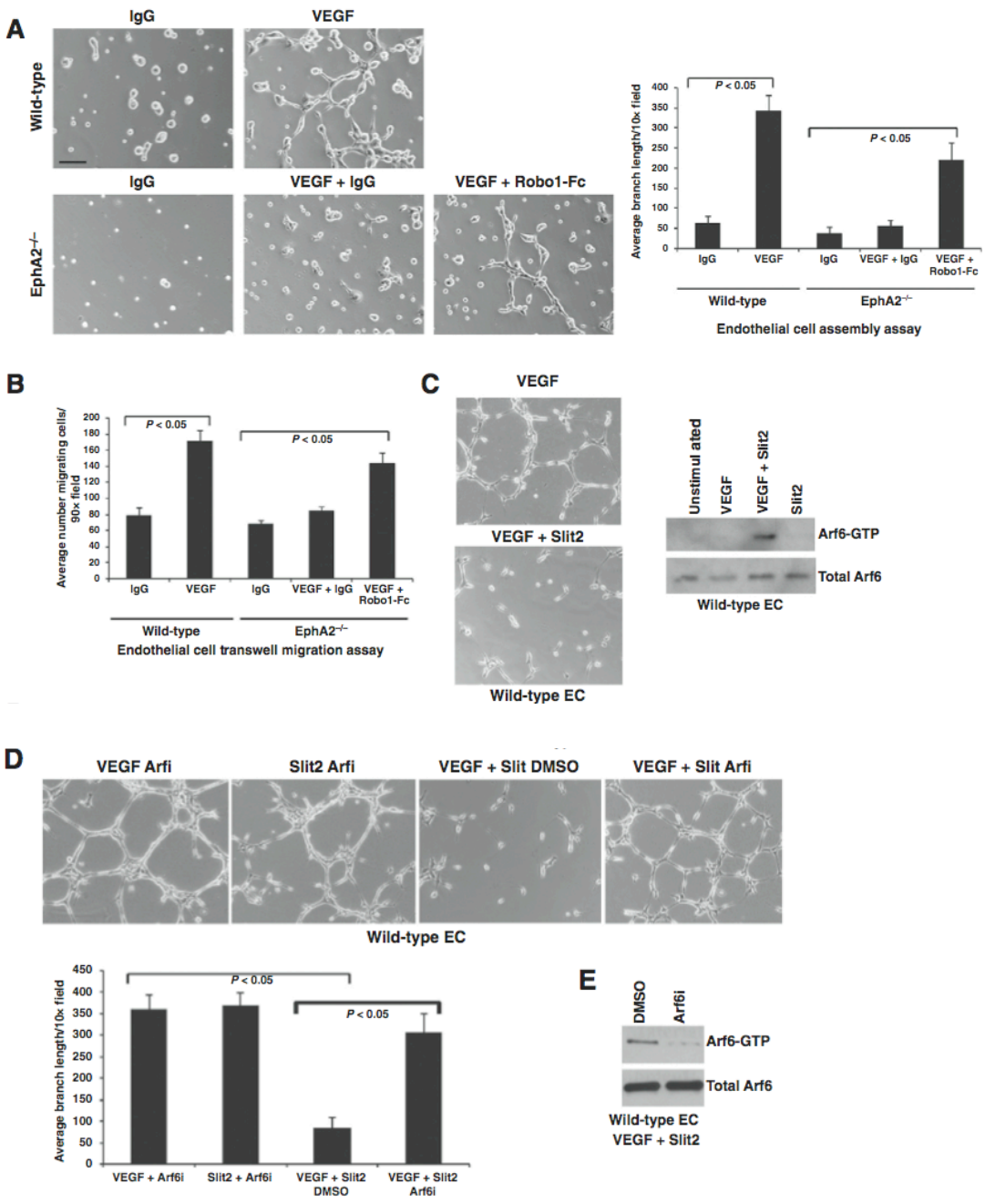

Figure 4.2 Inhibiting Slit activity rescues VEGF-induced vascular assembly and migration in EPHA2-deficient endothelial cells. (A) Endothelial cells were plated on a thin layer of growth factor-reduced Matrigel to score assembly into interconnected vascular networks in response to VEGF. EPHA2-deficiency impaired VEGF-induced assembly relative to wild-type controls. Addition of soluble Robo1-Fc receptor partially rescued VEGF-induced assembly of EPHA2-deficient endothelial cells relative to IgG control plus VEGF. Scale bar = 20 mm. **(B)** We observed a similar trend in endothelial cell motility as scored by transwell assay. Relative to wild-type endothelial cells, EPHA2-deficienct cells displayed impaired migration in response to VEGF, though addition of Robo1-Fc partially rescued VEGF-induced migration.

(C) Co-stimulation with VEGF and Slit2 impairs endothelial cell assembly relative to VEGF alone. We observed that co-stimulation induced activation of Arf6-GTPase, as measured by detection of GTP-bound (active) Arf6, in wild-type endothelial cells relative to untreated controls or cells treated with VEGF or Slit2 as single agents. (**D)** Treatment with an Arf inhibitor significantly rescued assembly in cells co-stimulated with VEGF and Slit2 relative to DMSO vehicle control. The inhibitor had no effect on assembly induced by VEGF or Slit2 as a single agent in wild-type endothelial cells. **(E)** We confirmed Arf6 inhibitor reduced levels of active, GTP-bound Arft6 in wild-type endothelial cells co-stimulated with VEGF and Slit2 by effector pull-down followed by western analysis. Data are a representation of three to five independent experiments, with replicate samples analyzed in each experiment, with average +/- standard deviation. Statistical significance was assessed by two-tailed, paired Student's t-test.

cells or cells stimulated with VEGF or Slit2 alone in our model system (Figure 4.2C), though VEGF was reported to activate Arf6 in HUVEC [279]. As high levels of Arf6 activity upon VEGF and Slit2 co-stimulation correlate with angiostasis, we wish to determine if blocking Arf6 restored angiogenesis in co-stimulated cells. Treatment with SecinH3 Arf inhibitor significantly rescued assembly in wild-type endothelial cells co-stimulated with VEGF and Slit2 relative to vehicle control (Figure 4.2D). Consistent with our activity assays, the Arf inhibitor did not affect angiogenesis induced by either VEGF or Slit2 alone (Figure 4.2D). We confirmed Arf6 inhibition of upon treatment with SecinH3 in wild-type endothelial cells co-stimulated with VEGF and Slit2 (Figure 4.2E).

Consistent with our previous studies [269], treatment of wild-type endothelial cells with Slit2 as a single agent induced endothelial assembly and migration (Figure 4.3A) Slit2 and VEGF co-stimulation inhibited assembly and migration of wild-type endothelial cells (Figure 4.3A) as previously reported [255, 257], and at a dose range consistent with levels observed in our ELISA analyses (Figure 4.4). Robo1-Fc did not induce assembly or migration in wild-type endothelium, nor did it enhance VEGF-induced assembly or migration (Figure 4.3A). Robo1-Fc treatment, however, partially rescued basal assembly in EPHA2-deficient endothelial cells, though to a lesser

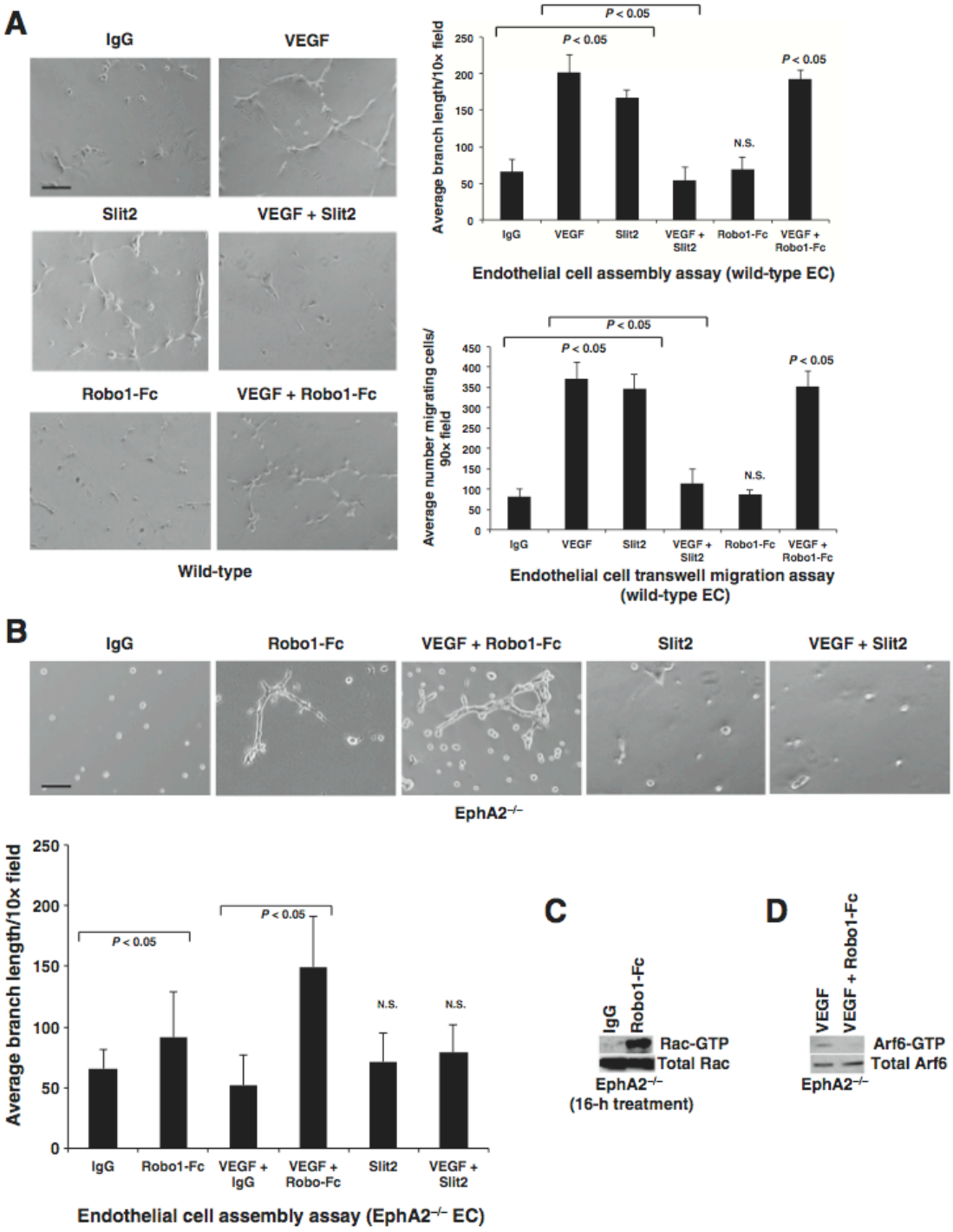

Figure 4.3 Slit2 inhibits VEGF-induced assembly and migration in wild-type cells, and inhibiting Slit activity in EPHA2-deficient cells rescues basal vascular assembly. (A) Individually, Slit2 or VEGF stimulated assembly and transwell migration in wild-type endothelial cells. The combination of VEGF and Slit2, however, significantly inhibited both assembly and migration. Robo1-Fc alone or in combination with VEGF did not significantly alter wild-type endothelial cell assembly or migration. (B) Addition of soluble Robo1-Fc

receptor partially rescued basal assembly of EPHA2-deficient endothelial cells in serum-free media after 24-hours, though to a lesser extent than in the presence of VEGF. Addition of Slit2 to EPHA2-deficient endothelial cells did not affect basal or VEGF-induced angiogenesis. **(C)** Consistent with these data, EPHA2-deficient endothelial cells treated with Robo1-Fc for 16-hours elevated basal Rac activity. **(D)** Levels of active, GTP-bound Arf6 were significantly reduced in VEGF-treated EPHA2-deficient endothelial cells upon co-treatment with Robo1-Fc, as observed using effector pull-down followed by western analysis. Data are a representation of two to three independent experiments, with replicate samples analyzed in each experiment, with average +/- standard deviation. Statistical significance was assessed by two-tailed, paired Student's t-test. N.S. = not significant (relative to IgG control).

extent relative to co-stimulation with VEGF (Figure 4.3B). Prolonged treatment with Robo1-Fc alone (16-hours) induced Rac activity (Figure 4.3C) in EPHA2-deficient endothelial cells, consistent with rescue of assembly by Robo1-Fc (24-hours; Figure 4.3B). Activated, GTP-bound Arf6 was detected in EPHA2-deficient endothelial cells stimulated with VEGF (Figure 4.3D). As expression of Slit2 is elevated in EPHA2-deficient endothelial cells, these data are consistent with activation of Arf6 in the context of Slit2 and VEGF co-stimulation (Figure 4.3C) and support an angiostatic function for Arf6 in our cell model. In addition, Arf6-GTP levels were reduced in

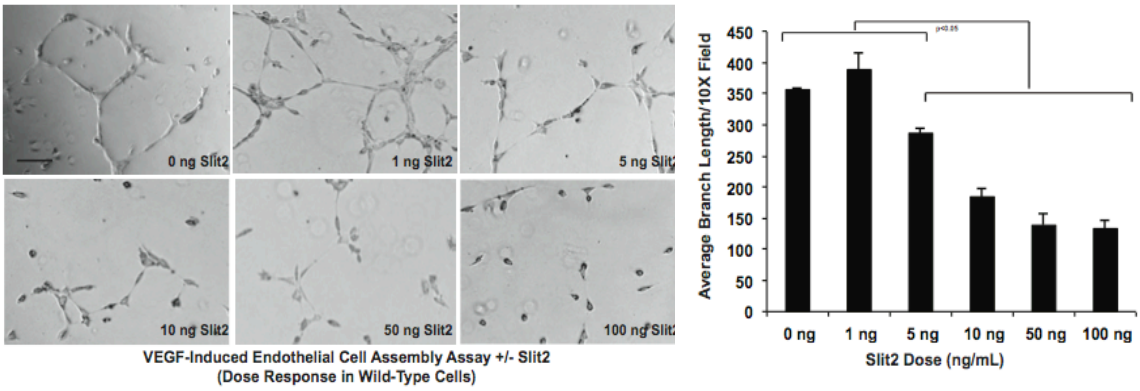

Figure 4.4: Dose response for Slit2-mediated inhibition of VEGF-induced vascular assembly. Wild-type endothelial cells were plated on a thin layer of growth factor-reduced Matrigel to score assembly into interconnected vascular networks in response to VEGF in the presence of increasing concentrations of Slit2. Doses between 10 and 100 ng/mL significantly impaired VEGF-induced assembly in culture. Scale bar = 20 µm. Data are a representation of three to five independent samples/condition with average +/- standard deviation. Statistical significance was assessed by two-tailed, paired Student's t-test.

EPHA2-deficient endothelial cells treated with VEGF in the presence of Robo1-Fc ligand trap (Figure 4.3D), supporting the hypothesis that Arf6 activation inhibits angiogenesis in Slit2/VEGF-stimulated microvascular endothelial cells. Addition of exogenous Slit2 did not induce assembly in EPHA2-deficient endothelial cells, nor did it affect assembly in the presence of VEGF (Figure 4.3B).

To confirm our results from EPHA2-deficient murine microvascular endothelial cells, we tested the impact of EPHA2 siRNA-mediated knockdown in human endothelial cells. EPHA2 knockdown in primary human retinal microvascular endothelial cells (HRMEC) significantly reduced assembly in response to VEGF relative to control siRNA expressing cells (Figure 4.5A). Addition of Robo1-Fc partially rescued VEGF-mediated assembly in EPHA2 knockdown lines, as did prolonged treatment of Robo1-Fc alone, albeit to a lesser extent. Exogenous Slit2 promoted assembly in control siRNA lines, whereas co-stimulation with Slit2 and VEGF impaired assembly (Figure 4.5A), consistent with our findings in murine cell lines and in previous studies [254-257]. We confirmed EPHA2 knockdown in lysates from HRMEC via immunoblot (Figure 4.5B) and upregulation of Slit2 expression by Real-Time qRT-PCR analysis (Figure 4.5C).

To confirm our results and to determine if blocking Slit2 expression specifically rescues VEGF-induced angiogenic remodeling, we generated two independent EPHA2-deficient cell lines stably expressing *slit2* shRNA sequences. Relative to vector control, VEGF induced a significant assembly response in EPHA2-deficient Slit2 knockdown lines (Figure. 4.6A). In addition, VEGF-induced migration was also rescued in Slit2 knockdown clones (Figure. 4.6B). Analysis and quantification of Slit2 protein in endothelial cell conditioned medium confirmed knockdown in shRNA clones relative to vector control (Figure 4.6C). Consistent with data derived from Robo1-Fc treatment, stable Slit2 shRNA knockdown in EPHA2-deficient endothelial cells rescued Src and Rac activity upon VEGF stimulation (Figure. 46D).

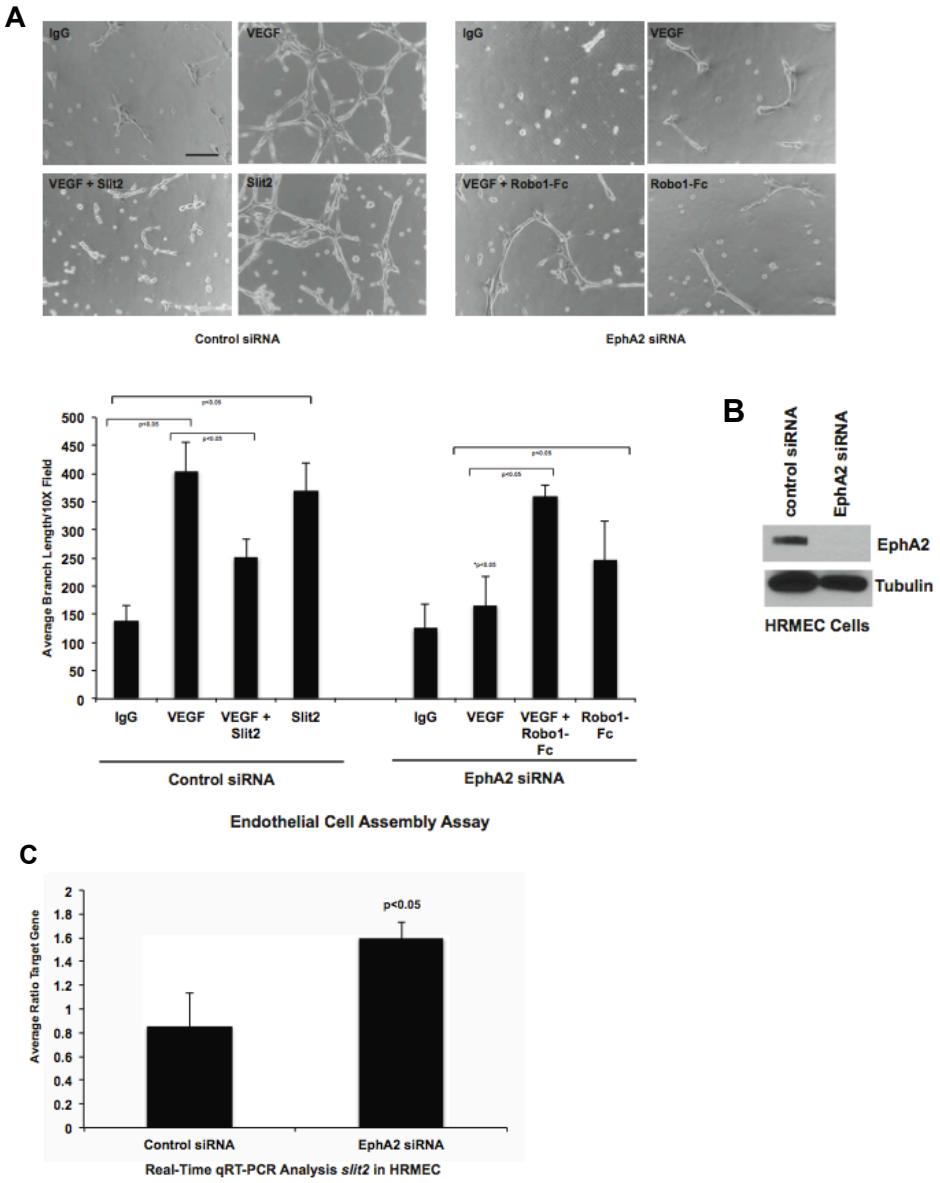

Figure 4.5 Inhibiting Slit activity rescues VEGF-induced vascular assembly and migration in EphA2 knockdown in human endothelial cells. (A) Human retinal microvascular endothelial cells (HRMEC) transfected with control versus EphA2 siRNA were plated on a thin layer of growth factor-reduced Matrigel to score assembly into interconnected vascular networks in response to VEGF. EphA2 knockdown impaired VEGF-induced assembly relative to Control siRNA. Addition of Robo1-Fc receptor partially rescued VEGF-induced assembly of EphA2 siRNA endothelial cells relative to IgG control plus VEGF. Slit2 alone promoted angiogenesis in Control siRNA cells, and prolonged treatment with Robo1-Fc partially rescued basal assembly in EphA2 siRNA treated cells. Scale bar=20µm. **(B)** EphA2 knockdown was confirmed by immuoblot. **(C)** qRT-PCR revealed significantly elevated levels of *slit2* mRNA in EphA2 siRNA treated endothelial cells relative to controls. Data represent 3 to 5 independent experiments, with replicate samples analyzed in each experiment, with average +/- standard deviation. Statistical significance was assessed by two-tailed, paired Student's t-test.

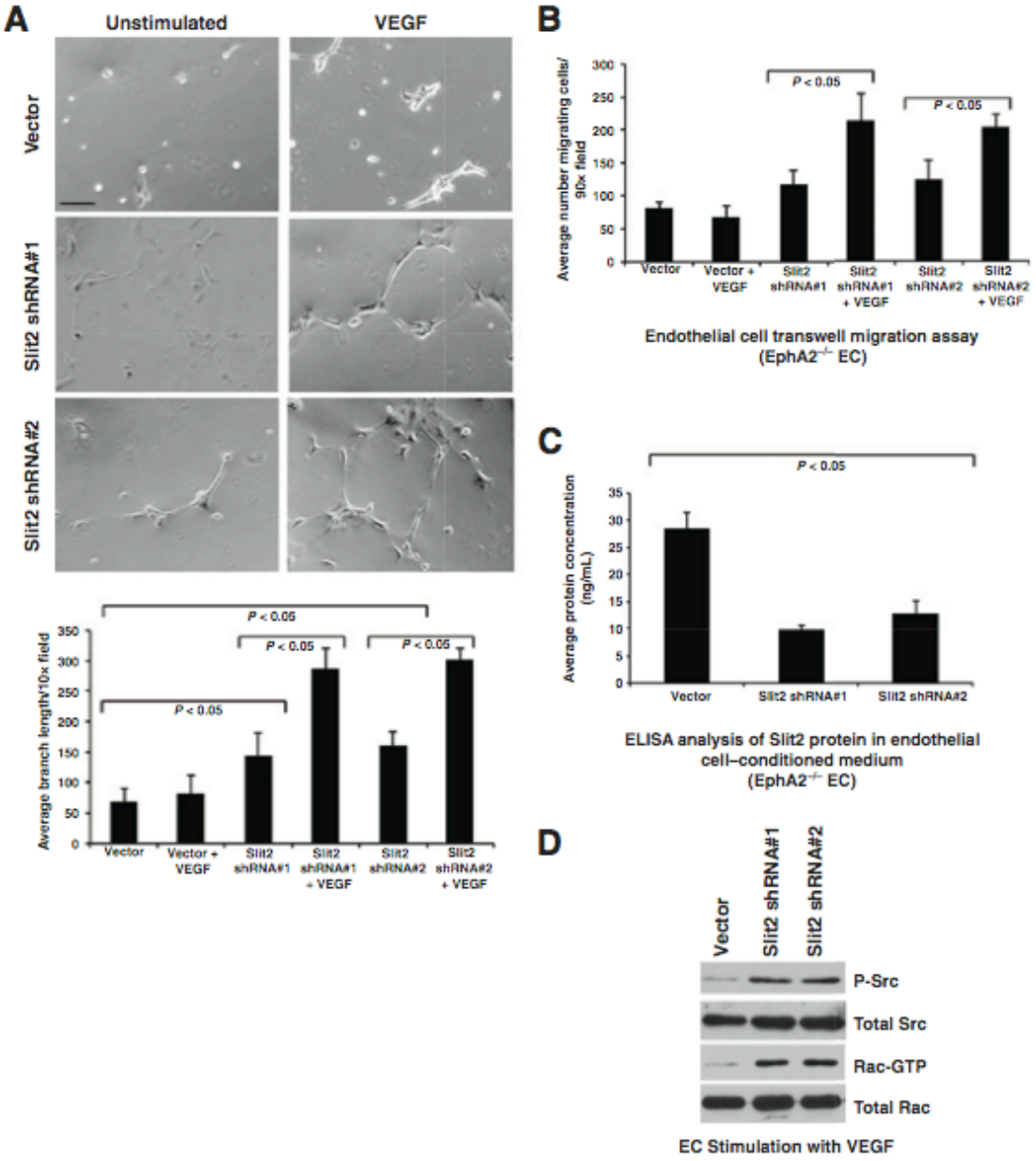

Figure 4.6 Slit2 knockdown rescues VEGF-induced vascular assembly and migration in EPHA2-deficient endothelial cells. (A) Relative to vector controls, EPHA2-deficient endothelial cells stably expressing two independent *slit2* shRNA constructs displayed increased basal and VEGF-induced assembly. **(B)** Stable *slit2* knockdown also rescued VEGF-induced migration of EPHA2-deficient endothelial cells relative to vector controls in transwell assays. **(C)** We confirmed decreased expression of Slit2 protein in knockdown clones relative to vector control lines by ELISA analysis. Data are a representation of two independent experiments, with replicate samples analyzed in each experiment, with average +/- standard deviation. Statistical significance was assessed by two-tailed, paired Student's t-test. **(D)** Consistent with data from treatment with Robo1-Fc, *slit2* knockdown rescued VEGF-induced Src and Rac activity.

EPHA2 gain-of-function significantly diminishes slit2 expression in endothelium

To determine if EPHA2 gain-of-function modulates Slit2 expression, we analyzed Slit2 protein levels in conditioned medium from EPHA2-deficient cells transduced with adenoviruses harboring control LacZ (Ad.LacZ) or wild-type EPHA2 (Ad.EPHA2) transgenes. Relative to Ad.LacZ controls, Ad.EPHA2-expressing cells secreted significantly lower levels of Slit2 protein into conditioned medium, comparable to levels detected in wild-type cells (Figure 4.7A) EPHA2-deficiency or knockdown results in elevated expression of *slit2*, which is at least partially responsible for EPHA2-mediated resistance to VEGF-induced angiogenesis. Overexpression of wild-type, but not kinase dead EPHA2 in EPHA2-deficient endothelial cells was sufficient to induce spontaneous assembly, with branch lengths significantly greater compared to partial rescue by Robo1-Fc plus VEGF (Figure 4.7B). Immunblot analysis confirmed overexpression of Ad.EPHA2 transgenes in transduced endothelial cells (Figure 4.7C). Consistent with data derived from wild-type endothelial cells, addition of exogenous Slit2 significantly inhibited assembly in Ad.EPHA2 overexpressing cells, both alone and in the presence of VEGF (Figure 4.7D). These data suggest that suppression of Slit2 expression by EPHA2 facilitates VEGF-induced angiogenesis.

Inhibiting Slit activity rescues VEGF-induced angiogenesis in EPHA2-deficient animals *in vivo*.

To determine if modulating Slit function affects vascular remodeling from intact vessels *in vivo*, we implanted sponges seeded with VEGF plus or minus IgG control versus recombinant Robo-1-Fc subcutaneously into the dorsal flank of recipient wild-type or EPHA2-deficient mice. One week following implantation, we injected mice intravenously with TRITC-dextran to visualize and quantify blood vessel infiltration into the sponge. Sponges harboring VEGF stimulated a robust angiogenic response in wild-type mice, with a significant increase in TRITC+ surface blood vessels (upper panels) and TRITC+ blood vessels infiltrating sponges in tissue sections (lower panels), relative to sponges containing IgG control (Figure 4.8A and B; data not

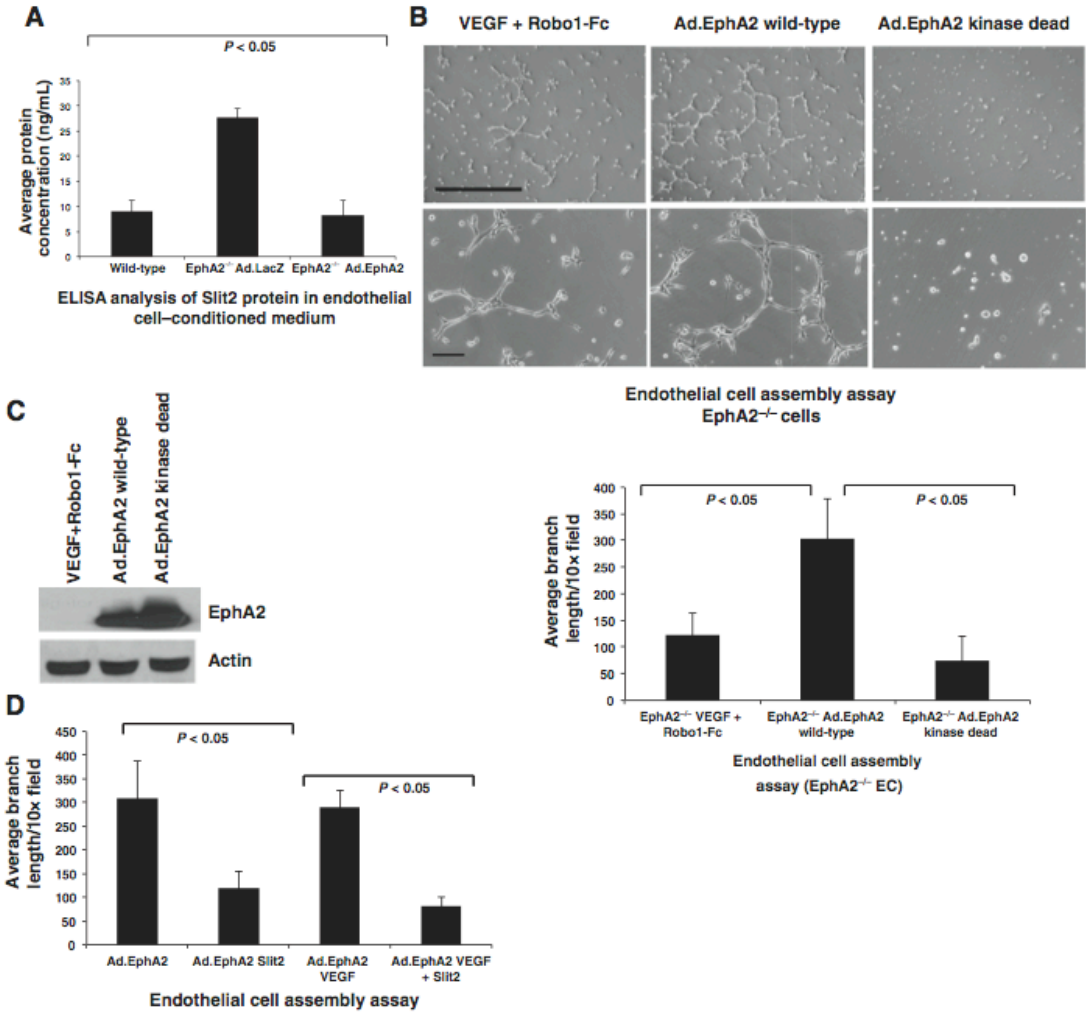

Figure 4.7 EPHA2 overexpression reduces Slit2 expression, and exogenous Slit2 inhibits endothelial cell assembly induced by EPHA2 gain-of-function. (A) EPHA2-deficient endothelial cells were transduced with adenoviruses harboring control LacZ (Ad.LacZ) or wild-type EPHA2 (Ad.EPHA2). Conditioned medium was harvested and protein expression of secreted murine Slit2 quantified by ELISA. Levels of secreted Slit2 were significantly higher in EPHA2-deficient endothelial cells expressing control Ad.LacZ relative to wild-type endothelial cells, and overexpression of Ad.EPHA2 reduced Slit2 protein levels back to the level observed in wild-type controls. **(B)** Overexpression of wild-type, but not kinase dead, EPHA2 rescued assembly in EPHA2-deficient cells to a greater extent than VEGF + Robo1-Fc, highlighting the importance of EPHA2 receptor function as an additional regulator of angiogenesis. Scale bar = 100 mm (upper panels) and 20 mm (lower panels). **(C)** Expression of adenoviral gene products was confirmed by immunoblot. **(D)** Consistent with data from wild-type endothelial cells, assembly induced by overexpression of Ad.EPHA2 was significantly reduced by treatment with exogenous Slit2 in the presence or absence of VEGF. Data are a representation of two independent experiments, with replicate samples analyzed in each experiment, with average +/- standard deviation. Statistical significance was assessed by two-tailed, paired Student's t-test.

shown). VEGF failed to induce angiogenesis in EPHA2-deficient mice in the presence of control IgG. In the presence of Robo1-Fc, however, we observed a partial rescue of subcutaneous angiogenesis (Figure 4.8A and B). The TRITC+ structures in sponge sections co-stained with von Willebrand Factor (vWF, green; Figure 4.8C), a marker for vascular endothelium, confirming that the TRITC+ structures observed were functional blood vessels. Consistent with our previous studies [269], single agent Slit2 induced angiogenesis in sponge assays (Figure 4.8D), whereas Slit2 impaired VEGF-induced subcutaneous vascular remodeling (Figure 4.8D and E; [254-257]), supporting the pro-angiogenic function of Slit2 as a single agent and its angiostatic funciton in the presence of VEGF co-stimulation. Taken together, these data support the hypothesis that elevated Slit2 in EPHA2-deficient endothelium, at least in part, mediates resistance to VEGF-mediated angiogenesis.

Inhibiting Slit activity rescues tumor-induced angiogenesis and growth in EPHA2-deficient animals *in vivo*

Given (i) the role of VEGF and EPHA2 in tumor angiogenesis, (ii) the observation that loss of EPHA2 impairs VEGF-induced angiogenesis, (iii) the known role of Slit2 in suppression of VEGF-induced angiogenesis and (iv) our data demonstrating that Slit2 is elevated in EPHA2-deficient endothelium, we wished to determine if Slit2 upregulation was, at least in part, responsible for defective tumor neovascularization in EPHA2-deficient animals. Indeed, EPHA2-deficiency and inhibition impairs angiogenesis and growth of VEGF-expressing tumors *in vivo* [131, 137, 197, 242-244]. To determine if Slit function mediates this phenotype, we first assessed endothelial cell migration in response to tumor cells in modified transwell chamber co-culture assays [Figure 4.9A; [197]]. 4T1-GFP tumor cells were plated on the lower surface of Matrigel-coated transwells. Endothelial cells were labeled with CellTracker dye and added to the upper chamber, and migration and intercalation of

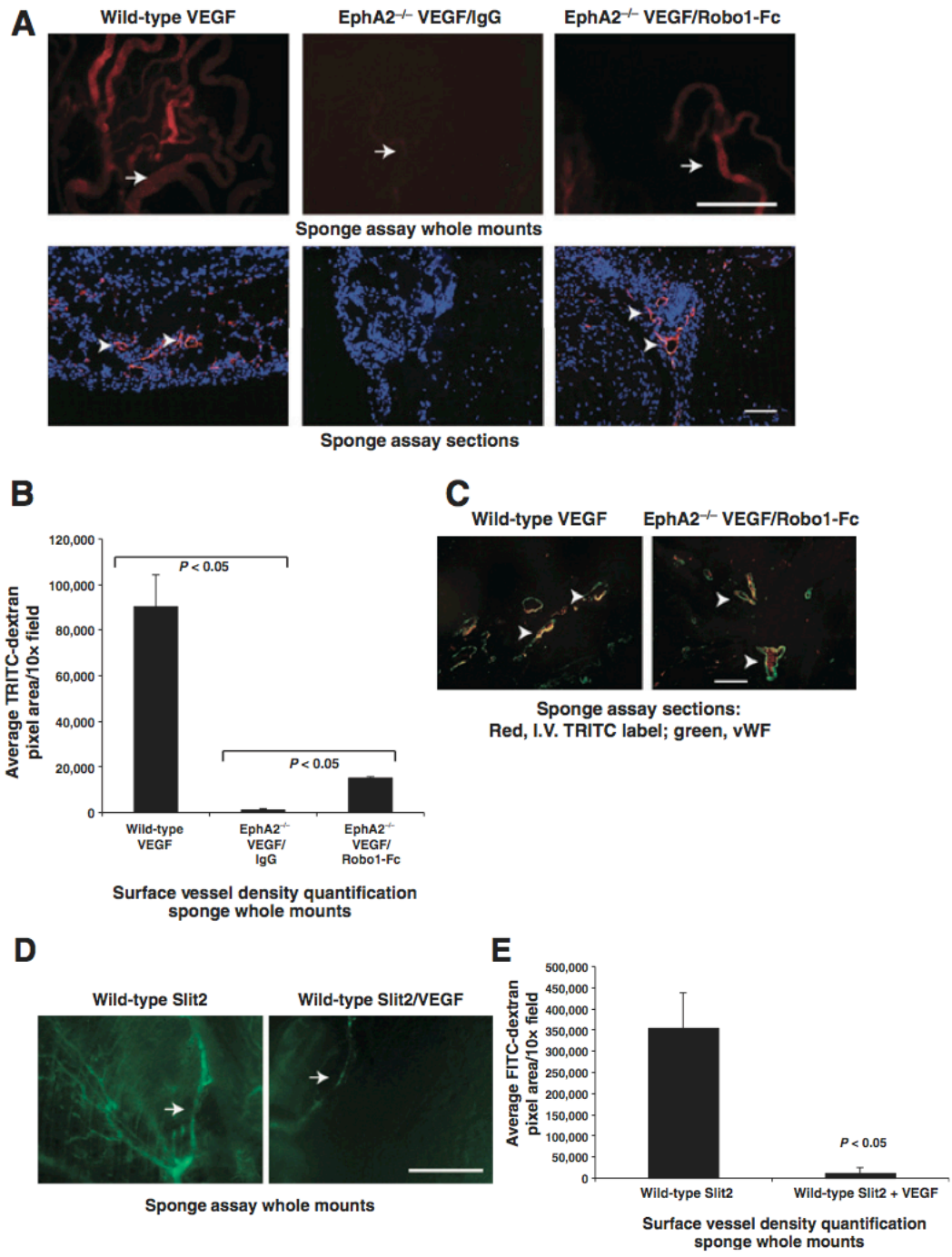

Figure 4.8 Inhibiting Slit activity rescues VEGF-induced angiogenesis in EPHA2-deficient animals *in vivo*. (A) Gelfoam sponges were loaded with VEGF plus or minus control IgG or Robo1-Fc and subcutaneously implanted the sponges into the dorsal flank of recipient mice. After 7 days, the mice were injected intravenously with TRITC-dextran to label vasculature and the sponges were excised for analysis. While wild-type recipients displayed a robust angiogenic remodeling response to sponges harboring VEGF, with numerous TRITC-positive

surface vessels (arrows in upper panels, whole mounts; arrowheads, sections), EPHA2-deficient recipients failed to respond to VEGF. Addition of Robo1-Fc partially rescued VEGF-induced vascular remodeling in EPHA2-deficient host animals. Scale bar = 5 mm (upper panels). Scale bar = 100 mm (lower panels). **(B)** We quantified surface vessel density in whole-mounts based TRITC+ pixel area using NIH Image J software analysis. **(C)** We confirmed that TRITC+ structures also expressed the endothelial marker von Willebrand factor (vWF, green staining; arrowheads indicate TRITC+/vWF+ blood vessels). **(D)** Slit2 alone induced subcutaneous angiogenic remodeling in wild-type animals, with numerous FITC-positive vessels observed on the surface of sponges (arrows), whereas Slit2 inhibited subcutaneous angiogenesis in the presence of VEGF. Scale bar = 5 mm. **(E)** We quantified surface vessel density in whole-mounts based FITC+ pixel area using NIH Image J software analysis. Data are a representation of 10 independent animals total/condition in analyzed in 2 independent experiments (5 animals/condition/experiment), with average +/- standard deviation. Statistical significance was assessed by two-tailed, paired Student's t-test.

endothelial cells was quantified by counting the number of red fluorescent cells on the lower surface (Figure 4.9A and B). Consistent with previous studies, migration of EPHA2-deficient endothelial cells was significantly lower than wild-type endothelial cell migration in response to tumor cells [131]. Addition of Slit2 inhibited migration of wild-type endothelial cells in response to 4T1 cells, whereas addition of Robo1-Fc partially rescued tumor-induced migration of EPHA2-deficient endothelial cells (Figure 4.9B). These data suggest that elevated Slit2 levels in EPHA2-deficient endothelium affects the ability of endothelial cell recruitment by VEGF-expressing tumor cells.

To confirm these findings *in vivo*, we scored changes in tumor angiogenesis and growth in wild-type versus EPHA2-deficient animals using cutaneous window chamber assays. VEGF-dependent 4T1 tumors [277, 280, 281] were co-transplanted into cutaneous window chambers with sponges impregnated with control IgG or Slit2 (wild-type hosts) or control IgG or Robo1-Fc (EPHA2-deficient hosts). Treatment with Slit2 significantly reduced tumor neovascularization in wild-type hosts, whereas Robo1-Fc partially rescued 4T1-induced tumor angiogenesis in EPHA2-deficient hosts as scored by branching from primary vessels (Figure 4.10A and B). We also tested

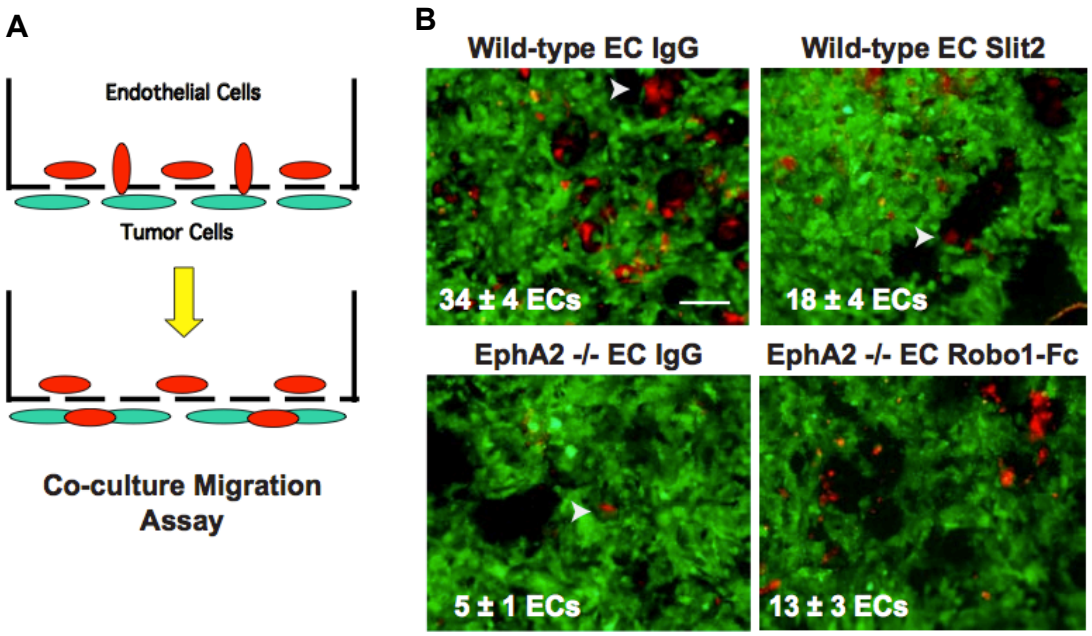

Figure 4.9 Inhibiting Slit activity rescues tumor cell-induced EphA2- deficient endothelial cell migration. (A) Schematic representation of tumor cell- endothelial co-culture migration assay used to quantify endothelial cells (labeled with red fluorescent cell-tracker dye) migration in response to GFP-expressing 4T1 tumor cells seeded on the lower surface of Matrigel-coated transwells. **(B)** Photomicrographs showing endothelial cells (arrowheads) that have migrated and intercalated into tumor cell layer on the underside of the transwell. $P<0.05$ for wild-type EC IgG versus EphA2 - /- EC IgG, wild-type EC IgG versus wild-type EC Slit2, and EphA2 -/- EC IgG versus EphA2 -/- EC Robo1-Fc. Scale bar = 50 µm.

the impact of modulating Slit activity in orthotopically-transplanted tumors. EPHA2-deficient hosts displayed a significant reduction in tumor volume relative to wild-type hosts, consistent with previous studies [131, 194]. Addition of Slit2 reduced tumor volume in wild-type hosts relative to IgG controls, whereas addition of Robo1-Fc rescued tumor volume in EPHA2-deficient hosts cells (Figure 4.10C). Consistent with our window assay data, Slit2 reduced, whereas Robo1-Fc partially rescued, microvascular density in orthotopic tumors implanted in wild-type or EPHA2-deficient hosts, respectively (Figure 4.10D and E).

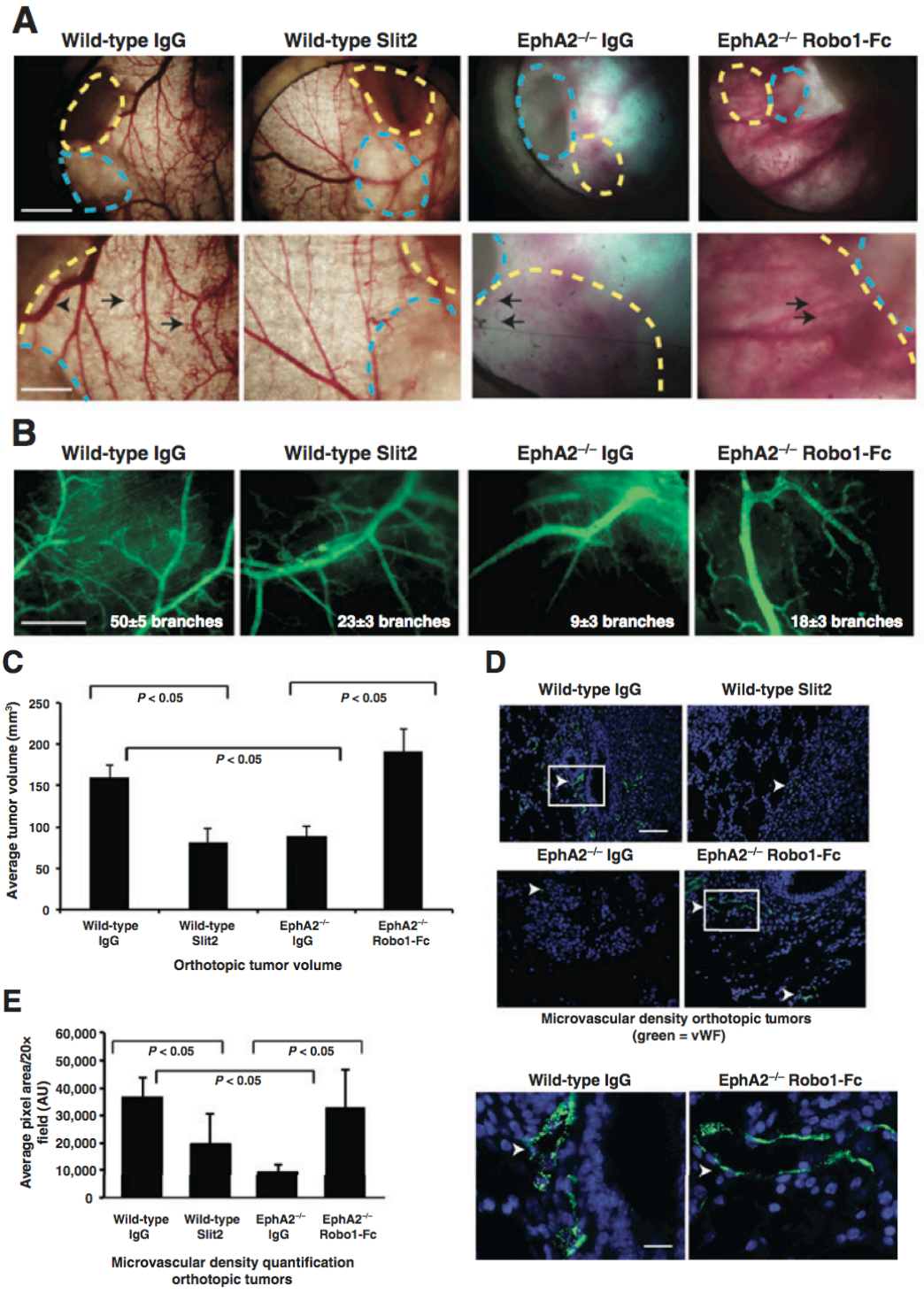

Figure. 4.10 Inhibiting Slit activity rescues tumor-induced angiogenesis and growth in EPHA2-deficient animals *in vivo*. (A) 4T1 tumors (outlined with yellow dashed lines) were co-transplanted with gelfoam sponges (outlined with blue dashed lines) plus or minus control IgG, Slit2, or Robo1-Fc and subcutaneously implanted into window chambers

mounted on the dorsal flank of recipient mice. After 7 days, FITC-conjugated dextran (2% in PBS, Sigma-Aldrich) was injected intravenously, and tumors vessels (arrows) in window chambers were photodocumented. Scale bar = 2 mm (upper panels) and 5 mm (lower panels). **(B)** Branches from host blood vessels within the window chambers were enumerated in at least three independent fields per mouse, and statistical significance was determined by two-tailed, paired Student's t-test ($p<0.05$ wild-type IgG versus EPHA2 -/- IgG; wild-type IgG versus Slit2; EPHA2 -/- IgG versus Robo1-Fc). Scale bar = 5 mm. Slit2 reduced tumor volume **(C)** and microvascular density (MVD; **D, E**) in orthotopically transplanted 4T1 tumors in wild-type hosts. By contrast, addition of Robo1-Fc partially rescued tumor volume and MVD in EPHA2 -/- hosts. Arrowheads indicate vWF+ blood vessels (green). Scale bar = 100 mm (upper panels) and 20 mm (lower panels). Lower panels are high magnification images of areas indicated by white boxes in upper panels. Data are a representation of 6-8 independent samples per condition with standard error of the mean, and statistical significance was assessed by two-tailed, paired Student's t-test.

Discussion

Emerging evidence suggests the effects of VEGF on vascular remodeling can be modulated by the activity of other signaling pathways. For example, VEGF-induced motility in tip cells versus proliferation in stalk cells is mediated by lateral inhibition upon Notch1 receptor activation by delta-like 4 (Dll4) ligand. VEGF migration versus proliferation in Notch-expressing stalk cells is further modulated by Jagged-1 ligand, which antagonizes Dll4 by competing for Notch receptor (Reviewed in [282]). In this study, we found that EPHA2 regulation of Slit2 also regulates endothelial cell response to VEGF. Slit2 mRNA and protein levels were significantly elevated in PHA2-deficient endothelium, including endothelium exposed to tumor-cell conditioned medium, as was Robo1 mRNA. EPHA2-deficient endothelium is resistant to VEGF-induced angiogenesis, and inhibition of Slit activity by soluble Robo receptors rescued EPHA2-deficient endothelial cell assembly, migration, subcutaneous vascular remodeling, and tumor angiogenesis mediated by VEGF.

Slit2 can either promote or inhibit angiogenesis, depending upon molecular context [249-253] [254-258]. Indeed, we recently reported that single agent Slit2 induces angiogenesis *in vitro* and *in vivo*, whereas co-stimulation with ephrin-A1 inhibits the

pro-angiogenic function of both factors [269]. Others observed similar inhibitory effects of Slit2 upon co-stimulation with VEGF [254-257]. These data are consistent with our observed alleviation of angiostasis in EPHA2-deficient endothelium upon inhibition of Slit function, though blocking this receptor likely affects a host of other molecular signaling pathways that culminate to inhibit angiogenesis. At least one mechanism through that appears to regulate the pro- versus anti-angiogenic functions of Slit2 is activation of Arf6 GTPase, an upstream regulator of Rac. While several previous studies showed that active Arf6 is necessary and sufficient for Rac1 activation [257, 283-285], Arf6 has also been reported to inhibit Rac activity by others [278, 286, 287], as we observed in our cell model systems. Activation of Arf6 by co-stimulation with Slit2 and VEGF, though not VEGF alone or Slit2 alone, may inhibit Rac-dependent angiogenesis, as supported by data from our model systems. Indeed, an Arf inhibitor rescued assembly in co-stimulated cells, supporting this model. Moreover, blocking Slit2 activity in EPHA2-deficient endothelial cells with Robo1-Fc significantly reduced Arf6 activation, which was elevated in the presence of VEGF. Thus, reduced Arf6 activity correlates with rescue of VEGF-induced Rac activity and angiogenic remodeling in EPHA2-deficient endothelial cells treated with Robo1-Fc.

It should be noted that other studies reported Slit2 inhibits Arf6 activity and that VEGF activates Arf6 as a single agent [257, 279]. Slit2-mediated inhibition of Arf6 was reportedly dependent on Robo4 activity [257], which may account for differential effects in our model systems that express relatively low levels of *robo4* and appear to primarily depend on Robo1 receptor function. In addition, most of the data from Jones et al. were derived from bovine aortic and human umbilical vein endothelial cells [257], large vessel sources, whereas our data were derived from microvascular endothelial cells from murine lung and human retina. Similarly, Hashimoto et al. reported VEGF-induced Arf6 activation in large-vessel-derived HUVEC [279]. Moreover, differences in stimulation conditions (e.g. culturing

endothelial cells on plates co-coated with Slit2 and fibronectin in Jones et al. versus acute stimulation of serum-starved endothelial cells with soluble Slit2 in our study) may also lead to differential signaling. Taken together, these differences in model systems, especially Robo receptor expression profiles, and experimental designs could account for differential regulation of Arf6/Rac by VEGF in the presence or absence of Slit2.

Our data support a model in which EPHA2 receptor suppresses Slit2 in microvascular endothelial cells, which enables microvascular endothelium to respond to VEGF and ephrins to promote angiogenesis. Indeed, our gain-of-function studies in which overexpression of wild-type EPHA2 reduced Slit2 expression support this model. As we observed elevated Robo1 levels in our EPHA2-deficient cells, it is possible that the angiostatic function of Slit2 in the absence of EPHA2 are enhanced by signaling through this receptor, a hypothesis that we are actively exploring.

In addition, EPHA2 regulation of Slit2 angiocrine function may alleviate tumor suppressive effects. Indeed, blocking Slit function in EPHA2-defcient endothelial cell conditioned media restored angiocrine-mediated tumor growth and motility in culture and *in vivo* [260]. Moreover, we observed an inverse correlation between EPHA2 and Slit2 expression in human breast tumor vasculature, supporting the clinical relevance of this observation [260]. Together, these data suggest that elevated Slit2 expression in the absence of EPHA2 is one mechanism of resistance to VEGF-induced angiogenesis, including tumor neovascularization.

Appendix B

LOSS OF EPHRIN-A1 IMPAIRS TUMOR ANGIOGENESIS AND PROGRESSION AND DECREASES VEGF RECEPTOR 2 ENDOCYTOSIS IN ENDOTHELIUM.

Abstract

Normal blood vessel remodeling in developing and mature tissues is coordinated by cooperative signaling between several distinct molecular signaling pathways, which are often hijacked by tumors. Understanding these pathways and their points of intersection is a key step in developing new, molecularly targeted anti-angiogenic therapies. Ephrin-A1, the primary ligand for EPHA2, a receptor tyrosine kinase (RTK), regulates cardiovascular development during embryogenesis and promotes angiogenic remodeling in cultured endothelial cells and *in vivo*. More recent studies have linked ephrin-A1 and VEGF-mediated cooperative signaling to tumor neovascularization, though the molecular mechanism(s) underlying this association remain unclear. Here, we report that ephrin-A1-deficiency inhibits VEGF-induced angiogenesis. Ephrin-A1 deficient microvascular endothelial cells fail to remodel in response to VEGF in culture and *in vivo*, and ephrin-A1 host deficiency significantly decreased tumor volume, microvascular density, and lung metastasis in a VEGF-dependent orthotropic transplant model of breast cancer. Moreover, loss of ephrin-A1 reduced VEGF-induced endothelial permeability *in vitro* and reduced extravasation/lung colonization in an experimental model of metastasis *in vivo*. Blocking ephrin-A1 reverse signaling in wild-type microvascular endothelial cells impaired VEGFR2, suggesting that ephrin-A1 reverse signaling is a critical component in VEGF signaling. Ephrin-A1-deficient cells also display decreased levels of activated

VEGFR2, AKT and p-38 in response to VEGF. Together these findings demonstrate a novel role for ephrin-A1 in VEGF signaling and tumor angiogenesis.

Introduction

Angiogenesis is the formation of blood vessels from a pre-existing vascular network and is required for solid tumor growth and progression [234]. Blood vessels can supply tumors with nutrients that support growth and this elevated vascular growth can also potentially provide increased opportunity for hematological dissemination and invasion [202]. Tumor microvascular density serves as a prognostic marker for malignancy, metastasis, and overall survival in multiple cancers, including breast [288-291]. The function of vascular endothelial growth factor-A (VEGF) in promoting and sustaining tumor angiogenesis is well-established, as is its association with poor patient prognosis across breast cancer molecular subtypes [292-305]. In breast cancer, carcinoma cells recruit endothelial cells by secreting growth factors, such as VEGF. VEGF-receptor 2 (VEGFR2) is expressed on endothelial cells and VEGF binding causes VEGFR2 phosphorylation and endocytosis, which are necessary events for VEGF-mediated signaling that promotes endothelial cell proliferation, migration, assembly and vascular permeability [306, 307]. In the clinical setting, anti-angiogenic therapies have been reported to reduce tumor size, but have had no overall effect on patient survival. Rapid vascular regrowth after treatment cessation, growth factor redundancy, and acquired drug resistance observed in both the research and clinical settings reinforce the need to explore alternative mechanisms that regulate tumor angiogenesis [308-315].

The EPH receptor tyrosine kinases (RTK) are the largest family of RTKs and are divided into classes, A and B, depending on their interactions with their ephrin-A or ephrin-B ligands [316-318]. We and others have demonstrated the critical role of EPH receptor tyrosine kinase A2 (EphA2) signaling in VEGF-dependent angiogenesis

and cancer progression [151, 197, 198, 242-246, 319, 320]. Ephrin-A1, the primary ligand for EphA2, promotes angiogenesis in culture and *in vivo* [197, 242, 245, 269, 273, 274, 321-324]. Moreover, when bound to EphA2, ephrin-A1 can engage in bi-directional signaling; a common characteristic of both A and B class Eph RTKs and ephrins. Ephrin-A1 reverse signaling has previously been implicated in axon guidance and mapping [325]. Unlike ephrin-B ligands, ephrin-A ligands lack a cytoplasmic domain and must facilitate reverse signaling through crosstalk with other transmembrane proteins [326]. Ephrin-A reverse signaling is significantly understudied compared to their B class counterparts, and to our knowledge has never been defined in an *in vivo* model of angiogenesis. Ephrin-A1 is expressed in several tissues, including the vascular endothelium; yet, the mechanisms in which membrane bound ephrin-A1 controls endothelial cell function and its potential contributions to tumor angiogenesis and cancer progression have yet to be elucidated.

To identify the role of ephrin-A1 in angiogenic processes, we used an *efna1* (ephrin-A1) knockout [A1KO; [199]] mouse model to evaluate potential changes in normal and tumor angiogenesis *in vivo*. Murine pulmonary microvascular endothelial cells (MPMECs) were also harvested from these mice to evaluate the role in ephrin-A1 specifically in endothelial cells *in vitro*. Here, we report that ephrin-A1-deficiency inhibits responses to VEGF both in tissue culture and *in vivo*. These defects are due, at least in part, to impaired VEGFR2 internalization. Notably, when we blocked ephrin-A1 reverse signaling in WT MPMECS, VEGFR2 internalization was impaired, suggesting that ephrin-A1 reverse signaling is a critical component in VEGF signaling. A1KO MPMECS also demonstrate decreased levels of activated VEGFR2, Akt, and p38 in response to VEGF. We also show that loss of ephrin-A1 in host animals significantly decreased tumor volume, microvascular density, and lung metastasis in an orthotropic transplant animal model of breast cancer. Loss of ephrin-A1 also impaired extravasation/lung colonization in an experimental metastasis model *in*

vivo as well as VEGF-induced permeability in culture. Together these findings demonstrate a novel role for ephrin-A1 in VEGF signaling and tumor angiogenesis.

Methods and Materials

Mouse model

Animals were housed under pathogen-free conditions, and experiments were performed in accordance with AAALAC guidelines and with Vanderbilt University Institutional Animal Care and Use Committee approval. EphrinA1$^{+/+}$ or Ephrin-A1$^{-/-}$ were identified by PCR analysis of genomic DNA using the following primers: Ephrin-A1 forward primer (5'-CCCAACAAAAACAAACAGCCG-3') and two allele specific reverse primers, WT (5'-GAGGTGGAGGAAGGGAAAAAGAC-3') and KO (5'-TGGATG TGGAATGTGTGCGAGG-3').

Cell culture

Primary murine pulmonary microvascular endothelial cells (MPMEC) were isolated from wild type or ephrin-A1-deficient animals as described previously [270]. HUVECs we purchased from the ATCC and used between passages 4-8. Endothelial cells were maintained in EGM-2 medium supplemented with penicillin-streptomycin and 10% fetal bovine serum. 4T1 mouse mammary adenocarcinoma cells were obtained from ATCC and were used at low passage. Cells were maintained in DMEM supplemented with penicillin-streptomycin and 10% fetal bovine serum, unles otherwise indicated. For RNAi experiments in HUVEC, *EFNA1* ON-TARGETplus Human SMARTpool siRNA (M-006369-01-005), and ON-TARGETplus Non-Targeting pool siRNA (D-001810-10-05) were purchased from Dharmacon/Thermo Scientific, and were used at a concentration on of 12.5-25nM in combination with Lipofectamine RNAiMAX transfection reagent (Invitrogen). Experiments were carried out after 72 hours.

In vivo sponge assay for angiogenesis

Sponge assays to evaluate *in vivo* vascular remodeling were performed as described previously [270, 274]. Briefly, gel foam sponges were cut into small pieces (2.5 to 3 mm wide by 5 mm long) and soaked with 100 mL of phosphate-buffered saline containing 100ng of VEGF or control IgG. The sponges were then implanted into the subcutaneous dorsal flank of Balb/c wild type or ephrin-A1-deficient recipient female mice. Each recipient received one pro-angiogenic factor impregnated sponge and one relevant control factor impregnated sponge implanted in the opposite flank. After 7 days, the mice were injected with a 2% tetramethyl rhodamine isothiocyanate (TRITC)-dextran-phosphate-buffered saline solution or 2% fluorescein isothiocyanate (FITC)-dextran-phosphate-buffered saline solution to label host blood vessels [270, 274], and the sponges were collected and analyzed. Whole-mount images were acquired on an Olympus CK40 inverted microscope through an Optronics DEI-750C charge-coupled-device video camera using CellSens capture software. Density of blood vessels within the sponges was quantified by fluorescence intensity (10X magnification) of TRITC-dextran or FITC-dextran using Scion Image software, version 1.62c. Data are a representation of results from five independent sponges under each condition. Statistical significance was determined by a two-tailed, paired Student's t test.

In vitro angiogenesis assays

In vitro vascular assembly assays were performed as described previously [270, 273]. Briefly, 12-well plates were coated with 100 mL of growth factor reduced Matrigel (BD Biosciences). After 24 hour starvation in Opti-MEM, 25,000 MPMEC were plated in wells in the presence or absence of VEGF (50 ng/mL) and photographed after 24-hours. Images were acquired using an Olympus CK40 inverted microscope through an Optronics DEI-750C CCD video camera using CellSens capture software. The degree of assembly was quantified by measuring branch length, the distance from branching point to the tip of assembled cells. The branch length in assembled

endothelial cell networks was expressed as arbitrary units per 10X field in four random fields from each well, with triplicate samples per condition, using Scion Image version 1.62c software.

For migration assays, endothelial cells were serum-starved for 24-hours in Opti-MEM medium. Transwells were coated with growth factor reduced Matrigel (1:20 dilution with Opti-MEM) for 30 minutes and blocked with 1% bovine serum albumin solution for an additional 30 minutes. One hundred thousand cells were plated in the upper chamber of the transwells, and 600 mL of Opti-MEM medium containing VEGF (50 ng/mL) or vehicle was added to the lower chamber. After 5-hours, cells were fixed and stained with crystal violet to visualize endothelial cells. Cells that migrated to the lower surface of transwell filters were counted in four random fields from each well, with triplicate samples per condition as described previously [270, 273].

Tumor-endothelial cell co-culture migration assays

For co-culture experiments, transwells were coated with growth factor-reduced Matrigel (1:20 dilution) and 1 x 10^5 4T1-GFP cells were plated on the lower surface of the transwell filter. Wild-type or ephrin-A1-deficient MPMEC or HUVEC, as indicated (1 x 10^5), labeled with CellTracker Orange CMTMR dye (Molecular Probes/Life Technologies) were added to upper transwell chambers. After 5-hours, cells were removed from the upper surface of the transwell filter using a cotton swab, and endothelial cells on the lower surface of the filter quantified. Similar experiments were performed comparing. Data are a representation of six to nine independent samples per condition with standard deviation, and statistical significance was assessed by two-tailed, paired Student's t test.

Orthotopic tumor transplantation

4T1 cells were collected and washed with PBS prior to injection. 250,000 cells were orthotopically transplanted in the mammary glands of recipient wild-type or ephrin-A1-deficient Balb/c female mice as described previously [131]. Tumors were harvested after 14 days, measured by digital caliper, and volume was calculated [length x width^2 x 0.52]. Tumor sections were stained for the endothelial marker vWF factor and microvascular density quantified based on pixel density as described previously [131, 194, 275].

VEGFR2 internalization assay

PMECs were plated onto gelatin-coated 8-well glass microscope slides. To analyse the internalization of VEGFR2 in vitro, cells were incubated with blocking solution containing (2% BSA, 4% goat serum in DPBS) for 10 minutes at 37°C. Anti-VEGFR2 (R&D) was delivered to cells in blocking solution (1:40 dilution) and incubated for 20 minutes at 37°C. Cells were washed with DPBS and then incubated in serum-free growth medium (OPTIMUM) containing 100 ng ml−1 VEGF-A for 30 min at 37 °C. Control wells received OPTIMUM with no VEGF. Samples were then fixed with fresh 4% PFA and 4% sucrose solution (in DPBS) on ice for 30 min. Cells were washed with DPBS. To visualize cell surface VEGFR2, cells were incubated with Alexa-Fluor-488-conjugated secondary antibody (Invitrogen, 1:100) for 2 h at room temperature/dark area. Cells were washed with DPBS and permeabilized with ice-cold blocking buffer solution contain 0.2% Triton-X100 for 30 min on ice. Cells were washed with DPBS and incubated with Alexa-Fluor-546-conjugated secondary antibody (Invitrogen, 1:400) for 1 h at room temperature to visualize internalized receptors. Cells were counterstained with DAPI and were mounted with slowfade mounting media. The number of VEGFR2 signals from each genotype was calculated from multiple frame shots containing at least ten cells from each group (generally 20+ cells); 4 independent experiments were performed each with 4 to 5 mice/genotype. Data points were calculated as a ratio of internal:surface (red:green) staining as

determine by microscopy, such that the number calculated is the fold change of internalized receptor staining for those giving cells.

Immunoblotting and immunoprecipitation

Cells were harvested and lysed with fresh, ice cold RIPA buffer supplemented with phosphatase and proteinase inhibitors. An aliquot of these lysates were set aside for total protein content. Cell lysates were incubated with anit-VEGFR2 antibody (cell signaling) for 16 hours at 4C with constant rotation. For immunoprecipitation experiments, agarose beads were then incubated the with cell lysates for 1 hour to allow for anti-VEGFR2 binding. Lysates were centrifuged and the pellet was washed with RIPA buffer, and the samples were boiled with loading buffer and then underwent electrophoresis and transfer to a cellulose membrane. Membrane was probed with anti-phospho-VEGFR2 (Y1175) mouse monoclonal antibody. Followed by anti-mouse antibody conjugated to HRP. The blot was stripped and re-probed for total VEGFR2., phosphor-p38, phospho-SRC, phosphor-AKT, and tubulin.

Results

Ephrin-A1-deficiency impairs VEGF-induced angiogenesis in culture and in vivo

To determine if eprhin-A1-deficiency in microvascular endothelium impairs angiogenesis, we isolated primary MPMEC from wild type and ephrin-A1-deficient mouse lungs and assessed vascular assembly on Matrigel-coated wells *in vitro*. Ephrin-A1-deficiency significantly reduced endothelial cell assembly into interconnected vascular networks in response to VEGF stimulation relative to wild-type control cells (Figure 5.1A). Consistent with this observation, ephrin-A1-deficient endothelial cells also displayed reduced motility in response to VEGF in transwell assays (Figure 5.1B). To assess VEGF-induced angiogenic remodeling responses in intact blood vessels, we performed *in vivo* vascular remodeling assays. Gelfoam sponges impregnated with vehicle control or recombinant VEGF were implanted subcutaneously into the dorsal flank of recipient wild type or ephrin-A1-deficient

mice. Mice were injected intravenously with TRITC-dextran 7 days post-implantation to label vessels to visualize functional vessels. While vehicle control did not induce a significant angiogenic remodeling response, VEGF induced new vessel sprouting from wild-type host vessels, as visualized by quantifying surface vessel area (Figure 5.1C). By contrast, VEGF-induced angiogenesis was significantly impaired in ephrin-A1-deficient hosts (Figure 5. 1C).

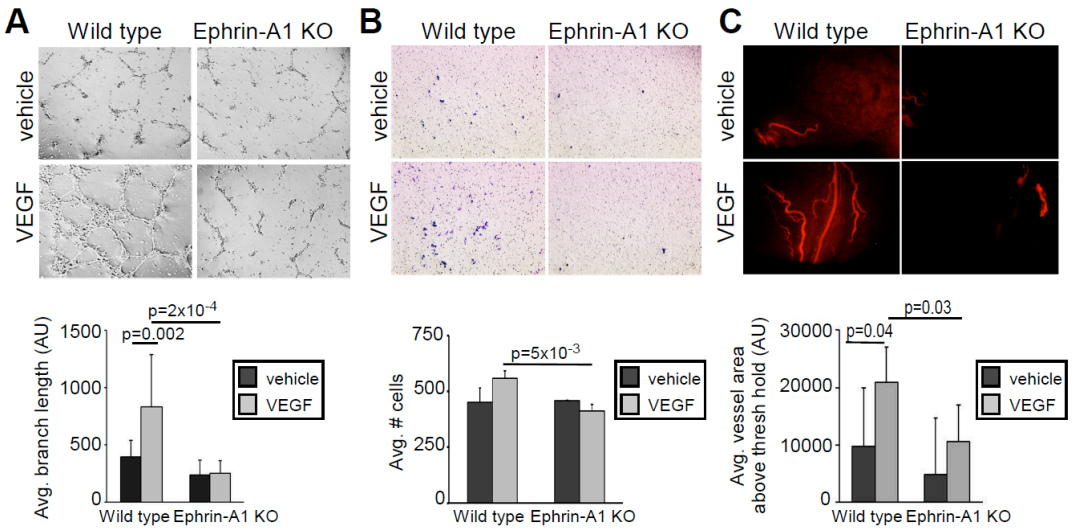

Figure 5.1 Loss of ephrin-A1 impairs VEGF-dependent angiogenesis. (A) Assembly assay: MPM- VECs were serum-starved for 14 hours and plated on Matrigel with vehicle or VEGF for 10 hours. Aver- age branch length was used to quantify assembly. Representative image from 1 of 3 independent exper- iments using 4 or more mice of each genotype. **(B)** Migration assay: MPMVECs were serum-starved and cultured onto Matrigel coated transwells with either vehicle or VEGF in the bottom chamber. Migrated cells were stained with crystal violet. Migration was quantified by number of cells on the under portion of the transwell. **(C)** Sponges saturated in VEGF or vehicle were surgically implanted into opposites sides of the dorsal flanks of wild type and ephrin-A1 KO mice mice. After 7 days mice were injected with TRITC- dextran and sponges were removed for imaging. Representative image from 1 of 2 independent experi ments using 4 or more mice from each genotype. Statistical significance determined by student's t-test.

To determine if ephrin-A1 host-deficiency also impairs tumor neovascularization and progression, we monitored tumor growth, microvascular density, and metastasis in an orthotopic allograft model of mammary adenocarcinoma *in vivo*. The 4T1 cell line

model was derived from a spontaneous Balb/C mouse mammary tumor and selected for its metastatic potential. It expresses high levels of VEGF, produces aggressive mammary adenocarcinoma when transplanted into Balb/C female hosts, and metastasizes via the hematologic route to lung [198, 327-329]. We transplanted 4T1 tumor cells into the mammary fat pad of congenic wild-type or eprhin-A1-deficient Balb/C female hosts and monitored tumor volume over several days. Tumors growing in ephrin-A1-deficient hosts displayed a significant reduction in tumor volume relative to wild-type controls (Figure 5.2A). We also observed a significant reduction in the frequency and number of lung metastases in ephrin-A1-deficient hosts relative to controls (Figure 5.2B). Consistent with our *in vitro* and sponge assay studies, we observed a significant decrease in microvessel density for tumors from ephrin-A1-deficient versus wild-type hosts, as quantified by immunofluorescent staining for von Willebrand Factor (vWF; Figure 5.2C). Tumor cell survival, as scored by TUNEL, was elevated (Figure 5.2D), and proliferation, measured and quantified by proliferating cell nuclear (PCNA) antigen expression (Figure 5.2E), was impaired in eprhin-A1-deficient hosts. Together, these data demonstrate that loss of ephrin-A1 in host endothelium, at least in part, reduces VEGF-induced angiogenesis, neovascularization, and tumor progression in culture and *in vivo*.

Loss of ephrin-A1 inhibits tumor cell intravasation and metastasis

Reduced metastasis frequency and lung metastatic burden in ephrin-A1-deficient hosts may be due to impaired vascular recruitment and decreased tumor survival/proliferation. Alternatively, this may be by directly impaired through decreased intravasation, survival in circulation, and/or extravasation and colonization of the lung. To test these possible mechanisms, we first performed co-culture intravasation assays in which we quantified migration and intercalation of GFP-labeled tumor cells into a monolayer of endothelial cells seeded on the lower transwell surface [260]. While endothelial cells isolated from wild-type mice induced

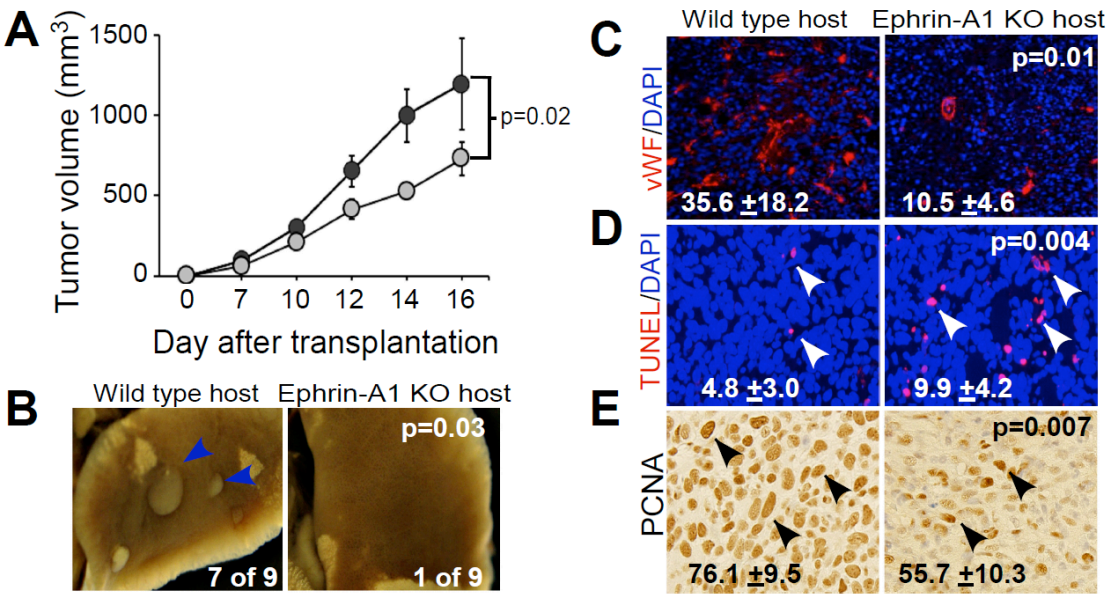

Figure 5.2 Ephrin-A1 host deficiency impairs tumor volume. (A) 4T1 cells were transplanted into mammary glands of 9 wild type (n=9) and ephrin-A1 KO (n=9) mice. Tumor volume was determined by caliper measurements on days 5,10,12,14 and 16. **(B)** Lungs from mice were harvested and surface metastases was evaluate (blue arrows). 7 of 9 WT mice had surface metastases compared to only 1 of 9 ephrin-A1 KO mice. Statistical significance determined by Chi Square Test. **(C)** Immunohistochemistry of vWF in tumor sections. vWF staining was measured using Image J software and is expressed in arbitrary units. **(D)** TUNEL-positive cells were evaluated in tumor sections to determine the apoptotic index. **(E)** PCNA-positive cells were evaluated in tumor sections to determine the proliferative index. Statistical significance was determined by student's t test.

a robust migratory response from 4T1-GFP tumor cells, significantly fewer tumor cells migrated and intercalated into monolayers of ephrin-A1-deficient endothelial cells (Figure 5.3A). We also confirmed this phenotype in HUVECs transfected with siNon-target control or siEphrin-A1, in that we observed a significant decrease in the number of human breast cancer cells (MDA-MB-231) able to migrate through HUVECs with ehrin-A1 knockdown (data not shown).

To assess tumor cell survival in circulation, extravasation/lung colonization, we performed tail vein injections in wild type versus ephrin-A1-deficient hosts and quantified surface lung lesions 1-week post injection. Lungs from ephrin-A1-deficient

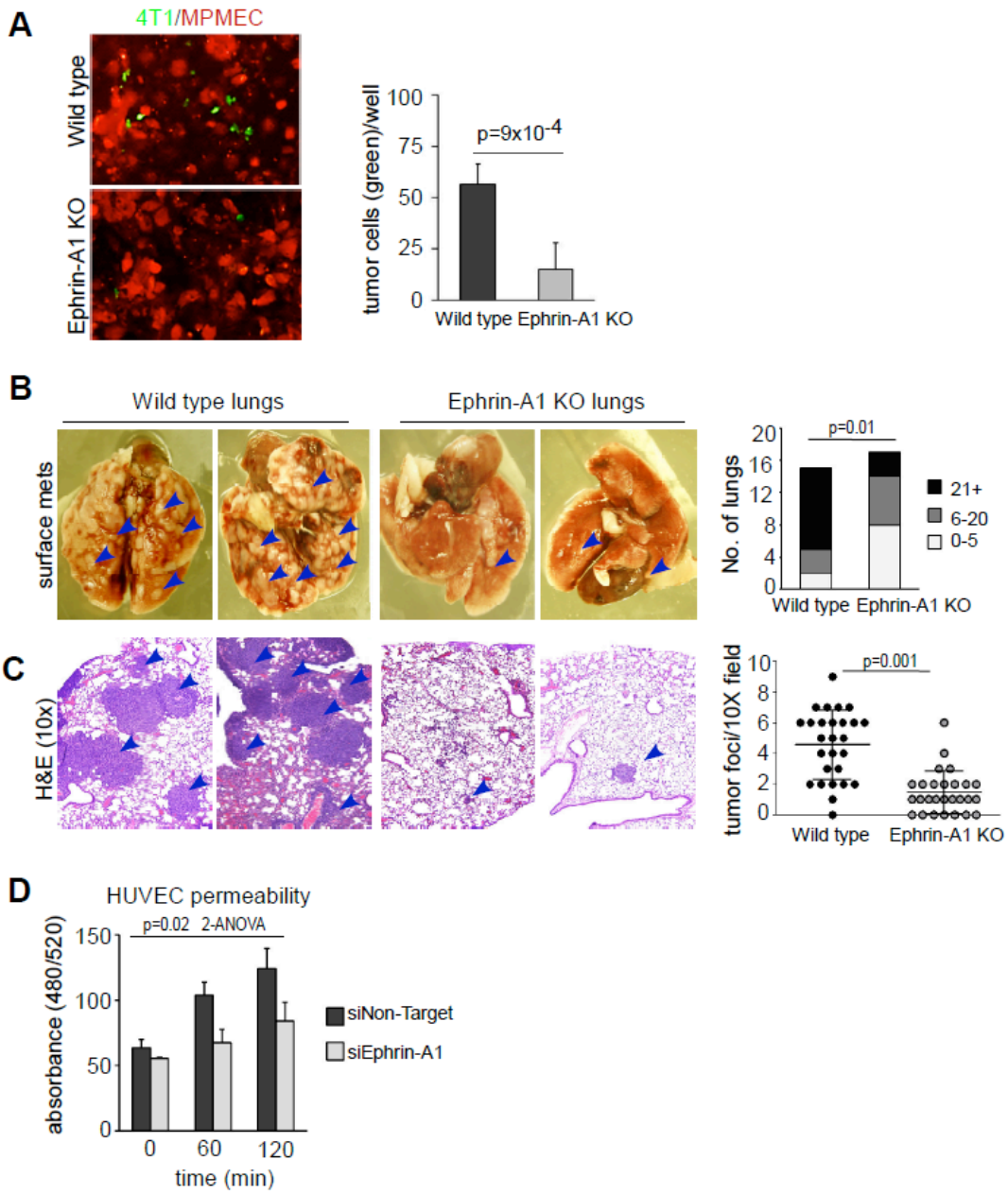

Figure 5.3 Loss of ephrin-A1 impairs tumor cell intravasation. **(A)** MPMECs were cultured on the under portion of transwell (red) and 4T1-GFP tumor cells (green) were cultured in the top portion. After 5 hours we quantified the number of tumor cells that migrated through the endothelial cell barrier. **(B)** Whole lungs from wild type or ephrin-A1-/- mice 1-week post tail vein injection with 4T1 cells. Grouped by the number of visual surface metastatic lesions (blue arrows) Chi Square to determine significance. **(C)** Lungs were sectioned and stained with haematoxylin and eosin (H&E) and the number of tumor foci (blue arrows) per field of view was determined. Significance determined by student's t-test. **(D)** Permeability assay in HUVEC; siNon-target control or siEphrin-A1 HUVECs were plated in transwells and the amount of FITC-dextran able to permeate through the cells upon VEGF treatment was determined. Data are expressed as absorbance, error bars, +SEM, one-way ANOVA was used to determine significance.

hosts harbored significantly fewer lung metastases relative to wild-type controls (Figure 5.3B and C). Together, these data suggest that endothelial ephrin-A1 mediates intravasation and lung colonization.

One potential mechanism through which endothelial ephrin-A1 might modulate VEGF function and intravasation/metastasis is through regulation of endothelial cell adhesion molecules. Indeed, recent studies reported that EphA2/ephrin-A1 upregulates expression of E-selectin and VCAM-1 in human endothelium, as well as ICAM-1, which regulates monocyte extravasation in atherosclerotic plaques and leukocyte-endothelial cell adhesion, respectively [330-333]. An impairment of cell-cell junction may contribute to cell permeability, a phenotype often associated with enhanced tumor cell intravasation and extravasation. In HUVECs we observed a significant reduction in cell permeability upon knockdown of ephrin-A1. HUVECs treated with siControl or siEphrin-A1 were cultured in transwells and the amount of FITC-dextran able to cross the endothelial barrier upon treatment of VEGF or vehicle was measured (Figure 5.3D).

Loss of ephrin-A1 impairs VEGFR2 internalization

Dysregulation of VEGF receptor 2 (VEGFR2) signaling can impact endothelial cell responses to VEGF, including motility and permeability [334, 335]. Upon VEGF binding, VEGFR2 is dissociated from the membrane and undergoes internalization. VEGFR2 signaling is not terminated in conjunction with internalization, rather the receptor continues to transduce signal from endosomes [336]. Since we observed ephrin-A1-deficient endothelial cells had significantly reduced responses to VEGF treatment, we sought to determine whether was due to impaired VEGFR2 internalization. We assessed VEGFR2 localization with wild-type versus ephrin-A1-deficient endothelial cells. Upon stimulation with VEGF, we observed reduced surface VEGFR2 and increased intracellular levels for wild-type endothelium (Figure 5.4A). By contrast, VEGFR2 cell surface localization persisted in ephrin-A1-deficient

endothelial cells treated with VEGF, with reduced internalization detected (Figure 5.4A) We also compared signaling downstream of VEGF in wild-type versus ephrin-A1-deficient endothelial cells. We observed a decrease in VEGFR2 phosphorylation in ephrin-A1 knockout cells 15 to 30 minutes post-stimulation, as well as P-Akt and P-p38, relative to wild-type controls, though P-src appeared unaffected (Figure 5.4B).

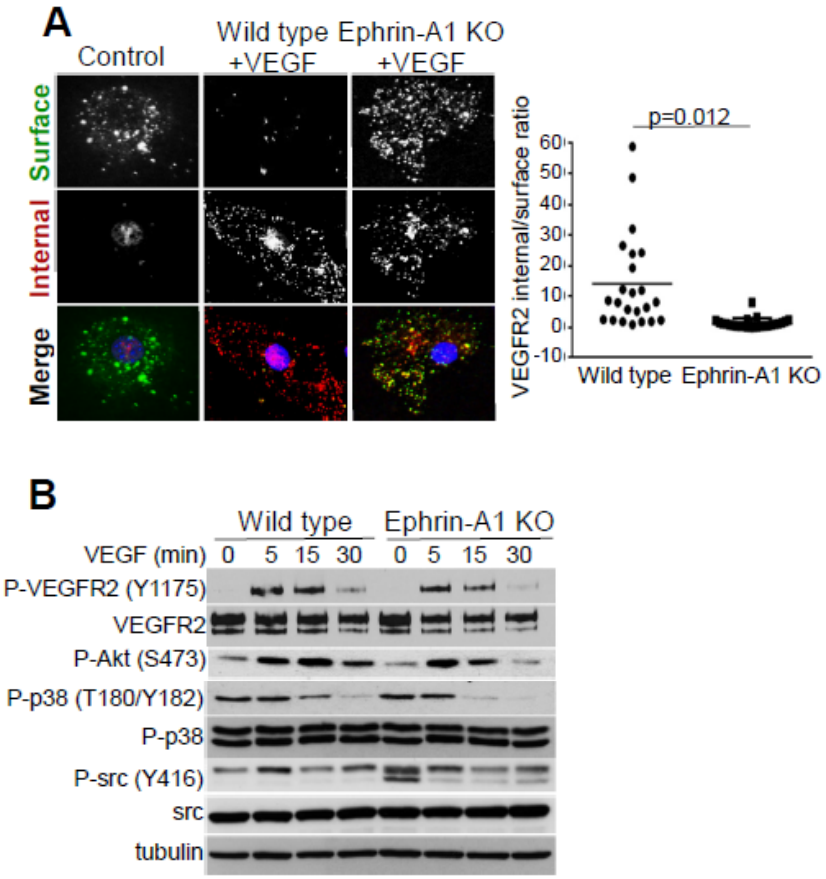

Figure 5.4 Loss of ephrin-A1 impairs VEGFR2 internalization and signaling. (A) Internalized (red) and surface (green) VEGFR2 was assessed in wild type and ephrin-A1-deficient MPMECS. Internal/surface ratio was calculated and significance was determined by student's t-test. **(B)** Wild type and ephrin-A1-deficient MPMECs were treated with VEGF for 1,5,15, or 30 minutes, were harvested in RIPA buffer and protein expression, as indicated was determined.

Discussion

The establishment of new blood vessel growth is essential for tumor cell growth and for metastatic spread. Tumor cells secrete a plethora of pro-angiogenic factors, such as VEGF, that aid in endothelial cell motility and vessel recruitment. The binding of VEGF to its receptor VEGFR2 causes the dissociation of VEGFR2 from the membrane surface and its rapid internalization to engage in signal transduction [336] that mediates endothelial cell motility, permeability and proliferation[335]. In this study we demonstrated that ephrin-A1 is critical for VEGF-driven angiogenic response, both *in vitro* and *in vivo*. Wild type 4T1 tumors cells that were transplanted into ephrin-A1 knockout mice displayed reduced tumor volume and vessel density. Notably, ephrin-A1-deficient animals had significantly decreased metastatic lung lesions compared to wild type animals, as evidenced in our tumor transplant model and in our tail vein model. This is consistent with observations made in human breast cancer patients that found vessel density in breast cancer patient tumors positively correlated with metastatic progression [337].

Our studies also revealed that loss of ephrin-A1 impaired VEGFR2 signaling in MPMECs that is at least in part due to stabilization of VEGFR2 to the membrane surface (Figure 5.4). Previously studies have linked VE-cadherin, which localizes to endothelial cell junctions and regulates vascular development and integrity [338, 339], to VEGFR localization and signaling. VE-cadherin is associated with VEGFR2 via β-catenin to stabilize the receptor at the cell surface, and the absence of VE-cadherin at the cell junction leads to a more rapid internalization of VEGFR2 [336, 340, 341]. Thus future investigations will focus on whether ephrin-A1 can impact VE-cadherin stability, and whether this is a mechanism of VEGFR2 surface stabilization. Together, our data suggests that ephrin-A1 regulates VEGFR2 signaling, tumor angiogenesis and tumor metastasis.

References

1. Siegel, R.L., K.D. Miller, and A. Jemal, *Cancer statistics, 2015.* CA Cancer J Clin, 2015. **65**(1): p. 5-29.
2. McPherson, K., C.M. Steel, and J.M. Dixon, *ABC of breast diseases. Breast cancer-epidemiology, risk factors, and genetics.* BMJ, 2000. **321**(7261): p. 624-8.
3. Lord, C.J. and A. Ashworth, *BRCAness revisited.* Nat Rev Cancer, 2016.
4. Pharoah, P.D., et al., *Family history and the risk of breast cancer: a systematic review and meta-analysis.* Int J Cancer, 1997. **71**(5): p. 800-9.
5. Collaborative Group on Hormonal Factors in Breast, C., *Familial breast cancer: collaborative reanalysis of individual data from 52 epidemiological studies including 58,209 women with breast cancer and 101,986 women without the disease.* Lancet, 2001. **358**(9291): p. 1389-99.
6. Moulis, S. and D.C. Sgroi, *Re-evaluating early breast neoplasia.* Breast Cancer Res, 2008. **10**(1): p. 302.
7. Kohler, B.A., et al., *Annual Report to the Nation on the Status of Cancer, 1975-2011, Featuring Incidence of Breast Cancer Subtypes by Race/Ethnicity, Poverty, and State.* J Natl Cancer Inst, 2015. **107**(6): p. djv048.
8. Kwan, M.L., et al., *Epidemiology of breast cancer subtypes in two prospective cohort studies of breast cancer survivors.* Breast Cancer Res, 2009. **11**(3): p. R31.
9. Howlader, N., et al., *US incidence of breast cancer subtypes defined by joint hormone receptor and HER2 status.* J Natl Cancer Inst, 2014. **106**(5).
10. Voduc, K.D., et al., *Breast cancer subtypes and the risk of local and regional relapse.* J Clin Oncol, 2010. **28**(10): p. 1684-91.
11. Bauer, K.R., et al., *Descriptive analysis of estrogen receptor (ER)-negative, progesterone receptor (PR)-negative, and HER2-negative invasive breast cancer, the so-called triple-negative phenotype: a population-based study from the California cancer Registry.* Cancer, 2007. **109**(9): p. 1721-8.
12. Slamon, D.J., et al., *Human breast cancer: correlation of relapse and survival with amplification of the HER-2/neu oncogene.* Science, 1987. **235**(4785): p. 177-82.
13. Warburg, O., *On the origin of cancer cells.* Science, 1956. **123**(3191): p. 309-14.
14. Warburg, O., *On respiratory impairment in cancer cells.* Science, 1956. **124**(3215): p. 269-70.
15. Souba, W.W., *Glutamine and cancer.* Ann Surg, 1993. **218**(6): p. 715-28.
16. Hensley, C.T., A.T. Wasti, and R.J. DeBerardinis, *Glutamine and cancer: cell biology, physiology, and clinical opportunities.* J Clin Invest, 2013. **123**(9): p. 3678-84.

17. Young, R.M., et al., *Dysregulated mTORC1 renders cells critically dependent on desaturated lipids for survival under tumor-like stress.* Genes Dev, 2013. **27**(10): p. 1115-31.
18. Wise, D.R., et al., *Myc regulates a transcriptional program that stimulates mitochondrial glutaminolysis and leads to glutamine addiction.* Proc Natl Acad Sci U S A, 2008. **105**(48): p. 18782-7.
19. Robey, R.B. and N. Hay, *Is Akt the "Warburg kinase"?-Akt-energy metabolism interactions and oncogenesis.* Semin Cancer Biol, 2009. **19**(1): p. 25-31.
20. Dang, C.V. and G.L. Semenza, *Oncogenic alterations of metabolism.* Trends Biochem Sci, 1999. **24**(2): p. 68-72.
21. Ying, H., et al., *Oncogenic Kras maintains pancreatic tumors through regulation of anabolic glucose metabolism.* Cell, 2012. **149**(3): p. 656-70.
22. Son, J., et al., *Glutamine supports pancreatic cancer growth through a KRAS-regulated metabolic pathway.* Nature, 2013. **496**(7443): p. 101-5.
23. Koppenol, W.H., P.L. Bounds, and C.V. Dang, *Otto Warburg's contributions to current concepts of cancer metabolism.* Nat Rev Cancer, 2011. **11**(5): p. 325-37.
24. Lim, H.Y., et al., *Respiratory competent mitochondria in human ovarian and peritoneal cancer.* Mitochondrion, 2011. **11**(3): p. 437-43.
25. Fantin, V.R., J. St-Pierre, and P. Leder, *Attenuation of LDH-A expression uncovers a link between glycolysis, mitochondrial physiology, and tumor maintenance.* Cancer Cell, 2006. **9**(6): p. 425-34.
26. Pfeiffer, T., S. Schuster, and S. Bonhoeffer, *Cooperation and competition in the evolution of ATP-producing pathways.* Science, 2001. **292**(5516): p. 504-7.
27. Dombrauckas, J.D., B.D. Santarsiero, and A.D. Mesecar, *Structural basis for tumor pyruvate kinase M2 allosteric regulation and catalysis.* Biochemistry, 2005. **44**(27): p. 9417-29.
28. Dhup, S., et al., *Multiple biological activities of lactic acid in cancer: influences on tumor growth, angiogenesis and metastasis.* Curr Pharm Des, 2012. **18**(10): p. 1319-30.
29. Wu, H., et al., *Central role of lactic acidosis in cancer cell resistance to glucose deprivation-induced cell death.* J Pathol, 2012. **227**(2): p. 189-99.
30. Vaupel, P., *Metabolic microenvironment of tumor cells: a key factor in malignant progression.* Exp Oncol, 2010. **32**(3): p. 125-7.
31. Lunt, S.Y. and M.G. Vander Heiden, *Aerobic glycolysis: meeting the metabolic requirements of cell proliferation.* Annu Rev Cell Dev Biol, 2011. **27**: p. 441-64.
32. Dang, C.V., *Links between metabolism and cancer.* Genes Dev, 2012. **26**(9): p. 877-90.
33. Boveris, A., *Mitochondrial production of superoxide radical and hydrogen peroxide.* Adv Exp Med Biol, 1977. **78**: p. 67-82.

34. Nogueira, V., et al., *Akt determines replicative senescence and oxidative or oncogenic premature senescence and sensitizes cells to oxidative apoptosis.* Cancer Cell, 2008. **14**(6): p. 458-70.
35. Macheda, M.L., S. Rogers, and J.D. Best, *Molecular and cellular regulation of glucose transporter (GLUT) proteins in cancer.* J Cell Physiol, 2005. **202**(3): p. 654-62.
36. Luo, X.M., S.H. Zhou, and J. Fan, *Glucose transporter-1 as a new therapeutic target in laryngeal carcinoma.* J Int Med Res, 2010. **38**(6): p. 1885-92.
37. Barron, C.C., et al., *Facilitative glucose transporters: Implications for cancer detection, prognosis and treatment.* Metabolism, 2016. **65**(2): p. 124-39.
38. Thorens, B. and M. Mueckler, *Glucose transporters in the 21st Century.* Am J Physiol Endocrinol Metab, 2010. **298**(2): p. E141-5.
39. Jun, Y.J., et al., *Clinicopathologic significance of GLUT1 expression and its correlation with Apaf-1 in colorectal adenocarcinomas.* World J Gastroenterol, 2011. **17**(14): p. 1866-73.
40. Basturk, O., et al., *GLUT-1 expression in pancreatic neoplasia: implications in pathogenesis, diagnosis, and prognosis.* Pancreas, 2011. **40**(2): p. 187-92.
41. Reinicke, K., et al., *Cellular distribution of Glut-1 and Glut-5 in benign and malignant human prostate tissue.* J Cell Biochem, 2012. **113**(2): p. 553-62.
42. Sakashita, M., et al., *Glut1 expression in T1 and T2 stage colorectal carcinomas: its relationship to clinicopathological features.* Eur J Cancer, 2001. **37**(2): p. 204-9.
43. Schwartzenberg-Bar-Yoseph, F., M. Armoni, and E. Karnieli, *The tumor suppressor p53 down-regulates glucose transporters GLUT1 and GLUT4 gene expression.* Cancer Res, 2004. **64**(7): p. 2627-33.
44. Binder, C., et al., *Deregulated simultaneous expression of multiple glucose transporter isoforms in malignant cells and tissues.* Anticancer Res, 1997. **17**(6D): p. 4299-304.
45. Robey, R.B. and N. Hay, *Mitochondrial hexokinases, novel mediators of the antiapoptotic effects of growth factors and Akt.* Oncogene, 2006. **25**(34): p. 4683-96.
46. Mathupala, S.P., A. Rempel, and P.L. Pedersen, *Glucose catabolism in cancer cells: identification and characterization of a marked activation response of the type II hexokinase gene to hypoxic conditions.* J Biol Chem, 2001. **276**(46): p. 43407-12.
47. Patra, K.C., et al., *Hexokinase 2 is required for tumor initiation and maintenance and its systemic deletion is therapeutic in mouse models of cancer.* Cancer Cell, 2013. **24**(2): p. 213-28.
48. Yi, W., et al., *Phosphofructokinase 1 glycosylation regulates cell growth and metabolism.* Science, 2012. **337**(6097): p. 975-80.
49. Chesney, J., *6-phosphofructo-2-kinase/fructose-2,6-bisphosphatase and tumor cell glycolysis.* Curr Opin Clin Nutr Metab Care, 2006. **9**(5): p. 535-9.

50. Christofk, H.R., et al., *The M2 splice isoform of pyruvate kinase is important for cancer metabolism and tumour growth.* Nature, 2008. **452**(7184): p. 230-3.
51. Chen, J., et al., *Shikonin and its analogs inhibit cancer cell glycolysis by targeting tumor pyruvate kinase-M2.* Oncogene, 2011. **30**(42): p. 4297-306.
52. Goldberg, M.S. and P.A. Sharp, *Pyruvate kinase M2-specific siRNA induces apoptosis and tumor regression.* J Exp Med, 2012. **209**(2): p. 217-24.
53. Aft, R.L., F.W. Zhang, and D. Gius, *Evaluation of 2-deoxy-D-glucose as a chemotherapeutic agent: mechanism of cell death.* Br J Cancer, 2002. **87**(7): p. 805-12.
54. Balinsky, D., C.E. Platz, and J.W. Lewis, *Enzyme activities in normal, dysplastic, and cancerous human breast tissues.* J Natl Cancer Inst, 1984. **72**(2): p. 217-24.
55. Shim, H., et al., *c-Myc transactivation of LDH-A: implications for tumor metabolism and growth.* Proc Natl Acad Sci U S A, 1997. **94**(13): p. 6658-63.
56. Townsend, D.W., *Physical principles and technology of clinical PET imaging.* Ann Acad Med Singapore, 2004. **33**(2): p. 133-45.
57. Dierickx, D., T. Tousseyn, and O. Gheysens, *How I treat posttransplant lymphoproliferative disorders.* Blood, 2015. **126**(20): p. 2274-83.
58. Jin, L., G.N. Alesi, and S. Kang, *Glutaminolysis as a target for cancer therapy.* Oncogene, 2015.
59. Harris, I.S., et al., *Glutathione and thioredoxin antioxidant pathways synergize to drive cancer initiation and progression.* Cancer Cell, 2015. **27**(2): p. 211-22.
60. Bhutia, Y.D. and V. Ganapathy, *Glutamine transporters in mammalian cells and their functions in physiology and cancer.* Biochim Biophys Acta, 2015.
61. Wang, Q., et al., *Targeting ASCT2-mediated glutamine uptake blocks prostate cancer growth and tumour development.* J Pathol, 2015. **236**(3): p. 278-89.
62. Shimizu, K., et al., *ASC amino-acid transporter 2 (ASCT2) as a novel prognostic marker in non-small cell lung cancer.* Br J Cancer, 2014. **110**(8): p. 2030-9.
63. van Geldermalsen, M., et al., *ASCT2/SLC1A5 controls glutamine uptake and tumour growth in triple-negative basal-like breast cancer.* Oncogene, 2015.
64. Patel, M., et al., *Functional characterization and molecular expression of large neutral amino acid transporter (LAT1) in human prostate cancer cells.* Int J Pharm, 2013. **443**(1-2): p. 245-53.
65. Zhao, Y., L. Wang, and J. Pan, *The role of L-type amino acid transporter 1 in human tumors.* Intractable Rare Dis Res, 2015. **4**(4): p. 165-9.
66. Huang, Q., et al., *Glutamine transporter ASCT2 was down-regulated in ischemic injured human intestinal epithelial cells and reversed by epidermal growth factor.* JPEN J Parenter Enteral Nutr, 2007. **31**(2): p. 86-93.
67. Carr, E.L., et al., *Glutamine uptake and metabolism are coordinately regulated by ERK/MAPK during T lymphocyte activation.* J Immunol, 2010. **185**(2): p. 1037-44.

68. Wang, H.S., M. Wasa, and A. Okada, *Amino acid transport in a human neuroblastoma cell line is regulated by the type I insulin-like growth factor receptor.* Life Sci, 2002. **71**(2): p. 127-37.
69. Wasa, M., et al., *Insulin-like growth factor-I stimulates amino acid transport in a glutamine-deprived human neuroblastoma cell line.* Biochim Biophys Acta, 2001. **1525**(1-2): p. 118-24.
70. Fuchs, B.C., et al., *ASCT2 silencing regulates mammalian target-of-rapamycin growth and survival signaling in human hepatoma cells.* Am J Physiol Cell Physiol, 2007. **293**(1): p. C55-63.
71. Nicklin, P., et al., *Bidirectional transport of amino acids regulates mTOR and autophagy.* Cell, 2009. **136**(3): p. 521-34.
72. Hara, K., et al., *Amino acid sufficiency and mTOR regulate p70 S6 kinase and eIF-4E BP1 through a common effector mechanism.* J Biol Chem, 1998. **273**(23): p. 14484-94.
73. Dann, S.G. and G. Thomas, *The amino acid sensitive TOR pathway from yeast to mammals.* FEBS Lett, 2006. **580**(12): p. 2821-9.
74. Aledo, J.C., et al., *Identification of two human glutaminase loci and tissue-specific expression of the two related genes.* Mamm Genome, 2000. **11**(12): p. 1107-10.
75. Szeliga, M., et al., *Silencing of GLS and overexpression of GLS2 genes cooperate in decreasing the proliferation and viability of glioblastoma cells.* Tumour Biol, 2014. **35**(3): p. 1855-62.
76. Gross, M.I., et al., *Antitumor activity of the glutaminase inhibitor CB-839 in triple-negative breast cancer.* Mol Cancer Ther, 2014. **13**(4): p. 890-901.
77. Gao, P., et al., *c-Myc suppression of miR-23a/b enhances mitochondrial glutaminase expression and glutamine metabolism.* Nature, 2009. **458**(7239): p. 762-5.
78. Csibi, A., et al., *The mTORC1/S6K1 pathway regulates glutamine metabolism through the eIF4B-dependent control of c-Myc translation.* Curr Biol, 2014. **24**(19): p. 2274-80.
79. Wang, J.B., et al., *Targeting mitochondrial glutaminase activity inhibits oncogenic transformation.* Cancer Cell, 2010. **18**(3): p. 207-19.
80. Suzuki, S., et al., *Phosphate-activated glutaminase (GLS2), a p53-inducible regulator of glutamine metabolism and reactive oxygen species.* Proc Natl Acad Sci U S A, 2010. **107**(16): p. 7461-6.
81. Qing, G., et al., *ATF4 regulates MYC-mediated neuroblastoma cell death upon glutamine deprivation.* Cancer Cell, 2012. **22**(5): p. 631-44.
82. Jin, L., et al., *Glutamate dehydrogenase 1 signals through antioxidant glutathione peroxidase 1 to regulate redox homeostasis and tumor growth.* Cancer Cell, 2015. **27**(2): p. 257-70.
83. Wise, D.R., et al., *Hypoxia promotes isocitrate dehydrogenase-dependent carboxylation of alpha-ketoglutarate to citrate to support cell growth and viability.* Proc Natl Acad Sci U S A, 2011. **108**(49): p. 19611-6.

84. Fan, J., et al., *Glutamine-driven oxidative phosphorylation is a major ATP source in transformed mammalian cells in both normoxia and hypoxia.* Mol Syst Biol, 2013. **9**: p. 712.
85. Mulcahy, R.T., S. Untawale, and J.J. Gipp, *Transcriptional up-regulation of gamma-glutamylcysteine synthetase gene expression in melphalan-resistant human prostate carcinoma cells.* Mol Pharmacol, 1994. **46**(5): p. 909-14.
86. Tew, K.D., *Glutathione-associated enzymes in anticancer drug resistance.* Cancer Res, 1994. **54**(16): p. 4313-20.
87. Godwin, A.K., et al., *High resistance to cisplatin in human ovarian cancer cell lines is associated with marked increase of glutathione synthesis.* Proc Natl Acad Sci U S A, 1992. **89**(7): p. 3070-4.
88. Benlloch, M., et al., *Acceleration of glutathione efflux and inhibition of gamma-glutamyltranspeptidase sensitize metastatic B16 melanoma cells to endothelium-induced cytotoxicity.* J Biol Chem, 2005. **280**(8): p. 6950-9.
89. Seitz, G., et al., *Inhibition of glutathione-S-transferase as a treatment strategy for multidrug resistance in childhood rhabdomyosarcoma.* Int J Oncol, 2010. **36**(2): p. 491-500.
90. Kiebala, M., et al., *Dual targeting of the thioredoxin and glutathione antioxidant systems in malignant B cells: a novel synergistic therapeutic approach.* Exp Hematol, 2015. **43**(2): p. 89-99.
91. Medes, G., A. Thomas, and S. Weinhouse, *Metabolism of neoplastic tissue. IV. A study of lipid synthesis in neoplastic tissue slices in vitro.* Cancer Res, 1953. **13**(1): p. 27-9.
92. Nagahashi, M., et al., *Sphingosine-1-phosphate produced by sphingosine kinase 1 promotes breast cancer progression by stimulating angiogenesis and lymphangiogenesis.* Cancer Res, 2012. **72**(3): p. 726-35.
93. Wymann, M.P. and R. Schneiter, *Lipid signalling in disease.* Nat Rev Mol Cell Biol, 2008. **9**(2): p. 162-76.
94. Hannun, Y.A. and L.M. Obeid, *Principles of bioactive lipid signalling: lessons from sphingolipids.* Nat Rev Mol Cell Biol, 2008. **9**(2): p. 139-50.
95. Nieman, K.M., et al., *Adipocytes promote ovarian cancer metastasis and provide energy for rapid tumor growth.* Nat Med, 2011. **17**(11): p. 1498-503.
96. Metallo, C.M., et al., *Reductive glutamine metabolism by IDH1 mediates lipogenesis under hypoxia.* Nature, 2012. **481**(7381): p. 380-4.
97. Menendez, J.A. and R. Lupu, *Fatty acid synthase and the lipogenic phenotype in cancer pathogenesis.* Nat Rev Cancer, 2007. **7**(10): p. 763-77.
98. Milgraum, L.Z., et al., *Enzymes of the fatty acid synthesis pathway are highly expressed in in situ breast carcinoma.* Clin Cancer Res, 1997. **3**(11): p. 2115-20.
99. Menendez, J.A., et al., *Inhibition of fatty acid synthase (FAS) suppresses HER2/neu (erbB-2) oncogene overexpression in cancer cells.* Proc Natl Acad Sci U S A, 2004. **101**(29): p. 10715-20.

100. Menendez, J.A., R. Lupu, and R. Colomer, *Targeting fatty acid synthase: potential for therapeutic intervention in her-2/neu-overexpressing breast cancer.* Drug News Perspect, 2005. **18**(6): p. 375-85.
101. Zhao, X., et al., *Regulation of lipogenesis by cyclin-dependent kinase 8-mediated control of SREBP-1.* J Clin Invest, 2012. **122**(7): p. 2417-27.
102. Puzio-Kuter, A.M., *The Role of p53 in Metabolic Regulation.* Genes Cancer, 2011. **2**(4): p. 385-91.
103. Wellberg, E.A., et al., *Modulation of tumor fatty acids, through overexpression or loss of thyroid hormone responsive protein spot 14 is associated with altered growth and metastasis.* Breast Cancer Res, 2014. **16**(6): p. 481.
104. Bandyopadhyay, S., et al., *Mechanism of apoptosis induced by the inhibition of fatty acid synthase in breast cancer cells.* Cancer Res, 2006. **66**(11): p. 5934-40.
105. Kridel, S.J., et al., *Orlistat is a novel inhibitor of fatty acid synthase with antitumor activity.* Cancer Res, 2004. **64**(6): p. 2070-5.
106. Kuhajda, F.P., et al., *Synthesis and antitumor activity of an inhibitor of fatty acid synthase.* Proc Natl Acad Sci U S A, 2000. **97**(7): p. 3450-4.
107. Menendez, J.A. and R. Lupu, *RNA interference-mediated silencing of the p53 tumor-suppressor protein drastically increases apoptosis after inhibition of endogenous fatty acid metabolism in breast cancer cells.* Int J Mol Med, 2005. **15**(1): p. 33-40.
108. Pizer, E.S., et al., *Inhibition of fatty acid synthesis induces programmed cell death in human breast cancer cells.* Cancer Res, 1996. **56**(12): p. 2745-7.
109. Pizer, E.S., et al., *Inhibition of fatty acid synthesis delays disease progression in a xenograft model of ovarian cancer.* Cancer Res, 1996. **56**(6): p. 1189-93.
110. Wong, K.K., J.A. Engelman, and L.C. Cantley, *Targeting the PI3K signaling pathway in cancer.* Curr Opin Genet Dev, 2010. **20**(1): p. 87-90.
111. Elstrom, R.L., et al., *Akt stimulates aerobic glycolysis in cancer cells.* Cancer Res, 2004. **64**(11): p. 3892-9.
112. Zoncu, R., A. Efeyan, and D.M. Sabatini, *mTOR: from growth signal integration to cancer, diabetes and ageing.* Nat Rev Mol Cell Biol, 2011. **12**(1): p. 21-35.
113. Morrison, M.M., et al., *mTOR Directs Breast Morphogenesis through the PKC-alpha-Rac1 Signaling Axis.* PLoS Genet, 2015. **11**(7): p. e1005291.
114. Porstmann, T., et al., *SREBP activity is regulated by mTORC1 and contributes to Akt-dependent cell growth.* Cell Metab, 2008. **8**(3): p. 224-36.
115. Hagiwara, A., et al., *Hepatic mTORC2 activates glycolysis and lipogenesis through Akt, glucokinase, and SREBP1c.* Cell Metab, 2012. **15**(5): p. 725-38.
116. Yuan, M., et al., *Identification of Akt-independent regulation of hepatic lipogenesis by mammalian target of rapamycin (mTOR) complex 2.* J Biol Chem, 2012. **287**(35): p. 29579-88.

117. Dang, C.V., A. Le, and P. Gao, *MYC-induced cancer cell energy metabolism and therapeutic opportunities.* Clin Cancer Res, 2009. **15**(21): p. 6479-83.
118. Osthus, R.C., et al., *Deregulation of glucose transporter 1 and glycolytic gene expression by c-Myc.* J Biol Chem, 2000. **275**(29): p. 21797-800.
119. Lewis, B.C., et al., *Tumor induction by the c-Myc target genes rcl and lactate dehydrogenase A.* Cancer Res, 2000. **60**(21): p. 6178-83.
120. David, C.J., et al., *HnRNP proteins controlled by c-Myc deregulate pyruvate kinase mRNA splicing in cancer.* Nature, 2010. **463**(7279): p. 364-8.
121. Hu, Y., et al., *K-ras(G12V) transformation leads to mitochondrial dysfunction and a metabolic switch from oxidative phosphorylation to glycolysis.* Cell Res, 2012. **22**(2): p. 399-412.
122. Pasquale, E.B., *Eph receptor signalling casts a wide net on cell behaviour.* Nat Rev Mol Cell Biol, 2005. **6**(6): p. 462-75.
123. Pasquale, E.B., *Eph-ephrin bidirectional signaling in physiology and disease.* Cell, 2008. **133**(1): p. 38-52.
124. Pasquale, E.B., *The Eph family of receptors.* Curr Opin Cell Biol, 1997. **9**(5): p. 608-15.
125. Himanen, J.P., et al., *Crystal structure of an Eph receptor-ephrin complex.* Nature, 2001. **414**(6866): p. 933-8.
126. Kullander, K. and R. Klein, *Mechanisms and functions of Eph and ephrin signalling.* Nat Rev Mol Cell Biol, 2002. **3**(7): p. 475-86.
127. Himanen, J.P., et al., *Ligand recognition by A-class Eph receptors: crystal structures of the EphA2 ligand-binding domain and the EphA2/ephrin-A1 complex.* EMBO Rep, 2009. **10**(7): p. 722-8.
128. Murai, K.K. and E.B. Pasquale, *'Eph'ective signaling: forward, reverse and crosstalk.* J Cell Sci, 2003. **116**(Pt 14): p. 2823-32.
129. Zisch, A.H., et al., *Replacing two conserved tyrosines of the EphB2 receptor with glutamic acid prevents binding of SH2 domains without abrogating kinase activity and biological responses.* Oncogene, 2000. **19**(2): p. 177-87.
130. Amato, K.R., et al., *Genetic and pharmacologic inhibition of EPHA2 promotes apoptosis in NSCLC.* J Clin Invest, 2014. **124**(5): p. 2037-49.
131. Brantley-Sieders, D.M., et al., *Impaired tumor microenvironment in EphA2-deficient mice inhibits tumor angiogenesis and metastatic progression.* FASEB J, 2005. **19**(13): p. 1884-6.
132. Wang, Y., et al., *Ephrin-B2 controls VEGF-induced angiogenesis and lymphangiogenesis.* Nature, 2010. **465**(7297): p. 483-6.
133. Pasquale, E.B., *Eph receptors and ephrins in cancer: bidirectional signalling and beyond.* Nat Rev Cancer, 2010. **10**(3): p. 165-80.
134. Pandy, M.G., B.A. Garner, and F.C. Anderson, *Optimal control of non-ballistic muscular movements: a constraint-based performance criterion for rising from a chair.* J Biomech Eng, 1995. **117**(1): p. 15-26.

135. Miao, H., et al., *Activation of EphA2 kinase suppresses integrin function and causes focal-adhesion-kinase dephosphorylation.* Nat Cell Biol, 2000. **2**(2): p. 62-9.
136. Shamah, S.M., et al., *EphA receptors regulate growth cone dynamics through the novel guanine nucleotide exchange factor ephexin.* Cell, 2001. **105**(2): p. 233-44.
137. Brantley-Sieders, D.M., et al., *The receptor tyrosine kinase EphA2 promotes mammary adenocarcinoma tumorigenesis and metastatic progression in mice by amplifying ErbB2 signaling.* J Clin Invest, 2008. **118**(1): p. 64-78.
138. Pratt, R.L. and M.S. Kinch, *Activation of the EphA2 tyrosine kinase stimulates the MAP/ERK kinase signaling cascade.* Oncogene, 2002. **21**(50): p. 7690-9.
139. Menges, C.W. and D.J. McCance, *Constitutive activation of the Raf-MAPK pathway causes negative feedback inhibition of Ras-PI3K-AKT and cellular arrest through the EphA2 receptor.* Oncogene, 2008. **27**(20): p. 2934-40.
140. Noren, N.K. and E.B. Pasquale, *Eph receptor-ephrin bidirectional signals that target Ras and Rho proteins.* Cell Signal, 2004. **16**(6): p. 655-66.
141. Fang, W.B., et al., *A kinase-dependent role for EphA2 receptor in promoting tumor growth and metastasis.* Oncogene, 2005. **24**(53): p. 7859-68.
142. Fang, W.B., et al., *Overexpression of EPHA2 receptor destabilizes adherens junctions via a RhoA-dependent mechanism.* J Cell Sci, 2008. **121**(Pt 3): p. 358-68.
143. Mancia, F. and L. Shapiro, *ADAM and Eph: how Ephrin-signaling cells become detached.* Cell, 2005. **123**(2): p. 185-7.
144. Holland, S.J., et al., *Bidirectional signalling through the EPH-family receptor Nuk and its transmembrane ligands.* Nature, 1996. **383**(6602): p. 722-5.
145. Palmer, A., et al., *EphrinB phosphorylation and reverse signaling: regulation by Src kinases and PTP-BL phosphatase.* Mol Cell, 2002. **9**(4): p. 725-37.
146. Bruckner, K., E.B. Pasquale, and R. Klein, *Tyrosine phosphorylation of transmembrane ligands for Eph receptors.* Science, 1997. **275**(5306): p. 1640-3.
147. Lu, Q., et al., *Ephrin-B reverse signaling is mediated by a novel PDZ-RGS protein and selectively inhibits G protein-coupled chemoattraction.* Cell, 2001. **105**(1): p. 69-79.
148. Brown, D., *The tyrosine kinase connection: how GPI-anchored proteins activate T cells.* Curr Opin Immunol, 1993. **5**(3): p. 349-54.
149. Davy, A., et al., *Compartmentalized signaling by GPI-anchored ephrin-A5 requires the Fyn tyrosine kinase to regulate cellular adhesion.* Genes Dev, 1999. **13**(23): p. 3125-35.
150. Walker-Daniels, J., D.J. Riese, 2nd, and M.S. Kinch, *c-Cbl-dependent EphA2 protein degradation is induced by ligand binding.* Mol Cancer Res, 2002. **1**(1): p. 79-87.
151. Miao, H., et al., *Activation of EphA receptor tyrosine kinase inhibits the Ras/MAPK pathway.* Nat Cell Biol, 2001. **3**(5): p. 527-30.

152. Miao, H., et al., *EphA2 mediates ligand-dependent inhibition and ligand-independent promotion of cell migration and invasion via a reciprocal regulatory loop with Akt.* Cancer Cell, 2009. **16**(1): p. 9-20.
153. Noren, N.K., et al., *The EphB4 receptor suppresses breast cancer cell tumorigenicity through an Abl-Crk pathway.* Nat Cell Biol, 2006. **8**(8): p. 815-25.
154. Sharfe, N., et al., *Ephrin stimulation modulates T cell chemotaxis.* Eur J Immunol, 2002. **32**(12): p. 3745-55.
155. Deroanne, C., et al., *EphrinA1 inactivates integrin-mediated vascular smooth muscle cell spreading via the Rac/PAK pathway.* J Cell Sci, 2003. **116**(Pt 7): p. 1367-76.
156. Larsen, A.B., et al., *Activation of the EGFR gene target EphA2 inhibits epidermal growth factor-induced cancer cell motility.* Mol Cancer Res, 2007. **5**(3): p. 283-93.
157. Tanaka, M., R. Kamata, and R. Sakai, *EphA2 phosphorylates the cytoplasmic tail of Claudin-4 and mediates paracellular permeability.* J Biol Chem, 2005. **280**(51): p. 42375-82.
158. Zantek, N.D., et al., *E-cadherin regulates the function of the EphA2 receptor tyrosine kinase.* Cell Growth Differ, 1999. **10**(9): p. 629-38.
159. Prevost, N., et al., *Eph kinases and ephrins support thrombus growth and stability by regulating integrin outside-in signaling in platelets.* Proc Natl Acad Sci U S A, 2005. **102**(28): p. 9820-5.
160. Yokote, H., et al., *Trans-activation of EphA4 and FGF receptors mediated by direct interactions between their cytoplasmic domains.* Proc Natl Acad Sci U S A, 2005. **102**(52): p. 18866-71.
161. Warner, N., L.E. Wybenga-Groot, and T. Pawson, *Analysis of EphA4 receptor tyrosine kinase substrate specificity using peptide-based arrays.* FEBS J, 2008. **275**(10): p. 2561-73.
162. Gu, C. and S. Park, *The EphA8 receptor regulates integrin activity through p110gamma phosphatidylinositol-3 kinase in a tyrosine kinase activity-independent manner.* Mol Cell Biol, 2001. **21**(14): p. 4579-97.
163. Dalva, M.B., et al., *EphB receptors interact with NMDA receptors and regulate excitatory synapse formation.* Cell, 2000. **103**(6): p. 945-56.
164. Cortina, C., et al., *EphB-ephrin-B interactions suppress colorectal cancer progression by compartmentalizing tumor cells.* Nat Genet, 2007. **39**(11): p. 1376-83.
165. Ethell, I.M., et al., *EphB/syndecan-2 signaling in dendritic spine morphogenesis.* Neuron, 2001. **31**(6): p. 1001-13.
166. Zisch, A.H., et al., *Tyrosine phosphorylation of L1 family adhesion molecules: implication of the Eph kinase Cek5.* J Neurosci Res, 1997. **47**(6): p. 655-65.
167. Salvucci, O., et al., *EphB2 and EphB4 receptors forward signaling promotes SDF-1-induced endothelial cell chemotaxis and branching remodeling.* Blood, 2006. **108**(9): p. 2914-22.

168. Trivier, E. and T.S. Ganesan, *RYK, a catalytically inactive receptor tyrosine kinase, associates with EphB2 and EphB3 but does not interact with AF-6.* J Biol Chem, 2002. **277**(25): p. 23037-43.
169. Luo, H., et al., *EphB6 crosslinking results in costimulation of T cells.* J Clin Invest, 2002. **110**(8): p. 1141-50.
170. Zhou, R., *The Eph family receptors and ligands.* Pharmacol Ther, 1998. **77**(3): p. 151-81.
171. Stein, E., et al., *Eph receptors discriminate specific ligand oligomers to determine alternative signaling complexes, attachment, and assembly responses.* Genes Dev, 1998. **12**(5): p. 667-78.
172. Huynh-Do, U., et al., *Surface densities of ephrin-B1 determine EphB1-coupled activation of cell attachment through alphavbeta3 and alpha5beta1 integrins.* EMBO J, 1999. **18**(8): p. 2165-73.
173. Brantley-Sieders, D.M., et al., *Eph/ephrin profiling in human breast cancer reveals significant associations between expression level and clinical outcome.* PLoS One, 2011. **6**(9): p. e24426.
174. Brannan, J.M., et al., *Expression of the receptor tyrosine kinase EphA2 is increased in smokers and predicts poor survival in non-small cell lung cancer.* Clin Cancer Res, 2009. **15**(13): p. 4423-30.
175. Kinch, M.S., M.B. Moore, and D.H. Harpole, Jr., *Predictive value of the EphA2 receptor tyrosine kinase in lung cancer recurrence and survival.* Clin Cancer Res, 2003. **9**(2): p. 613-8.
176. Duxbury, M.S., et al., *EphA2: a determinant of malignant cellular behavior and a potential therapeutic target in pancreatic adenocarcinoma.* Oncogene, 2004. **23**(7): p. 1448-56.
177. Han, L., et al., *The clinical significance of EphA2 and Ephrin A-1 in epithelial ovarian carcinomas.* Gynecol Oncol, 2005. **99**(2): p. 278-86.
178. Miyazaki, T., et al., *EphA2 overexpression correlates with poor prognosis in esophageal squamous cell carcinoma.* Int J Cancer, 2003. **103**(5): p. 657-63.
179. Zelinski, D.P., et al., *EphA2 overexpression causes tumorigenesis of mammary epithelial cells.* Cancer Res, 2001. **61**(5): p. 2301-6.
180. Lu, C., et al., *EphA2 overexpression promotes ovarian cancer growth.* Cancer Biol Ther, 2008. **7**(7): p. 1098-103.
181. Zhuang, G., et al., *Elevation of receptor tyrosine kinase EphA2 mediates resistance to trastuzumab therapy.* Cancer Res, 2010. **70**(1): p. 299-308.
182. Lu, M., et al., *EphA2 overexpression decreases estrogen dependence and tamoxifen sensitivity.* Cancer Res, 2003. **63**(12): p. 3425-9.
183. Miao, B., et al., *EPHA2 is a mediator of vemurafenib resistance and a novel therapeutic target in melanoma.* Cancer Discov, 2015. **5**(3): p. 274-87.
184. Amato, K.R., et al., *EPHA2 Blockade Overcomes Acquired Resistance to EGFR Kinase Inhibitors in Lung Cancer.* Cancer Res, 2016. **76**(2): p. 305-18.

185. Song, W., et al., *JNK signaling mediates EPHA2-dependent tumor cell proliferation, motility, and cancer stem cell-like properties in non-small cell lung cancer.* Cancer Res, 2014. **74**(9): p. 2444-54.
186. Landen, C.N., Jr., et al., *Therapeutic EphA2 gene targeting in vivo using neutral liposomal small interfering RNA delivery.* Cancer Res, 2005. **65**(15): p. 6910-8.
187. Munarini, N., et al., *Altered mammary epithelial development, pattern formation and involution in transgenic mice expressing the EphB4 receptor tyrosine kinase.* J Cell Sci, 2002. **115**(Pt 1): p. 25-37.
188. Folkman, J., *Role of angiogenesis in tumor growth and metastasis.* Semin Oncol, 2002. **29**(6 Suppl 16): p. 15-8.
189. Weis, S.M. and D.A. Cheresh, *Tumor angiogenesis: molecular pathways and therapeutic targets.* Nat Med, 2011. **17**(11): p. 1359-70.
190. Senger, D.R., et al., *Vascular permeability factor (VPF, VEGF) in tumor biology.* Cancer Metastasis Rev, 1993. **12**(3-4): p. 303-24.
191. Brantley-Sieders, D.M. and J. Chen, *Eph receptor tyrosine kinases in angiogenesis: from development to disease.* Angiogenesis, 2004. **7**(1): p. 17-28.
192. Sawamiphak, S., et al., *Ephrin-B2 regulates VEGFR2 function in developmental and tumour angiogenesis.* Nature, 2010. **465**(7297): p. 487-91.
193. Herath, N.I., et al., *Over-expression of Eph and ephrin genes in advanced ovarian cancer: ephrin gene expression correlates with shortened survival.* BMC Cancer, 2006. **6**: p. 144.
194. Vaught, D., D.M. Brantley-Sieders, and J. Chen, *Eph receptors in breast cancer: roles in tumor promotion and tumor suppression.* Breast Cancer Res, 2008. **10**(6): p. 217.
195. Gyorffy, B., et al., *An online survival analysis tool to rapidly assess the effect of 22,277 genes on breast cancer prognosis using microarray data of 1,809 patients.* Breast Cancer Res Treat, 2010. **123**(3): p. 725-31.
196. Evans, A.M., et al., *Integrated, nontargeted ultrahigh performance liquid chromatography/electrospray ionization tandem mass spectrometry platform for the identification and relative quantification of the small-molecule complement of biological systems.* Anal Chem, 2009. **81**(16): p. 6656-67.
197. Brantley, D.M., et al., *Soluble Eph A receptors inhibit tumor angiogenesis and progression in vivo.* Oncogene, 2002. **21**(46): p. 7011-26.
198. Brantley-Sieders, D.M., et al., *Ephrin-A1 facilitates mammary tumor metastasis through an angiogenesis-dependent mechanism mediated by EphA receptor and vascular endothelial growth factor in mice.* Cancer Res, 2006. **66**(21): p. 10315-24.
199. Frieden, L.A., et al., *Regulation of heart valve morphogenesis by Eph receptor ligand, ephrin-A1.* Dev Dyn, 2010. **239**(12): p. 3226-34.

200. Tawadros, T., et al., *Ligand-independent activation of EphA2 by arachidonic acid induces metastasis-like behaviour in prostate cancer cells.* Br J Cancer, 2012. **107**(10): p. 1737-44.
201. Muller, W.J., et al., *Single-step induction of mammary adenocarcinoma in transgenic mice bearing the activated c-neu oncogene.* Cell, 1988. **54**(1): p. 105-15.
202. Hanahan, D. and R.A. Weinberg, *Hallmarks of cancer: the next generation.* Cell, 2011. **144**(5): p. 646-74.
203. Furuta, E., et al., *Metabolic genes in cancer: their roles in tumor progression and clinical implications.* Biochim Biophys Acta, 2010. **1805**(2): p. 141-52.
204. Pemble, C.W.t., et al., *Crystal structure of the thioesterase domain of human fatty acid synthase inhibited by Orlistat.* Nat Struct Mol Biol, 2007. **14**(8): p. 704-9.
205. Thornburg, J.M., et al., *Targeting aspartate aminotransferase in breast cancer.* Breast Cancer Res, 2008. **10**(5): p. R84.
206. Parri, M., et al., *EphA2 reexpression prompts invasion of melanoma cells shifting from mesenchymal to amoeboid-like motility style.* Cancer Res, 2009. **69**(5): p. 2072-81.
207. Miao, H. and B. Wang, *EphA receptor signaling--complexity and emerging themes.* Semin Cell Dev Biol, 2012. **23**(1): p. 16-25.
208. Gokmen-Polar, Y., et al., *Dual targeting of EphA2 and ER restores tamoxifen sensitivity in ER/EphA2-positive breast cancer.* Breast Cancer Res Treat, 2011. **127**(2): p. 375-84.
209. Noblitt, L.W., et al., *Decreased tumorigenic potential of EphA2-overexpressing breast cancer cells following treatment with adenoviral vectors that express EphrinA1.* Cancer Gene Ther, 2004. **11**(11): p. 757-66.
210. Hanahan, D. and R.A. Weinberg, *Hallmarks of cancer: the next generation.* Cell, 2011. **144**: p. 646-674.
211. Furuta, E., et al., *Fatty acid synthase gene is up-regulated by hypoxia via activation of Akt and sterol regulatory element binding protein-1.* Cancer Res, 2008. **68**(4): p. 1003-11.
212. Yang, Y., et al., *Regulation of fatty acid synthase expression in breast cancer by sterol regulatory element binding protein-1c.* Exp Cell Res, 2003. **282**(2): p. 132-7.
213. Hatzivassiliou, G., et al., *ATP citrate lyase inhibition can suppress tumor cell growth.* Cancer Cell, 2005. **8**(4): p. 311-21.
214. DeBerardinis, R.J., et al., *Beyond aerobic glycolysis: transformed cells can engage in glutamine metabolism that exceeds the requirement for protein and nucleotide synthesis.* Proc Natl Acad Sci U S A, 2007. **104**(49): p. 19345-50.
215. Wise, D.R. and C.B. Thompson, *Glutamine addiction: a new therapeutic target in cancer.* Trends Biochem Sci, 2010. **35**(8): p. 427-33.

216. Kung, H.N., J.R. Marks, and J.T. Chi, *Glutamine synthetase is a genetic determinant of cell type-specific glutamine independence in breast epithelia.* PLoS Genet, 2011. **7**(8): p. e1002229.
217. Choi, Y., et al., *Discovery and structural analysis of Eph receptor tyrosine kinase inhibitors.* Bioorg Med Chem Lett, 2009. **19**(15): p. 4467-70.
218. Cairns, R.A., I.S. Harris, and T.W. Mak, *Regulation of cancer cell metabolism.* Nat Rev Cancer, 2011. **11**(2): p. 85-95.
219. Rouzier, R., et al., *Breast cancer molecular subtypes respond differently to preoperative chemotherapy.* Clin Cancer Res, 2005. **11**(16): p. 5678-85.
220. Wolff, A.C., et al., *American Society of Clinical Oncology/College of American Pathologists guideline recommendations for human epidermal growth factor receptor 2 testing in breast cancer.* J Clin Oncol, 2007. **25**(1): p. 118-45.
221. Slamon, D.J., et al., *Use of chemotherapy plus a monoclonal antibody against HER2 for metastatic breast cancer that overexpresses HER2.* N Engl J Med, 2001. **344**(11): p. 783-92.
222. Shen, H., et al., *Enhancing chemotherapy response with sustained EphA2 silencing using multistage vector delivery.* Clin Cancer Res, 2013. **19**(7): p. 1806-15.
223. Wang, S., et al., *Targeted delivery of paclitaxel to EphA2-expressing cancer cells.* Clin Cancer Res, 2013. **19**(1): p. 128-37.
224. Wang, Y., et al., *Ephrin typeA receptor 2 regulates sensitivity to paclitaxel in nasopharyngeal carcinoma via the phosphoinositide 3kinase/Akt signalling pathway.* Mol Med Rep, 2015. **11**(2): p. 924-30.
225. Dunne, P.D., et al., *EphA2 Expression Is a Key Driver of Migration and Invasion and a Poor Prognostic Marker in Colorectal Cancer.* Clin Cancer Res, 2016. **22**(1): p. 230-42.
226. Taddei, M.L., et al., *EphA2 induces metastatic growth regulating amoeboid motility and clonogenic potential in prostate carcinoma cells.* Mol Cancer Res, 2011. **9**(2): p. 149-60.
227. Shiraishi, T., et al., *Glycolysis is the primary bioenergetic pathway for cell motility and cytoskeletal remodeling in human prostate and breast cancer cells.* Oncotarget, 2015. **6**(1): p. 130-43.
228. Currie, E., et al., *Cellular fatty acid metabolism and cancer.* Cell Metab, 2013. **18**(2): p. 153-61.
229. Jin, Q., et al., *Fatty acid synthase phosphorylation: a novel therapeutic target in HER2-overexpressing breast cancer cells.* Breast Cancer Res, 2010. **12**(6): p. R96.
230. Zaytseva, Y.Y., et al., *Inhibition of fatty acid synthase attenuates CD44-associated signaling and reduces metastasis in colorectal cancer.* Cancer Res, 2012. **72**(6): p. 1504-17.
231. Kim, M.J., et al., *Expression of metabolism-related proteins in triple-negative breast cancer.* Int J Clin Exp Pathol, 2014. **7**(1): p. 301-12.

232. Cao, M.D., et al., *Metabolic characterization of triple negative breast cancer.* BMC Cancer, 2014. **14**: p. 941.
233. Macrae, M., et al., *A conditional feedback loop regulates Ras activity through EphA2.* Cancer Cell, 2005. **8**(2): p. 111-8.
234. Potente, M., H. Gerhardt, and P. Carmeliet, *Basic and therapeutic aspects of angiogenesis.* Cell, 2011. **146**(6): p. 873-87.
235. Tie, J. and J. Desai, *Antiangiogenic therapies targeting the vascular endothelia growth factor signaling system.* Crit Rev Oncog, 2012. **17**(1): p. 51-67.
236. Waldner, M.J. and M.F. Neurath, *Targeting the VEGF signaling pathway in cancer therapy.* Expert Opin Ther Targets, 2012. **16**(1): p. 5-13.
237. Brantley-Sieders, D., et al., *Eph receptor tyrosine kinases in tumor and tumor microenvironment.* Curr Pharm Des, 2004. **10**(27): p. 3431-42.
238. Kuijper, S., C.J. Turner, and R.H. Adams, *Regulation of angiogenesis by Eph-ephrin interactions.* Trends Cardiovasc Med, 2007. **17**(5): p. 145-51.
239. Ahmed, Z. and R. Bicknell, *Angiogenic signalling pathways.* Methods Mol Biol, 2009. **467**: p. 3-24.
240. Holderfield, M.T. and C.C. Hughes, *Crosstalk between vascular endothelial growth factor, notch, and transforming growth factor-beta in vascular morphogenesis.* Circ Res, 2008. **102**(6): p. 637-52.
241. Chung, A.S. and N. Ferrara, *Developmental and pathological angiogenesis.* Annu Rev Cell Dev Biol, 2011. **27**: p. 563-84.
242. Cheng, N., et al., *Blockade of EphA receptor tyrosine kinase activation inhibits vascular endothelial cell growth factor-induced angiogenesis.* Mol Cancer Res, 2002. **1**(1): p. 2-11.
243. Cheng, N., et al., *Inhibition of VEGF-dependent multistage carcinogenesis by soluble EphA receptors.* Neoplasia, 2003. **5**(5): p. 445-56.
244. Dobrzanski, P., et al., *Antiangiogenic and antitumor efficacy of EphA2 receptor antagonist.* Cancer Res, 2004. **64**(3): p. 910-9.
245. Chen, J., et al., *Inhibition of retinal neovascularization by soluble EphA2 receptor.* Exp Eye Res, 2006. **82**(4): p. 664-73.
246. Landen, C.N., Jr., et al., *Efficacy and antivascular effects of EphA2 reduction with an agonistic antibody in ovarian cancer.* J Natl Cancer Inst, 2006. **98**(21): p. 1558-70.
247. Legg, J.A., et al., *Slits and Roundabouts in cancer, tumour angiogenesis and endothelial cell migration.* Angiogenesis, 2008. **11**(1): p. 13-21.
248. Zhang, B., et al., *Repulsive axon guidance molecule Slit3 is a novel angiogenic factor.* Blood, 2009. **114**(19): p. 4300-9.
249. Kaur, S., et al., *Robo4 signaling in endothelial cells implies attraction guidance mechanisms.* J Biol Chem, 2006. **281**(16): p. 11347-56.
250. Kaur, S., et al., *Silencing of directional migration in roundabout4 knockdown endothelial cells.* BMC Cell Biol, 2008. **9**: p. 61.

251. Sheldon, H., et al., *Active involvement of Robo1 and Robo4 in filopodia formation and endothelial cell motility mediated via WASP and other actin nucleation-promoting factors.* Faseb J, 2009. **23**(2): p. 513-22.
252. Urbich, C., et al., *HDAC5 is a repressor of angiogenesis and determines the angiogenic gene expression pattern of endothelial cells.* Blood, 2009. **113**(22): p. 5669-79.
253. Yang, X.M., et al., *Slit-Robo signaling mediates lymphangiogenesis and promotes tumor lymphatic metastasis.* Biochem Biophys Res Commun, 2010. **396**(2): p. 571-7.
254. Park, K.W., et al., *Robo4 is a vascular-specific receptor that inhibits endothelial migration.* Dev Biol, 2003. **261**(1): p. 251-67.
255. Jones, C.A., et al., *Robo4 stabilizes the vascular network by inhibiting pathologic angiogenesis and endothelial hyperpermeability.* Nat Med, 2008. **14**(4): p. 448-53.
256. Liu, D., et al., *Neuronal chemorepellent Slit2 inhibits vascular smooth muscle cell migration by suppressing small GTPase Rac1 activation.* Circ Res, 2006. **98**(4): p. 480-9.
257. Jones, C.A., et al., *Slit2-Robo4 signalling promotes vascular stability by blocking Arf6 activity.* Nat Cell Biol, 2009. **11**(11): p. 1325-31.
258. Han, X. and M.C. Zhang, *Potential anti-angiogenic role of Slit2 in corneal neovascularization.* Exp Eye Res, 2010. **90**(6): p. 742-9.
259. Yu, J., et al., *Slit2N and Robo4 regulate lymphangiogenesis through the VEGF-C/VEGFR-3 pathway.* Cell Commun Signal, 2014. **12**: p. 25.
260. Brantley-Sieders, D.M., et al., *Angiocrine factors modulate tumor proliferation and motility through EphA2 repression of Slit2 tumor suppressor function in endothelium.* Cancer Res, 2011. **71**(3): p. 976-87.
261. Prasad, A., et al., *Slit protein-mediated inhibition of CXCR4-induced chemotactic and chemoinvasive signaling pathways in breast cancer cells.* J Biol Chem, 2004. **279**(10): p. 9115-24.
262. Dallol, A., et al., *SLIT2, a human homologue of the Drosophila Slit2 gene, has tumor suppressor activity and is frequently inactivated in lung and breast cancers.* Cancer Res, 2002. **62**(20): p. 5874-80.
263. Schmid, B.C., et al., *The neuronal guidance cue Slit2 induces targeted migration and may play a role in brain metastasis of breast cancer cells.* Breast Cancer Res Treat, 2007. **106**(3): p. 333-42.
264. Marlow, R., et al., *SLITs suppress tumor growth in vivo by silencing Sdf1/Cxcr4 within breast epithelium.* Cancer Res, 2008. **68**(19): p. 7819-27.
265. Prasad, A., et al., *Slit-2 induces a tumor-suppressive effect by regulating beta-catenin in breast cancer cells.* J Biol Chem, 2008. **283**(39): p. 26624-33.
266. Yuasa-Kawada, J., et al., *Deubiquitinating enzyme USP33/VDU1 is required for Slit signaling in inhibiting breast cancer cell migration.* Proc Natl Acad Sci U S A, 2009. **106**(34): p. 14530-5.

267. Macias, H., et al., *SLIT/ROBO1 signaling suppresses mammary branching morphogenesis by limiting basal cell number.* Dev Cell, 2011. **20**(6): p. 827-40.
268. Chang, P.H., et al., *Activation of Robo1 signaling of breast cancer cells by Slit2 from stromal fibroblast restrains tumorigenesis via blocking PI3K/Akt/beta-catenin pathway.* Cancer Res, 2012. **72**(18): p. 4652-61.
269. Dunaway, C.M., et al., *Cooperative signaling between Slit2 and Ephrin-A1 regulates a balance between angiogenesis and angiostasis.* Mol Cell Biol, 2011. **31**(3): p. 404-16.
270. Brantley-Sieders, D.M., et al., *EphA2 receptor tyrosine kinase regulates endothelial cell migration and vascular assembly through phosphoinositide 3-kinase-mediated Rac1 GTPase activation.* J Cell Sci, 2004. **117**(Pt 10): p. 2037-49.
271. Jat, P.S., et al., *Direct derivation of conditionally immortal cell lines from an H-2Kb-tsA58 transgenic mouse.* Proc Natl Acad Sci U S A, 1991. **88**(12): p. 5096-100.
272. Langley, R.R., et al., *Tissue-specific microvascular endothelial cell lines from H-2K(b)-tsA58 mice for studies of angiogenesis and metastasis.* Cancer Res, 2003. **63**(11): p. 2971-6.
273. Fang, W.B., et al., *Identification and functional analysis of phosphorylated tyrosine residues within EphA2 receptor tyrosine kinase.* J Biol Chem, 2008. **283**(23): p. 16017-26.
274. Hunter, S.G., et al., *Essential role of Vav family guanine nucleotide exchange factors in EphA receptor-mediated angiogenesis.* Mol Cell Biol, 2006. **26**(13): p. 4830-42.
275. Brantley-Sieders, D.M., et al., *Host deficiency in Vav2/3 guanine nucleotide exchange factors impairs tumor growth, survival, and angiogenesis in vivo.* Mol Cancer Res, 2009. **7**(5): p. 615-23.
276. Muraoka, R.S., et al., *Blockade of TGF-beta inhibits mammary tumor cell viability, migration, and metastases.* J Clin Invest, 2002. **109**(12): p. 1551-9.
277. Li, C.Y., et al., *Initial stages of tumor cell-induced angiogenesis: evaluation via skin window chambers in rodent models.* J Natl Cancer Inst, 2000. **92**(2): p. 143-7.
278. Donaldson, J.G., *Multiple roles for Arf6: sorting, structuring, and signaling at the plasma membrane.* J Biol Chem, 2003. **278**(43): p. 41573-6.
279. Hashimoto, A., et al., *GEP100-Arf6-AMAP1-cortactin pathway frequently used in cancer invasion is activated by VEGFR2 to promote angiogenesis.* PLoS One, 2011. **6**(8): p. e23359.
280. Mitra, S.K., et al., *Intrinsic FAK activity and Y925 phosphorylation facilitate an angiogenic switch in tumors.* Oncogene, 2006. **25**(44): p. 5969-84.
281. Roland, C.L., et al., *Cytokine levels correlate with immune cell infiltration after anti-VEGF therapy in preclinical mouse models of breast cancer.* PLoS One, 2009. **4**(11): p. e7669.

282. Thomas, J.L., et al., *Interactions between VEGFR and Notch signaling pathways in endothelial and neural cells.* Cell Mol Life Sci, 2013. **70**(10): p. 1779-92.
283. Tushir, J.S. and C. D'Souza-Schorey, *ARF6-dependent activation of ERK and Rac1 modulates epithelial tubule development.* EMBO J, 2007. **26**(7): p. 1806-19.
284. Hu, B., et al., *ADP-ribosylation factor 6 regulates glioma cell invasion through the IQ-domain GTPase-activating protein 1-Rac1-mediated pathway.* Cancer Res, 2009. **69**(3): p. 794-801.
285. Muralidharan-Chari, V., et al., *ADP-ribosylation factor 6 regulates tumorigenic and invasive properties in vivo.* Cancer Res, 2009. **69**(6): p. 2201-9.
286. Bhanot, H., et al., *Induction of nonapoptotic cell death by activated Ras requires inverse regulation of Rac1 and Arf6.* Mol Cancer Res, 2010. **8**(10): p. 1358-74.
287. Kawaguchi, K., et al., *ADP ribosylation factor 6 (Arf6) acts through FilGAP protein to down-regulate Rac protein and regulates plasma membrane blebbing.* J Biol Chem, 2014. **289**(14): p. 9675-82.
288. Folkman, J., *What is the evidence that tumors are angiogenesis dependent?* J Natl Cancer Inst, 1990. **82**(1): p. 4-6.
289. Gasparini, G., *Clinical significance of determination of surrogate markers of angiogenesis in breast cancer.* Crit Rev Oncol Hematol, 2001. **37**(2): p. 97-114.
290. Rau, K.M., et al., *Neovascularization evaluated by CD105 correlates well with prognostic factors in breast cancers.* Exp Ther Med, 2012. **4**(2): p. 231-236.
291. Uzzan, B., et al., *Microvessel density as a prognostic factor in women with breast cancer: a systematic review of the literature and meta-analysis.* Cancer Res, 2004. **64**(9): p. 2941-55.
292. Gasparini, G., et al., *Prognostic significance of p53, angiogenesis, and other conventional features in operable breast cancer: subanalysis in node-positive and node-negative patients.* Int J Oncol, 1998. **12**(5): p. 1117-25.
293. Foekens, J.A., et al., *High tumor levels of vascular endothelial growth factor predict poor response to systemic therapy in advanced breast cancer.* Cancer Res, 2001. **61**(14): p. 5407-14.
294. Konecny, G.E., et al., *Association between HER-2/neu and vascular endothelial growth factor expression predicts clinical outcome in primary breast cancer patients.* Clin Cancer Res, 2004. **10**(5): p. 1706-16.
295. Linderholm, B., et al., *Correlation of vascular endothelial growth factor content with recurrences, survival, and first relapse site in primary node-positive breast carcinoma after adjuvant treatment.* J Clin Oncol, 2000. **18**(7): p. 1423-31.

296. Burstein, H.J., et al., *VEGF as a marker for outcome among advanced breast cancer patients receiving anti-VEGF therapy with bevacizumab and vinorelbine chemotherapy.* Clin Cancer Res, 2008. **14**(23): p. 7871-7.
297. Gasparini, G., *Prognostic value of vascular endothelial growth factor in breast cancer.* Oncologist, 2000. **5 Suppl 1**: p. 37-44.
298. Linderholm, B., et al., *Vascular endothelial growth factor is of high prognostic value in node-negative breast carcinoma.* J Clin Oncol, 1998. **16**(9): p. 3121-8.
299. Gasparini, G., et al., *Clinical relevance of vascular endothelial growth factor and thymidine phosphorylase in patients with node-positive breast cancer treated with either adjuvant chemotherapy or hormone therapy.* Cancer J Sci Am, 1999. **5**(2): p. 101-11.
300. Linderholm, B.K., et al., *Vascular endothelial growth factor is a strong predictor of early distant recurrences in a prospective study of premenopausal women with lymph-node negative breast cancer.* Breast, 2008. **17**(5): p. 484-91.
301. Linderholm, B.K., et al., *Significantly higher levels of vascular endothelial growth factor (VEGF) and shorter survival times for patients with primary operable triple-negative breast cancer.* Ann Oncol, 2009. **20**(10): p. 1639-46.
302. Linderholm, B., et al., *Shorter survival-times following adjuvant endocrine therapy in oestrogen- and progesterone-receptor positive breast cancer overexpressing HER2 and/or with an increased expression of vascular endothelial growth factor.* Med Oncol, 2009. **26**(4): p. 480-90.
303. Mylona, E., et al., *The prognostic value of vascular endothelial growth factors (VEGFs)-A and -B and their receptor, VEGFR-1, in invasive breast carcinoma.* Gynecol Oncol, 2007. **104**(3): p. 557-63.
304. Mylona, E., et al., *Clinicopathological and prognostic significance of vascular endothelial growth factors (VEGF)-C and -D and VEGF receptor 3 in invasive breast carcinoma.* Eur J Surg Oncol, 2007. **33**(3): p. 294-300.
305. Moran, M.S., et al., *Evaluation of vascular endothelial growth factor as a prognostic marker for local relapse in early-stage breast cancer patients treated with breast-conserving therapy.* Int J Radiat Oncol Biol Phys, 2011. **81**(5): p. 1236-43.
306. Claesson-Welsh, L. and M. Welsh, *VEGFA and tumour angiogenesis.* J Intern Med, 2013. **273**(2): p. 114-27.
307. Shibuya, M., *VEGFR and type-V RTK activation and signaling.* Cold Spring Harb Perspect Biol, 2013. **5**(10): p. a009092.
308. Afranie-Sakyi, J.A. and G.L. Klement, *The toxicity of anti-VEGF agents when coupled with standard chemotherapeutics.* Cancer Lett, 2015. **357**(1): p. 1-7.
309. Tredan, O., et al., *Angiogenesis and tumor microenvironment: bevacizumab in the breast cancer model.* Target Oncol, 2014.
310. Kumler, I., O.G. Christiansen, and D.L. Nielsen, *A systematic review of bevacizumab efficacy in breast cancer.* Cancer Treat Rev, 2014. **40**(8): p. 960-73.

311. Wadhwa, R., et al., *Anti-angiogenic agent ramucirumab: meaningful or marginal?* Expert Rev Anticancer Ther, 2014. **14**(4): p. 367-79.
312. Huang, H., et al., *An updated meta-analysis of fatal adverse events caused by bevacizumab therapy in cancer patients.* PLoS One, 2014. **9**(3): p. e89960.
313. Wang, Z., et al., *Multitargeted antiangiogenic tyrosine kinase inhibitors combined to chemotherapy in metastatic breast cancer: a systematic review and meta-analysis.* Eur J Clin Pharmacol, 2014. **70**(5): p. 531-8.
314. Vasudev, N.S. and A.R. Reynolds, *Anti-angiogenic therapy for cancer: current progress, unresolved questions and future directions.* Angiogenesis, 2014. **17**(3): p. 471-94.
315. Kerbel, R.S., et al., *Preclinical recapitulation of antiangiogenic drug clinical efficacies using models of early or late stage breast cancer metastatis.* Breast, 2013. **22 Suppl 2**: p. S57-65.
316. Lisabeth, E.M., G. Falivelli, and E.B. Pasquale, *Eph receptor signaling and ephrins.* Cold Spring Harb Perspect Biol, 2013. **5**(9).
317. Chen, J., W. Song, and K. Amato, *Eph receptor tyrosine kinases in cancer stem cells.* Cytokine Growth Factor Rev, 2015. **26**(1): p. 1-6.
318. Tognolini, M., et al., *Therapeutic perspectives of Eph-ephrin system modulation.* Drug Discov Today, 2014. **19**(5): p. 661-9.
319. Youngblood, V., et al., *Elevated Slit2 Activity Impairs VEGF-Induced Angiogenesis and Tumor Neovascularization in EphA2-Deficient Endothelium.* Mol Cancer Res, 2015. **13**(3): p. 524-37.
320. Miao, Z., et al., *VEGF increases paracellular permeability in brain endothelial cells via upregulation of EphA2.* Anat Rec (Hoboken), 2014. **297**(5): p. 964-72.
321. Pandey, A., et al., *Role of B61, the ligand for the Eck receptor tyrosine kinase, in TNF-alpha-induced angiogenesis.* Science, 1995. **268**(5210): p. 567-9.
322. Jing, X., et al., *Ephrin-A1-mediated dopaminergic neurogenesis and angiogenesis in a rat model of Parkinson's disease.* PLoS One, 2012. **7**(2): p. e32019.
323. Song, Y., et al., *Ephrin-A1 is up-regulated by hypoxia in cancer cells and promotes angiogenesis of HUVECs through a coordinated cross-talk with eNOS.* PLoS One, 2013. **8**(9): p. e74464.
324. Hassan-Mohamed, I., et al., *UniPR129 is a competitive small molecule Eph-ephrin antagonist blocking in vitro angiogenesis at low micromolar concentrations.* Br J Pharmacol, 2014. **171**(23): p. 5195-208.
325. Xu, N.J. and M. Henkemeyer, *Ephrin reverse signaling in axon guidance and synaptogenesis.* Semin Cell Dev Biol, 2012. **23**(1): p. 58-64.
326. Daar, I.O., *Non-SH2/PDZ reverse signaling by ephrins.* Semin Cell Dev Biol, 2012. **23**(1): p. 65-74.
327. Aslakson, C.J. and F.R. Miller, *Selective events in the metastatic process defined by analysis of the sequential dissemination of subpopulations of a mouse mammary tumor.* Cancer Res, 1992. **52**(6): p. 1399-405.

328. Prewett, M., et al., *Antivascular endothelial growth factor receptor (fetal liver kinase 1) monoclonal antibody inhibits tumor angiogenesis and growth of several mouse and human tumors.* Cancer Res, 1999. **59**(20): p. 5209-18.
329. Pidgeon, G.P., et al., *Vascular endothelial growth factor (VEGF) upregulates BCL-2 and inhibits apoptosis in human and murine mammary adenocarcinoma cells.* Br J Cancer, 2001. **85**(2): p. 273-8.
330. Funk, S.D., et al., *EphA2 activation promotes the endothelial cell inflammatory response: a potential role in atherosclerosis.* Arterioscler Thromb Vasc Biol, 2012. **32**(3): p. 686-95.
331. Ley, K., et al., *Getting to the site of inflammation: the leukocyte adhesion cascade updated.* Nat Rev Immunol, 2007. **7**(9): p. 678-89.
332. Chan, B. and V.P. Sukhatme, *Receptor tyrosine kinase EphA2 mediates thrombin-induced upregulation of ICAM-1 in endothelial cells in vitro.* Thromb Res, 2009. **123**(5): p. 745-52.
333. Coulthard, M.G., et al., *Eph/Ephrin signaling in injury and inflammation.* Am J Pathol, 2012. **181**(5): p. 1493-503.
334. Sun, Z., et al., *VEGFR2 induces c-Src signaling and vascular permeability in vivo via the adaptor protein TSAd.* J Exp Med, 2012. **209**(7): p. 1363-77.
335. Koch, S. and L. Claesson-Welsh, *Signal transduction by vascular endothelial growth factor receptors.* Cold Spring Harb Perspect Med, 2012. **2**(7): p. a006502.
336. Lampugnani, M.G., et al., *Vascular endothelial cadherin controls VEGFR-2 internalization and signaling from intracellular compartments.* J Cell Biol, 2006. **174**(4): p. 593-604.
337. Weidner, N., et al., *Tumor angiogenesis and metastasis--correlation in invasive breast carcinoma.* N Engl J Med, 1991. **324**(1): p. 1-8.
338. Vestweber, D., *VE-cadherin: the major endothelial adhesion molecule controlling cellular junctions and blood vessel formation.* Arterioscler Thromb Vasc Biol, 2008. **28**(2): p. 223-32.
339. Vestweber, D., et al., *Cell adhesion dynamics at endothelial junctions: VE-cadherin as a major player.* Trends Cell Biol, 2009. **19**(1): p. 8-15.
340. Coon, B.G., et al., *Intramembrane binding of VE-cadherin to VEGFR2 and VEGFR3 assembles the endothelial mechanosensory complex.* J Cell Biol, 2015. **208**(7): p. 975-86.
341. Tzima, E., et al., *VE-cadherin links tRNA synthetase cytokine to anti-angiogenic function.* J Biol Chem, 2005. **280**(4): p. 2405-8.